Universidade de Vigo

Escola de Enxeñaría de Telecomunicación

Proxecto de Fin de Carreira

Evaluation of New Link Adaptation Techniques for Mobile Satellite Channels

Autor
Anxo Tato Arias

Titor
Carlos Mosquera Nartallo

Titulación
Enxeñaría de Telecomunicación

Curso 2015-2016

Evaluation of New Link Adaptation Techniques for Mobile Satellite Channels

Autor: Anxo Tato Arias
Titor: Carlos Mosquera Nartallo

Resumo

Neste proxecto abórdase o problema de adaptación de enlace no estándar S-UMTS (compoñente satélite de UMTS). A adaptación de enlace consiste en elixir a modulación e a codificación de cada trama co obxectivo de maximizar a eficiencia espectral e ao mesmo tempo garantir que a taxa de erro de trama (FER) non supera un limiar obxectivo. En primeiro lugar faise unha introdución do proxecto falando da compoñente satélite das IMT-2000. Despois faise un resumo da familia SL do estándar S-UMTS. A continuación explícanse o modelo do sistema e o modelo da canle LMS (Land Mobile Satellite) e finalmente o último capítulo dedícase á adaptación de enlace en S-UMTS. Nel preséntanse unhas ferramentas novidosas para analizar os resultados obtidos cos algoritmos de adaptación de enlace e propóñense novos algoritmos tanto para o enlace directo (forward link) como para o enlace de retorno (return link). Os algoritmos mostran un bo comportamento tanto en termos de eficiencia espectral como de taxa de error de trama, achegándose ao límite teórico de eficiencia, determinado pola informed outage capacity, e garantindo a FER obxectivo para un amplo abano de SNRs.

Palabras clave: adaptación de enlace, S-UMTS, codificación e modulación adaptativas, satélite móbil, canle LMS.

Resumen

Este proyecto aborda el problema de la adaptación de enlace en el estándar S-UMTS (componente de satélite de UMTS). La adaptación de enlace consiste en elegir la modulación y la codificación de cada trama con el fin de maximizar la eficiencia espectral y al mismo tiempo garantizar que la tasa de error de trama (FER) no supera un umbral objetivo. En primer lugar se realiza una introducción del proyecto hablando de la componente de satélite de las IMT-2000. Después se resume la familia SL del estándar S-UMTS. A continuación se explica el modelo del sistema y el modelo del canal LMS (Land Mobile Satellite) y, finalmente, el último capítulo está dedicado a la adaptación de enlace en S-UMTS. En él se presentan herramientas innovadoras para analizar los resultados obtenidos con los algoritmos de adaptación de enlace y se proponen nuevos algoritmos tanto para el enlace directo

(forward link) como para el enlace de retorno (return link). Los algoritmos muestran un buen comportamiento tanto en términos de eficiencia espectral como de tasa de error de trama, acercándose al límite teórico de la eficiencia, determinada por la informed outage capacity, y cumpliendo la FER objetivo para un amplio rango de SNRs.

Palabras clave: adaptación de enlace, S-UMTS, codificación y modulación adaptativas, satélite móbil, canal LMS.

Abstract

This project deals with link adaptation in the standard S-UMTS (satellite component of UMTS). The link adaptation consists on selecting the modulation and coding scheme (MCS) for each frame with the purpose of maximize the spectral efficiency and, at the same time, guarantee that the frame error rate (FER) does not exceed a target value. In first place, it is made an introduction to the satellite component of IMT-2000. Then it is summed up the SL family of the standard S-UMTS. After that, the system model and the LMS (Land Mobile Satellite) channel model are explained and, finally, the last chapter deals with link adaptation in S-UMTS. In this chapter some innovative tools for analysing the results obtained with the link adaptation algorithms are presented. Also we propose new algorithms for the forward link and return link. The algorithms show a good behaviour in terms of spectral efficiency and frame error rate, reaching the theoretical limit of efficiency, determined by the informed outage capacity, and guaranteeing the objective FER for a wide range of SNRs.

Keywords: link adaptation, S-UMTS, adaptive coding and modulation, mobile satellite, LMS channel.

Acknowledgement

This work was partially funded by the Spanish Government and the European Regional Development Fund under project TACTICA.

Agradecementos

En primeiro lugar quero agradecerlle á miña familia, que é a primeira escola da sociedade e un mundo en pequeno, a educación que me deu. E especialmente a meu pai, Ricardo Tato, porque, grazas ao seu sabio consello, agora estou rematando Enxeñaría de Telecomunicación, titulación que me apaixona e que me habilita para exercer unha profesión bonita e coa que podo achegar o meu grao de area á sociedade para facer un mundo mellor actuando localmente no meu país, Galicia.

Unha consideración especial merece a miña moza, Rocío Toxo que, co seu amor, me axudou a superar os momentos difíciles e non só iso, senón que me dá as ás para voar cara a un futuro de soños en común.

Non me quero esquecer tampouco do meu cuñado Serxio Toxo que, a pesar de non ter formación técnica, coa súa paixón pola música e pola electrónica me fixo entender na práctica conceptos que os profesores da carreira debullaban nas clases.

Un só dá o mellor de si no ámbito profesional e académico cando está ben consigo mesmo e coa súa contorna, e a nosa contorna máis inmediata despois da familia e da parella son os amigos. Grazas, amigos, vós xa sabedes quen sodes, non fai falta que vos cite un a un. Aínda así gustaríame nomear a Iago Fernández e a Iria Domínguez: a súa axuda foi imprecindible «per desfer-me d'aquella mala estaca que em lligava i no em deixava avançar», en termos de Lluís Llach. A Miguel Domínguez, bo amigo e excelente matemático, modelo que me gustaría seguir como investigador. A Xosé Antonio Arias, co que compartín grandes momentos e soños. Mención especial merecen aqueles amigos que chegaron á miña vida despois de aterrar en Vigo, ou cuxa relación se intensificou aquí: Samuel López, Carlos Patiño, Noelia Devesa, Javi Gómez... grazas por convertir esta cidade industrial na miña segunda Compostela.

E non tería chegado ata aquí, ou polo menos non sendo o que son e como son, de non ser por tantos mestres que, dando a súa vida por unha ensinanza pública e de calidade, me formaron como persoa e como cidadán. Un emotivo recordo para todo o profesorado do CPI Fonte-Díaz de Touro, do Instituto Rosalía de Castro de Santiago de Compostela e da Escola de Enxeñaría de Telecomunicación. Entre as súas paredes gardo moitas das que son as mellores lembranzas da miña vida.

Quero citar tamén a aquelas persoas que fixeron posible que puidese levar á práctica aquelas ensinanzas que ía adquirindo na Escola de Enxeñaría de Telecomunicación. Teresa Prat, grazas por confiar en min e darme a oportunidade de ser colaborador-bolseiro na Residencia Xuvenil Altamar. Jorge Munir, grazas por acollerme entre o equipo de Comunicacións de Gradiant e por facerme sentir un máis.

Unha parte importante da miña estancia en Vigo foi a Asociación Trabalingua. Cos compañeiros e coas compañeiras da asociación aprendín o que é traballar en equipo, con ilusión, por cambiar a realidade e achegala algo máis ao que son os nosos soños. O traballo na asociación axudounos a evolucionar interiormente e a adquirir moitas habilidades que agora cada un de nós está aplicando no lugar ao que a vida o levou.

Este proxecto non sería posible se o meu titor Carlos Mosquera non tivese depositado a súa confianza en min. Grazas, Carlos, por ofrecerme a oportunidade de ser o teu «aprendiz»durante todos estes meses. E grazas a AtlantTIC, *Atlantic Research Center for Information and Communication Technologies*, e especialmente á súa directora, Nuria González, que froito do seu traballo e dedicación fixo posible a existencia do proxecto Táctica, dentro do cal puiden facer este Proxecto de Fin de Carreira, traballando como persoal colaborador en investigación e desenvolvemento.

Moitas veces, a xente de enxeñaría peca de soberbia subestimando as persoas do ámbito das Humanidades ou das Ciencias Sociais. Fano sen darse conta de que, por exemplo, as palabras son a base da comunicación e de que a función da enxeñaría é resolver problemas que teñen as persoas, membros dunha sociedade, coa axuda da ciencia, das matemáticas e empregando a tecnoloxía existente. Quero aproveitar tamén para enviarlle un saúdo a todas as amigas e os amigos de Filoloxía e de Tradución e Interpretación, e darlle as grazas a Antía Veres Gesto por corrixirme esta sección.

Para ir rematando, quixera agradecerlle a Isaac Martínez a súa compañía durante as últimas semanas de redacción do proxecto. A súa alegría e as nosas parolas fixeron que garde uns bonitos recordos do que foron as últimas semanas como estudante de Enxeñaría.

E podería seguir citando e citando a xente, porque somos o que somos grazas a moitos dos que nos precederon e a moitos dos nosos coetáneos, pero non podo estender máis esta sección.

Por último, vendo a situación económica que vive o noso país actualmente, gustaríame traer aquí uns versos do poemario *Follas novas* que tomo prestadas da nosa gran poeta, Rosalía de Castro:

Este vaise i aquel vaise,
e todos, todos se van,
Galicia sin homes quedan
que te poidan traballar.[1]

E aquí quero aproveitar este parágrafo para pedirlle aos poderes públicos de Galicia que fagan por cumprir a súa obrigación estatutaria de *asumir, como un dos principios rectores da súa política social e económica, o dereito dos galegos a viviren e traballaren na propia terra*[2] e por frear esta perda de capital humano que mina o futuro da nosa terra.

E para rematar teño que confesar que non son nada pesimista. Coma os *Scorpions I am listening to the wind of change* ou, como Rosalía pregobaba na alborada do Rexurdimento, eu tamén canto na praza da vila:

Vaite, noi-
te, —vai fuxin-

[1] Rosalía de Castro. *Follas novas*. 1880
[2] *Estatuto de Autonomía de Galicia*. 1981

do—. Vente, auro-
ra, —vente abrin-
do–, co te ros-
tro —que, sorrin-
do—, ¡¡¡a sombra espanta!!![3]

[3]Rosalía de Castro. *Cantares gallegos.* 1863

Contents

Chapter 1

Introduction

Spectrum is the lifeblood of communication systems.

The radio spectrum is one of scarcest resources of the humanity and it is a task of the Telecommunication Engineers to take the most of it to allow the transmission of as much data as possible. And, in satellite communications, spectrum is even more scarce, because due to the large footprint of a satellite spot beam, a channel in frequency is shared among a lot of users in a big geographical area. Therefore, it is important to increase the spectral efficiency of the communication systems, measured in bit/s/Hz.

The standard under study in this project, S-UMTS family SL, disposes up to 41 MHz for downlink and 41 MHz for uplink in the user link at L-band. This small quantity of bandwidth should be shared among tens of thousands of users over large terrestrial areas, hence the need to make an efficient use of the allocated spectrum.

Also, users demand each year bigger data rates and the ubiquitous access to communication networks and even on the move. S-UMTS family SL allows the access to Internet and the realisation of phone calls in places not covered by terrestrial networks and access to those services even while they are in movement.

As the title says, this project evaluates new link adaptation techniques for the mobile satellite channels. This means that some new algorithms are explored in order to increase the spectral efficiency of satellite communication systems involving mobile users. The algorithms proposed here are easy to implement and allow to achieve the most of the spectrum while maintaining the rate of errors, measured in Framer Error Ratio (FER), under a pre-set value.

The main objectives of the project are the following:

- Study of the standard S-UMTS family SL.
- Study the Land Mobile Satellite (LMS) channel.
- Program in Matlab an implementation of the multi-state LMS channel model.
- Study the previous work realised by GPSC members related with link adaptation.
- Modify the algorithm for the return link presented in [3] and adapt it to operate in the forward link.

- Validate the correct operation of the algorithms under the LMS channel.
- Propose new link adaptation algorithms for mobile satellite communications.

Finally, the project is structured as follows. In the Chapter 2 the framework of the third generation of mobile telecommunications technologies, named IMT-2000 (International Mobile Telecommunications - 20000), is explained. This chapter is focused on the satellite component of IMT-2000. Then, Chapter 3 is a summary of the standard S-UMTS family SL, which is one of the Satellite Radio Interfaces proposed in the IMT-2000. After that, Chapter 4 describes the system model emphasizing the Fontán channel model. Lastly, in Chapter 5, which is focused on link adaptation in S-UMTS, the main results of the project are exposed. Finally, Chapter 6 collects the Conclusions and the Future Work.

Chapter 2

Satellite component of IMT-2000

2.1 GSM over GEO satellite

After the standardization of GSM in the late 1980s and deployment of the first GSM networks, the ETSI and the American organisation TIA (Telecommunications Industry Association) started the adaptation of this standard to the satellite scenario. Their objective was to standardize a new system, a expansion of GSM, that provides the same services as the terrestrial digital cellular standard GSM provides but by means of a GEO satellite. The developed standard was called GMR, that stands for GEO Mobile Radio Interface [4]. The new system is compatible with the GSM core network and the user terminals, named MES (Mobile Earth Stations), are implemented as dual mode devices, which can be operated in either cellular or GMR mode.

GSM and GMR are a good example of integration of satellite and terrestrial systems to provide mobile communication services. In maritime and aeronautical markets satellite systems are the unique option due to its wide coverage, but in land applications they have a different role. The fact that eighty per cent of the population lives in urban/suburban areas where terrestrial networks are well-developed leaves the satellite systems a secondary role to complement them in rural and remote areas. The exception to that is the TV delivering, where the inherent broadcast capabilities encourage satellite television to be a popular alternative to terrestrial television. This integration is also mentioned in [5], they offer a view of the future of satellite communications where they are integrated with terrestrial systems for offering services economically and using a single terminal for both systems. However, in spite of having a complementary role to terrestrial systems, satellite communications have an important advantage since satellites are not affected by natural disasters on Earth as terrestrial systems are. For example, an earthquake, a hurricane or a flood can destroy some BTS (Base Transceiver Station), disrupting the mobile telephony service in the vicinity, while satellite mobile phones in that area could still work properly.

Returning to the subject of GMR, this system provides mainly voice, data and fax services to mobile users with worldwide connectivity because the core network is connected to the public and private communication networks. They main elements of the system are:

- the Gateways
- the GEO satellite

- the User Terminals (named Mobile Earth Stations, MES)
- the Satellite Control Facility
- the Network Control Center and
- the Customer Management Information System

There are several on-ground Gateways, on one hand they are connected to the fixed terrestrial networks and, on the other hand, they send the data and signalling traffic to the satellite via a feeder link that operates in C-band (4-8 GHz). The User Terminal, however, uses a lower frequency, the link is in L-band (1-2 GHz) in the frequency bands assigned to Mobile Satellite Services. This band allows the use of hemispherical coverage antennas with no need to perform any cast of pointing. In Figure 2.1 we show the main elements of a GMR system.

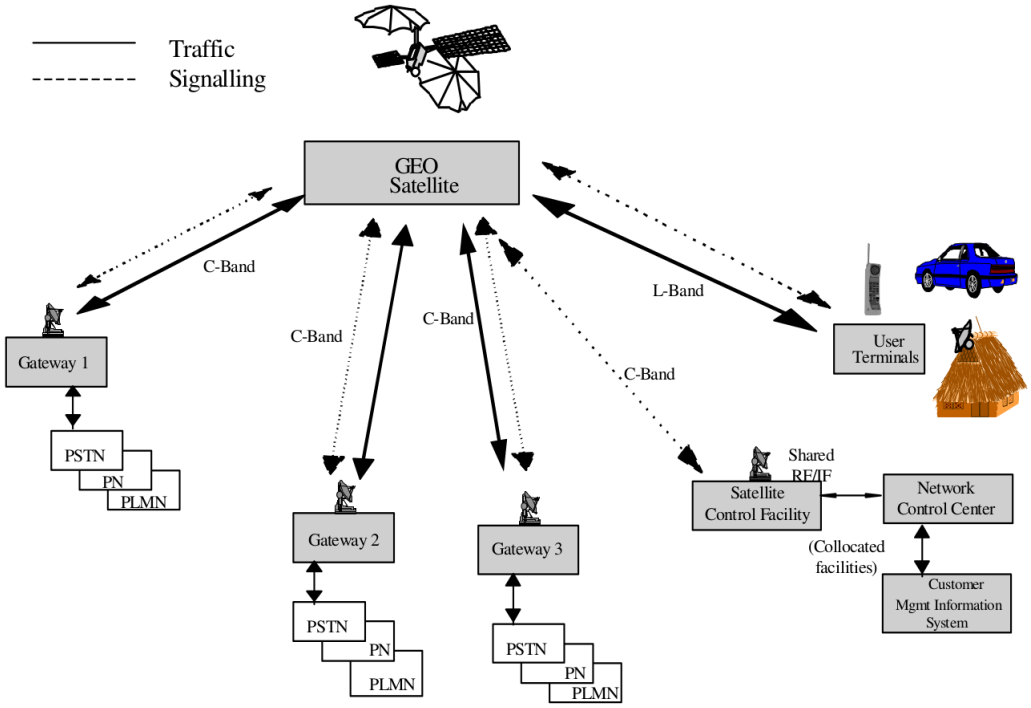

Figure 2.1: GMR system elements

Regarding the versions of GMR, there are two sets of different specifications, GMR-1 and GMR-2, which were developed by different groups of companies. The GMR-1, the first version of the standard, was developed by Hughes Electronics for the satellite communication company Thuraya and it was used by its spacecraft Thuraya-1 (launched in 2000) [6]. The two current operational satellites of Thuraya, Thuraya-2 and Thuraya-3, also use an evolution of this air interface [7]. Figure 2.2 depicts the evolution of GMR-1 along with the evolution of the terrestrial GMS towards 3G, as can be seen in the aforementioned figure, GMR-1 has three different revisions:

- GMR-1: This first version, published in 2001, offers circuited switched voice and data and it is based on GSM protocol architecture.
- GmPRS: This release adds IP data services using GPRS techonology. The latest

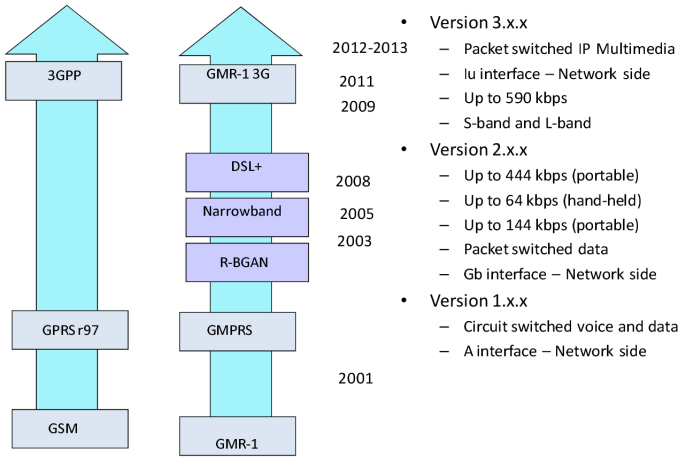

Figure 2.2: Evolution of GMR-1 specifications

versions (2008) support dynamic link adaptation and data rates of 444 kbit/s on the downlink and 202 kbit/s on the uplink for A5 size transportable terminals [2].

- GMR-1 3G: It is based on the adaptation of the terrestrial air interface EDGE. It also adds some changes in the core network to be compatible with 3GPP Release 6. GMR-1 3G is designed to meet the requirements of the satellite component of 3G (IMT-2000) [2].

The air interface GMR-2, developed by Ericsson and Lockheed Martin Global Telecommunications, is employed by the Asia Cellular System (ACeS) and its satellite Garuda-1 [6].

2.2 3G over satellite

Initial standardization efforts for the third generation of mobile telecommunications technology started during the mid-1980s within the ITU. The final result is the so called IMT-2000 "International Mobile Telecommunications", a family of technologies for 3rd Generation mobile services with worldwide roaming and compatibility [8]. IMT-2000 intend to provide higher capacity and enhanced network functionalities, which allows advanced services and applications, including multimedia. In words of the ITU-R Recommendation M.687 [8], that defines the objectives to be met by IMT-2000 and provides the overall IMT-2000 concept, some of the primary general objectives are:

- to make available to users who are on the move or whose location may change (nomadic users), irrespective of their location (i.e. national and international roaming), a wide range of telecommunication services (voice and non-voice), allowing communication between mobile users and other mobile users, users of the fixed public networks (PSTN, PDNs and ISDN) or other telecommunication networks as appropriate.
- to provide these services over a wide range of user densities and geographic coverage areas.
- to make efficient and economical use of the radio spectrum consistent with providing

service at an acceptable cost.

- to adopt a phased approach for the definition of IMT-2000 where the first phase (Phase 1) includes those services supported by user bit rates up to approximately 2 Mbit/s. In the case of the satellite component, although relatively high bit rates are achievable the bulk of the services and terminals are should be targeted to low bit rates, less than 64 kbit/s.

As said in the second point, IMT-2000 tries to provide services over a wide range of geographic areas but where there is low user density it may no be profitable to deploy a IMT-2000 terrestrial network. In those cases a mobile-satellite component is desirable due to the wide coverage of a satellite compared with a terrestrial cell. From the beginning of the standardization process it was contemplated the existence of a satellite component of IMT-2000 as can be seen in the section 3.3.2 of ITU-R M.687. After this, the Recommendation ITU-R M.818 [9] analyses the reasons why IMT-2000 should have a satellite component and present the services it should provide and its main characteristics. In this document they admit that in order for IMT-2000 to be available to users anywhere on land, ships and aircraft, a satellite component of IMT-2000 will be required. The Recommendation also expresses some advantages of it like the following ones:

- the satellite operation within IMT-2000 will enhance the overall coverage and attractiveness of the services.
- the satellite operation within IMT-2000 could facilitate the development of telecommunication services in developing countries.
- satellite systems (including the satellite component of IMT-2000) could be useful for the provision of services in emergency and disaster relief situations.

Here below in figure 2.3 we include a diagram taken from [9] which shows different configurations within the satellite component of IMT-2000.

2.2.1 Recommendation ITU-R M.1167: Framework for the satellite component of IMT-2000 [1]

This Recommendation describes those capabilities and features that are specific of the satellite component and expose some aspects of the integration with the terrestrial component, the radio interfaces and the services provided. It makes a brief introduction to those aspects that are developed with more detail in subsequent Recommendations like ITU-R M.1182 that deals with the integration of terrestrial and satellite mobile communication systems or ITU-R M.1850 which details the specifications of the radio interfaces for the satellite component of International Mobile Telecommunications-2000 (IMT-2000). This section summarizes the aspects of that Recommendation that have a stronger connection with the present work.

A key feature of the satellite component of IMT-2000 is that, contrary to the terrestrial component, the coverage is provided by means of a number of spot beams from one or more satellites being the geographical area covered by one satellite much bigger than a terrestrial cell, spanning over different countries and even having a global coverage. Regarding the space segment there can be different configurations, from big constellations of LEO satellites to MEO, GEO or HEO constellations, having each option its own features

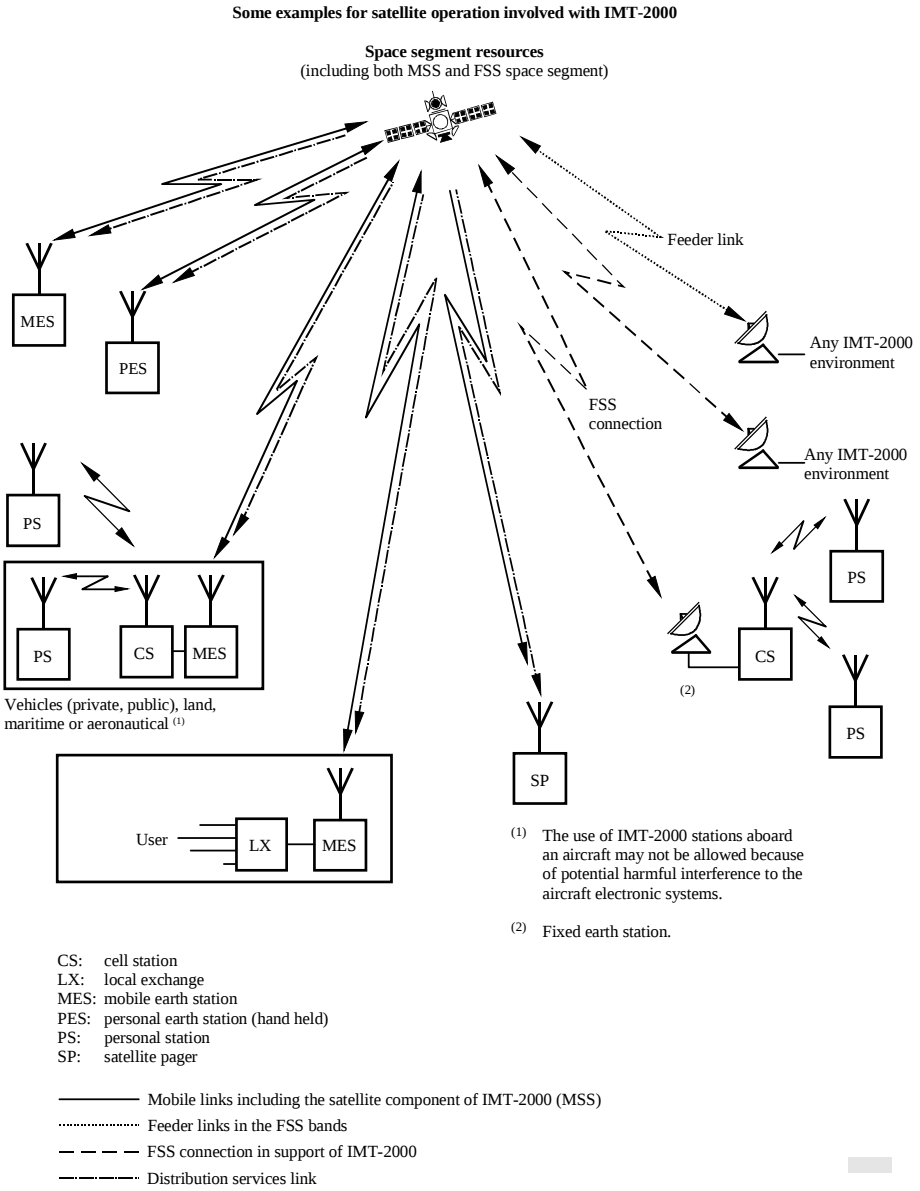

Figure 2.3: Satellite operation within the IMT-2000. *Source: ITU-R M.818 Fig 1*

and implications in the design of the IMT-2000 system. Another important issue is the frequencies used by the system. The user link employs those frequencies allocated to mobile satellite services, being desirable not being shared with the terrestrial component; the feeder links and the inter-satellite links, if they exist, must operate outside the IMT-2000 band.

The handover, the action of switching a call in progress from one cell to another (intercell) or between radio channels in the same cell (intracell) without interruption of the call [10] also applies to the satellite component. For non-geostationary satellites the footprints of beams are in motion and calls in progress may need to be transferred from one beam to another and even for geostationary satellites with users on the move a handover could be also required. Handovers must be performed through appropriate air interface protocols which involve functionalities both in the mobile and in the satellite component. Finally,

another type of handover that occurs only to equipments able to access both the terrestrial and satellite components is the intercomponent handover, which intends to maintain continuity of calls in progress as the user crosses the boundary between the components.

With respect to the integration of satellite and terrestrial components, they are fully integrated in the network level so they support identical management services, and functional entities, that can be shared between both components, are standardized together with network protocols. Concerning service integration it can be said that it is not practical to offer all services in all the environments but in order to achieve service integration if both components have common services they have to be offered in the same way. Another important matter is the commonality between terrestrial and satellite radio interfaces. In principle a high degree of concordance is desirable however, due to critical design constraints such as spectral and power efficiency, there are different radio interfaces for the components. A last point related to integration is the roaming between the terrestrial and satellite components. IMT-2000 should support roaming between the terrestrial and satellite components and the user must be able to be reached by dialling a single number, whether the mobile terminal is in the terrestrial or the satellite component.

Satellite and terrestrial components, although designed for inter-work and be integration at network level can be deployed in several ways. One option is a self-contained satellite IMT-2000 network (see Figure 2.4) which has all the elements needed for work in a standalone mode. It has interfaces to other IMT-2000 networks and other networks. Another option is an integrated IMT-2000 network as that showed in figure 2.5 that provides both terrestrial and satellite components. Finally other option is that the terrestrial and satellite components be a extension of other intelligent fixed network which can deploy some of the functionality entities of the IMT-2000 networks.

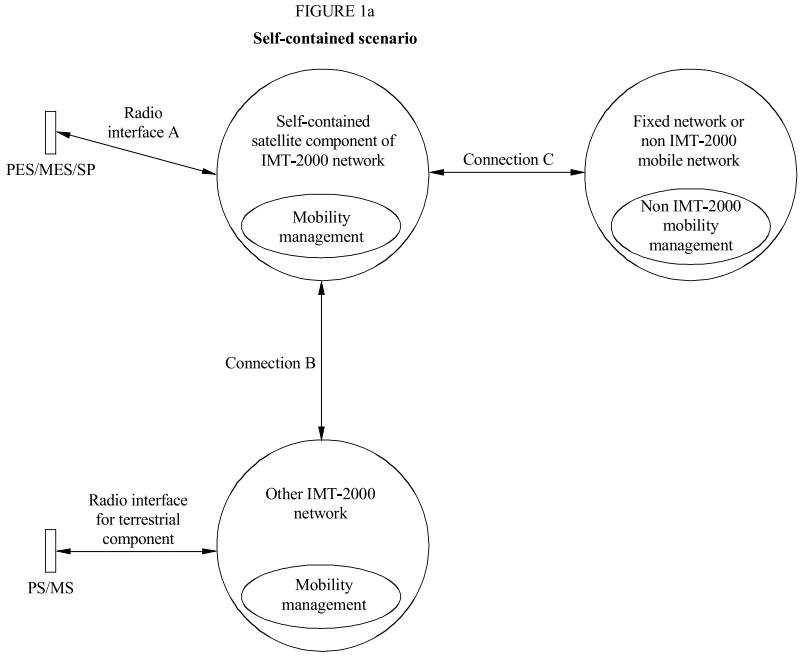

Figure 2.4: Self-contained scenario. *Source: ITU-R M.1167 Fig 1A*

Let us now introduce the problem of the design of the satellite radio interface. The eco-

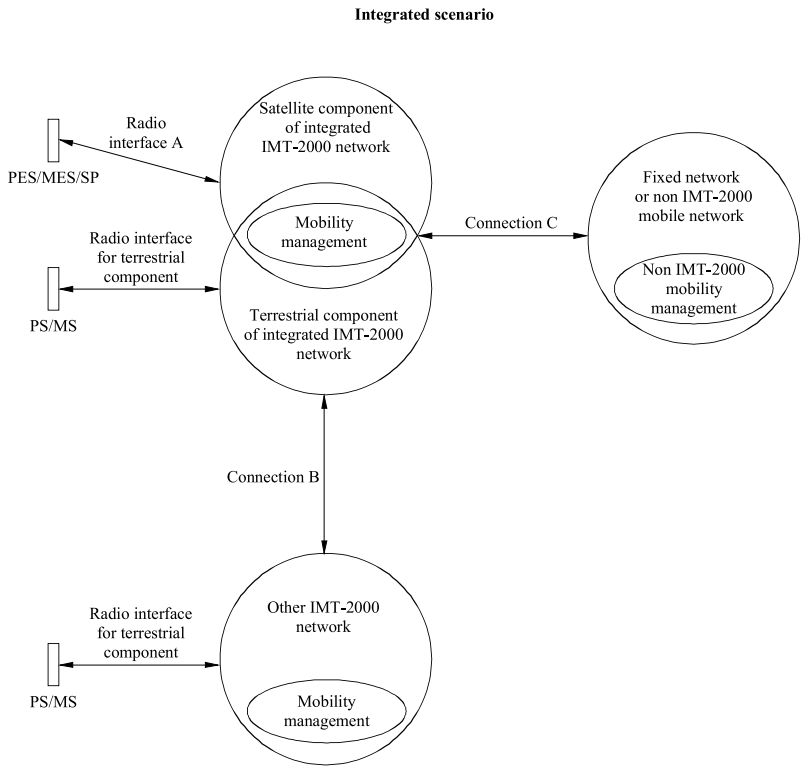

Figure 2.5: Integrated scenario. *Source: ITU-R M.1167 FIg 1B*

nomics of worldwide satellite systems dictate that for the system to be profitable it has to operate very close to the optimum point of bandwidth and information rate and a minimum deviation could make it economically unviable. Remember that many of the companies who build a mobile satellite communication system in the 90's went into bankruptcy, therefore, it shows that this is of paramount importance. When designing and selecting the radio interface some features need to be taken into account:

- Hand-held satellite terminals require the use of narrow spot satellite beams.
- The scarcity of the satellite spectrum force to reduce the channel overheads to the minimum.
- Satellite signalling and broadcast channels will generally operate at higher powers or with more robust protection than traffic channels.
- Radio access techniques must be tolerant of signal acquisition delays, variable propagation delays, Doppler shifts, and delay or Doppler jumps.
- Radio multiple access techniques such as CDMA, FDMA and TDMA are all potential candidate solutions for the satellite component, each one offering particular advantages and disadvantages dependent on the service requirements and the orbital/system characteristics.
- The shadowing caused by buildings etc may and other obstacles countered by techniques such as link margin, coding, satellite diversity, among others.

2.2.2 Recommendation ITU-R M.1850: Detailed specifications of the radio interfaces for the satellite component of IMT-2000 [2]

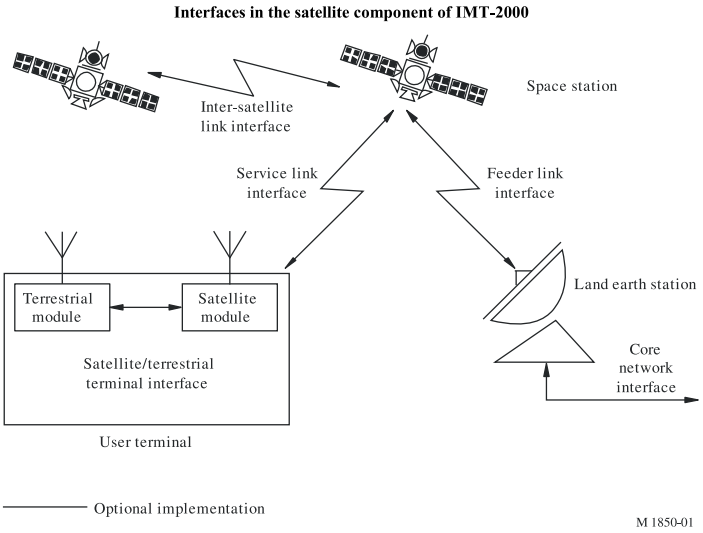

Figure 2.6: Interfaces in the satellite component of IMT-2000. *Source: ITU-RM.1850 Fig1*

As the Recommendation ITU-R M.1457 details the specifications of the radio interfaces of the terrestrial component of IMT-2000, this Recommendation does the same with the satellite component. As said previously, there are a set of different satellite radio interfaces (SRIs). The strong dependency between technical design and business objectives and the system optimization process to exploit the scarce resources (power and spectrum) lead to this flexibility in the definition of the SRIs.

The specifications identified in this Recommendation have been developed by the ITU in collaboration with some companies, global partnership projects and standards development organizations (SDOs) like the ETSI (which has standardized the SRIs families A and G for S-UMTS).

Before getting into the details of the radio interfaces of the satellite component, a overview of the main interfaces of the system will be made. Figure 2.6 shows the existence of five different interfaces. Two of them, the inter-satellite link interface (if any) and the feeder link interface, are outside the scope of IMT-2000 and are considered as an implementation issue. The satellite/terminal interfaces applies to user terminals which incorporate both components of IMT-2000 and is the interface between the satellite and terrestrial modules within a user terminal. The core network (CN) interface, called Ius, is the interface between the radio access part of a Land Earth Station (LES) and the CN and it is designed to achieve as much commonality as possible with the equivalent interface of the terrestrial component (Iu). Finally, the Uus interface is the satellite service link radio interface, or simply satellite radio interface (SRI), that will be explained hereafter in detail. The user terminal employs this interface to communicate with the SRAN (satellite radio access network), the union of the LES, the satellite and the feeder and inter-satellite links as depicted in Figure 2.7.

The Recommendation comprises seven different satellite radio interfaces (SRIs), each one named with a letter. Hereafter we include seven tables (Table 2.1, 2.2, 2.3, 2.4, 2.5, 2.6, 2.7)

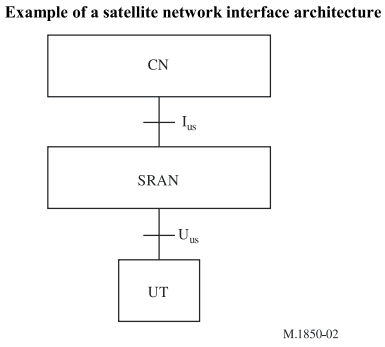

Figure 2.7: Satellite network architecture

that summarize the main characteristics of each SRI. Then, in the next section the family SL of the S-UMTS ETSI standard, that developes the satellite radio interface SRI-E, will be explained in detail before start with the link adaptation applied to S-UMTS.

Characteristic	**Value**
Name	SW-CDMA
Standard	ETSI S-UMTS A family
Based on	WCDMA or CDMA direct spread terrestrial radio interface
Multiple access	CDMA
Duplex method	FDD
Bit rates	Voice and data services (1.2 - 144 kbit/s, BER $10^{-3} - 10^{-6}$)
Constellation	Any (LEO, MEO, GEO, HEO)
Satellite	Any (bent-pipe transparent satellite transponder or regenerative transponder)
Terminal features	Hand-held, vehicular, transportable, fixed
Modulation	↓QPSK or BPSK. ↑Dual-code BPSK
FEC	convolutional, Red Solomon (RS), turbo coder
Other	Great degree of commonality with the terrestrial radio interface

Table 2.1: Features of SRI-A

Characteristic	**Value**
Name	W-C/TDMA
Standard	Examining by ETSI SES Technical Comittee
Multiple access	Hybrid C/TDMA
Duplex method	Baseline FDD. TDD/FDD supported
Bit rates	Voice and data services (1.2 - 144 kbit/s, BER $10^{-3} - 10^{-6}$)
Constellation	Any (LEO, MEO, GEO, HEO)
Satellite	Any (bent-pipe transparent satellite transponder or regenerative transponder)
Terminal features	Hand-held, vehicular, transportable, fixed
Modulation	↓QPSK or BPSK. ↑QPSK, Dual-code BPSK
FEC	Convolutional, Red Solomon (RS), turbo coder
Other	High penetration paging channel

Table 2.2: Features of SRI-B

Characteristic	**Value**
Name	W-C/TDMA
Proponent organization	ICO (Inmarsat)
Multiple access	FDMA and TDMA
Duplex method	FDD
Bit rates	Voice (BER 4%) and data services (up to 38.4 kbit/s, BER 10^{-6})
Constellation	10 MEO satellites at 10390 km with 12 LES
Satellite	163 beams, digital beam forming and channelization. onboard digital processor
Terminal features	Hand-held, ruggedized transportable, private vehicle, commercial vehicle, semi-fixed
Modulation	↓QPSK, BPSK. ↑GMSK, S-BPSK
FEC	Convolutional

Table 2.3: Features of SRI-D

Characteristic	**Value**
Standard	ETSI S-UMTS SL family (TS 102 744)
Multiple access	TDM/TDMA
Duplex method	FDD
Bit rates	↓19.2 - 512 kbit/s. ↑21.6 - 512 kbit/s
Constellation	3 GEO satellites
Satellite	State-of-the-art GEO technology. 300 spot-beams
Terminal features	Primary type: palmtop computer. From stationary to aircraft speeds
Modulation	↓QPSK, 16-QAM. ↑π/4-QPSK, 16-QAM
FEC	Turbo codes
Others	Link adaptation through variable coding

Table 2.4: Features of SRI-E

Characteristic	**Value**
Name	Satcom2000
Proponent organization	INX-Motorola
Multiple access	Hybrid: FDMA/TDMA and FDMA/CDMA
Duplex method	TDD/FDD
Bit rates	TDMA (2.4 - 4 kbit/s). CDMA 9.6 kbit/s (up to 144 kbit/s with multiple channels)
Constellation	96 LEO satellites
Satellite	228 spot beams
Terminal features	Hand-held (500 km/h), portable, nomadic, fixed, aeronautical (5000 km/h), maritime, others
Modulation	QPSK (TDMA). QPSK, 16-QAM (CDMA)
FEC	Red Solomon, convolutional

Table 2.5: Features of SRI-F

Characteristic	**Value**
Based on	IMT-2000 CDMA DS
Standard	ETSI S-UMTS family G (TS 101 851)
Multiple access	DS-CDMA
Duplex method	FDD
Bit rates	Voice (2.4 - 12.2 kbit/s). data (1.2 - 384 kbit/s)
Constellation	Any (LEO, MEO, GEO, HEO)
Satellite	7 beams or 30 beams (extended multi-beam)
Terminal features	Hand-held, portable, vehicular, transportable (all 500 km/h) and aeronautical (5000 km/h)
Modulation	OC-QPSK (orthogonal complex). QPSK
FEC	Convolutional and turbo coding
Observation	Harmonized result of ancient SRI-C and SRI-G, with optional A and C modes
Others	Intermediate Module Repeaters (IMRs) provide coverage continuity in shadowed areas. Deep paging service. Multicasting

Table 2.6: Features of SRI-G

Characteristic	**Value**
Name on	GMR-1 3G
Standard	ETSI GMR1- 3G (TS 101 376) Adaptation of EDGE to the satellite scenario
Multiple access	↓TDM. ↑TDMA
Duplex method	FDD
Bit rates	1.2 - 592 kbit/s. Voice, fax, data, SMS...
Constellation	Any (LEO, MEO, GEO, HEO)
Terminal features	Hand-held, PDA, vehicular, portable, fixed, maritime, aeronautical
Modulation	32-APSK, 16-APSK. $\pi/2$-BPSK, $\pi/4$-QPSK, Dual chirp
FEC	LDPC, CRC, Extended Golay code, Red Solomon, Turbo code, convolutional
Others	Efficient multicast. High penetration alerting. Dynamic link adaptation (modulation-code rate adaptation).

Table 2.7: Features of SRI-H

Chapter 3

Family SL of S-UMTS standard

The ETSI has a Technical Specification, still in a draft stage, that specifies the family SL satellite radio interface of the satellite component of UMTS. It is the ETSI TS 102 744 [11] which develops the SRI-E of the ITU-R Recommendation M.1850 presented briefly in Table 2.4 of the previous chapter. The version of the technical specification is v.0.0.9 of October 2012. In this work we evaluate new link adaptation techniques applied to Mobile Satellite Channels using this standard to test the algorithms. For this reason this satellite radio interface will be explained in detail. This section is a summary of the aforementioned technical specification and all information has been obtained from it, [11].

First of all, before explaining the satellite radio interface of this S-UMTS family, let's make a brief introduction to the main elements and the network architecture of a S-UMTS system. This can be divided into three different segments: a space segment, a user segment and a ground segment [12].

The space segment is made of one or several GEO satellites and some elements in the Earth as the Tracking, Control and Ranging (TCR) stations and the Satellite Control Centre (SCC).

The user segment comprises the User Equipments (UE) also named Mobile Earth Stations (MES). An UE is an entity capable of accessing a set of IMT-2000 satellite services. This entity may be stationary or in motion within the IMT-2000 service area while accessing IMT-2000 satellite services and may simultaneously serve one or more users which may also have several simultaneous connections with the network [10].

And lastly, the ground segment includes the gateways (GW) or Fixed Earth Stations (FES) and the Network Control Centre (NCC) which coordinates the use of satellite resources among all gateways. The gateway is composed of the Radio Network Controller (RNC) and the Node-B. This last entity performs mainly RF functions and it is located within the gateway in the case of transparent satellite payloads or within the satellite, when this is of regenerative type. On the other hand, the RNC interfaces with the core network and realises tasks of paramount importance as manage radio resources, channel allocation, admission control and handover control [13]. Figure 3.1, taken from [13], shows some of the previously cited elements.

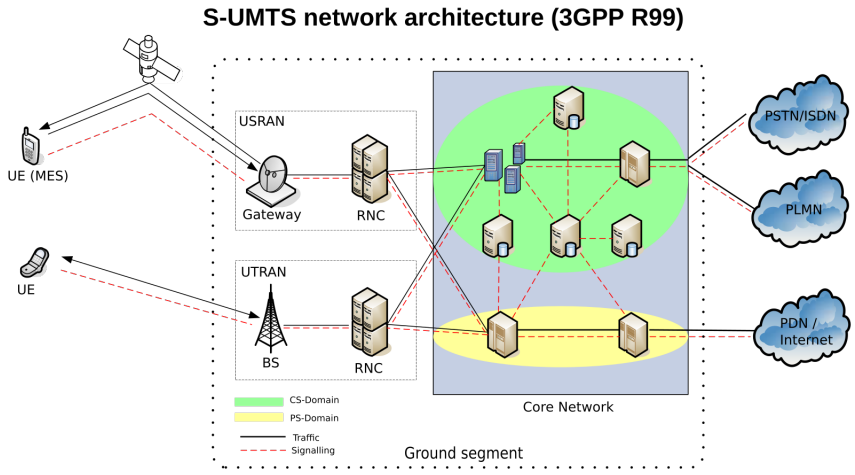

Figure 3.1: S-UMTS network architecture
Source: Thesis Radio Resource management for Satellite UMTS, Kai XU

3.1 Radio interface layering

The satellite radio interface is divided in two group of layers: the Non-Access Stratum (NAS) and the Access Stratum (AS). On the one hand, the Non-Access Stratum includes entities and protocols that are independent of the radio access technology, on the user plane they include protocols generating the data streams to be transported by lower layers and, on the control plane, it manages the set up, maintenance and closure of the connections and sessions. This layer is very similar to its equivalent in the terrestrial UMTS. On the other hand, the main differences between terrestrial and satellite component are in the layers below that, the Access Stratum. The Access Stratum provides a set of services that support the entities residing in the Non-Access Stratum and is made up of four different communication layers, as can be seen in Figure 3.2:

- Adaptation Layer (AL),
- Bearer Connection Layer (BCn),
- Bearer Control Layer (BCt) and
- Physical Layer (L1).

Each one of this layers communicates with its peer in the other extreme, for example, the Bearer Connection Layer of the User Equipment (UE) establishes a communication with its peer, the Bearer Connection Layer of the Radio Network Controller (RNC). They also communicate with the layer above and the layer below sending primitives through a Service Access Point (SAP). For example, when the Adaptation Layer receives the command to create a new connection, it sends a message (a primitive with some input parameters) to the Bearer Connection Layer in order to create in that layer the necessary structures to handle the new connection. The BCn also communicates with the Adaptation Layer in order to inform if the task ordered was successfully realized or not.

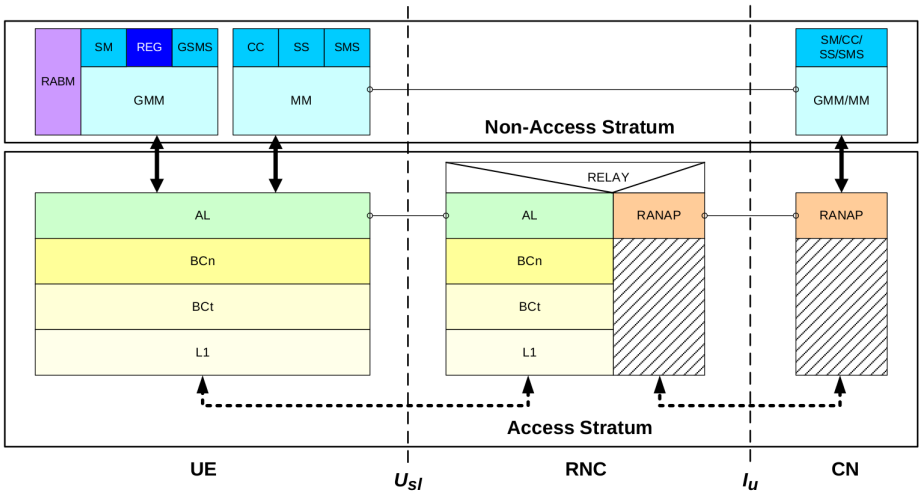

Figure 3.2: Control plane Protocol Stack Layering*Source: ETSI TS 102 744-1-3 Fig. 4.1*

The communication among the different layers is possible by means of a set of protocols that specify the format of the messages and how they are interchanged. The messages are encapsulated in a basic unit called Protocol Data Unit (PDU). The PDUs can carry data of the users as well as control messages, the Signalling Data Units (SDUs), used for the purpose of establishing, maintaining and termination a connection. The interfaces between two contiguous layers are the Services Access Points (SAPs), it is via the SAPs how a layer sends PDUs to a contiguous one.

The encapsulation of PDUs and SDUs is shown in Figure 3.3 where it can be seen how some portion of the user data goes trough the different layers and finally it is allocated in a frame of the physical layer. In first place the adaptation layer, named PDCP (Packet Data Convergence Protocol) in the case of a packet switched connection, builds a segment with part of the user data and sends it to the Bearer Connection Layer. This layer ciphers the data and builds a PDU, a BCn PDU, adding a proper header to the user data. Next, it sends this BCn PDU to the below layer, the Bearer Control Layer. Here the BCnPDU is encapsulated in a BCt PDU along with the control messages of the Signalling Data Units (SDUs), the BCt PDU header and a CRC used to check the integrity of the BCt PDU in the other extreme. Finally, several BCt PDUs are allocated in a frame which is transmitted in the forward or return link.

Regarding the user plane, the protocol stack of the Packet Switched Domain (Figure 3.4) is different from the protocol stack of the Circuit Switched Domain (Figure 3.5). The main differences between them are in the Non-Access Stratum and in the Adaptive Layer.

3.2 Adaptation Layer operation

This layer,equivalent the Radio Resource Control (RRC) layer of T-UMTS, performs the following functions [11]:

- Registration management: spot beam selection, registration and deregistration...
- GMM (GPRS Mobility Mangagement) Handling

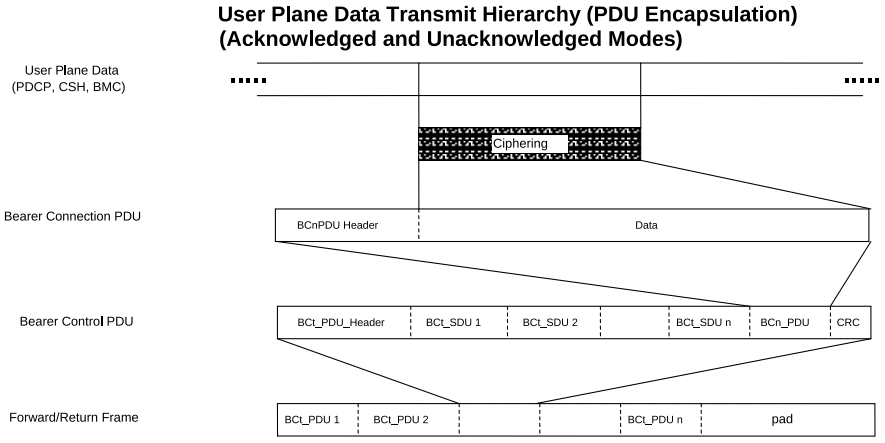

Figure 3.3: User plane Data Transmit Hierarchy (PDU Encapsulation)
Source: ETSI TS 102 744-1-3 Fig. 4.5

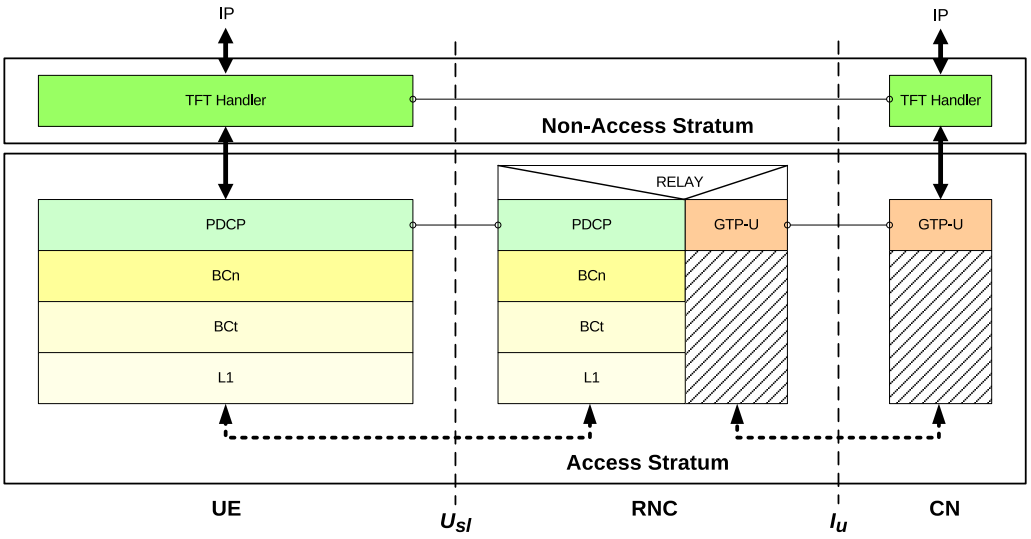

Figure 3.4: Packet Switched User Plane Protocol Stack Layering
Source: ETSI TS 102 744-1-3 Fig. 4.2

- MM (Mobility Mangagement) Handling to the Circuit Switched Domain

- Radio Bearer Control. This function is more related with the present work. The Adaptation Layer handles the signalling related to setup, modification and release of radio bearers (it requests lower layers to create a new connection, to change its parameters or to destroy it). It also does ciphering and notifies NAS entities of resource assignments.

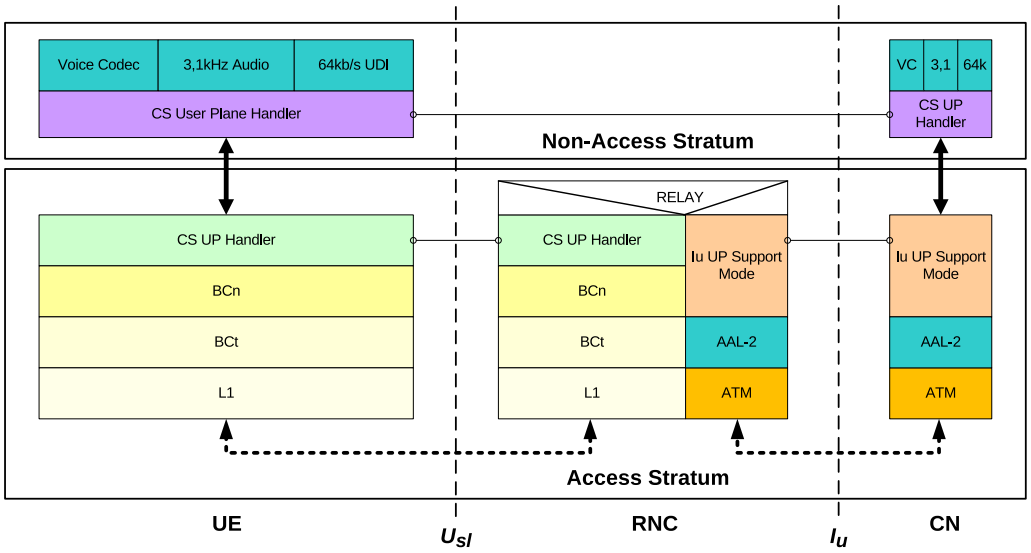

Figure 3.5: Circuit Switched User Plane Protocol Stack Layering
Source: ETSI TS 102 744-1-3 Fig. 4.3

3.3 Bearer Connection Layer

3.3.1 Introduction

The Bearer Connection Layer, BCn, performs similar functions to the Radio Link Control (RLC) layer of T-UMTS, provides a number of different data transport services to upper layers. Its main functions are:

- Buffering and flow control of information
- Quality of Service (QoS) policing
- Segmentation and reassembly of information
- Automatic Repeat Request (ARQ) for Acknowledge Mode connections
- Ciphering

3.3.2 Buffering and flow control

The BCn layer includes an input buffer for receiving the Protocol Data Units (PDUs) of the layer above (Adaptation Layer). When this buffer is reaching its maximum size it performs flow control functions notifying layer above of this situation. Also, each PDU in the buffer has its own maximum lifetime, if it is not transmitted before its discard time the PDU is thrown since it may be retransmitted by higher layers. This parameter is specified in the Quality of Service parameters during the establishment of each connection.

3.3.3 QoS policing

When the Adaptation Layer requests the creation of a connection to the BCn layer it specifies the QoS parameters, then BCn layer transfers the query to Bearer Control (BCt) layer and if there are bearers to satisfy that request both layers prepare themselves to transmit data within that connection. The set of QoS parameters contain:

- Rate Parameters: Mean Rate and Peak Rate;
- Delay Parameters: Target Latency and Discard Latency; and
- Connection Type and Priority.

Also, the BCn layer is responsible for guaranteeing that the traffic generated by the connections fits the requested QoS specified during the establishment, otherwise, if there is not any available resources in the network, it can discard some data.

3.3.4 Segmentation and Reassembly

Another function the BCn performs is the segmentation and reassembly of PDUs. The length of PDUs sent by Adaptation Layer is usually bigger than length of the data blocks within the frames of the shared access bearers. Therefore, the BCn layer should split the large Adaptation Layer PDUs into smaller BCn PDUs and number the segments in order to, in the receiver side, reconstruct correctly the above layer PDU putting in order the BCn segments.

3.3.5 Ciphering

Ciphering is another task of the BCn layer. Depending on the transmission mode (there are three different transmission modes) the ciphering and de-ciphering is realised in this layer or in the Bearer Control Layer. In the Acknowledged Mode and in the Unacknowledged Mode the ciphering is done with the standard UMTS KASUMI ciphering algorithm, named f8, with some minor changes due to the adaptation of that algorithm from T-UMTS to S-UMTS [11]-3-4. Figure 3.6 represent the process of ciphering and de-ciphering. Conversely, for Transparent Mode operation ciphering is carried out in the Bearer Control layer.

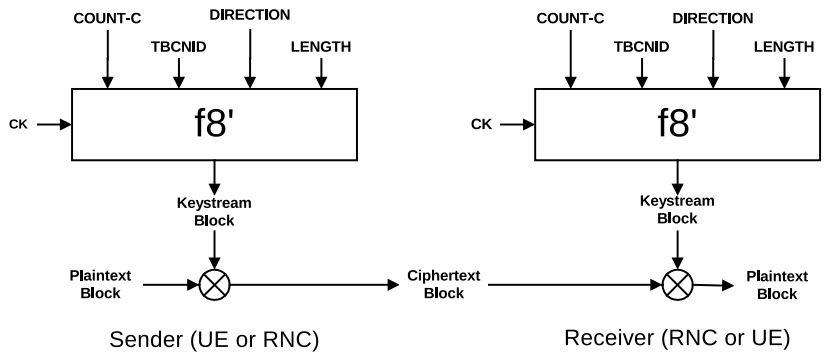

Figure 3.6: Ciphering of data transmitted over satellite radio interface.
(Source: ETSI TS 102 744-3-4 Fig. 5.10)

3.3.6 Transport modes

As already mentioned in the previous paragraph, the BCn layer provides three different types of data transport modes [11]-3-4 to the upper layers:

- Acknowledged Mode (AM)
- Transparent Mode (TM)
- Unacknowledged (Numbered Frame) Mode (UM)

The **Acknowledged Mode** is employed when a reliable deliverable of messages is required, e.g. for packet data and signalling connections. The reliability is guaranteed using an ARQ mechanism based on the standard HDLC (High Level Data Link Control). This mode of operation also guarantees the in-order delivery of packets and provide ciphering of the data. On the other hand, the **Transparent Mode** is more oriented to support circuit switched traffic. It is no added any overhead and no ciphering is perform at this layer. Finally, **Unacknowledged Mode** provides in-sequence delivery, segmentation and reassembly, and ciphering of data but packet delivery is not guaranteed due to the non use of ARQ.

3.3.7 General architecture

Through this section it is described the entities resident in the BCn layer, their main functions and interfaces with upper and lower layers. In first place let us focus our attention in the control plane of the BCn layer, represented in Figure 3.7. One of the main elements, existing either in the User Equipment (UE) as in the Radio Network Controller (RNC), is the Bearer Connection Manager. This entity communicates with the Adaptation Layer via CBCn-SAP and receives the command of creating a connection with a specific QoS or remove it. It is also responsible for monitoring the queue status of the data handlers and send it to the Bearer Control Layer. The other elements of the BCn layer are instances of different data handlers. On the one hand there always exists an AM_DH for the UE Specific Signalling connection and a COM_DH for managing the Common Signalling connection. Furthermore, in the user plane (see Figure 3.8) the Bearer Connection Manager creates an instance of a data handler for each new connection of a type depending on the class of connection: AM_DH for Acknowledged Mode connections, TM_DH for Transparent Mode and UM_DH for Unacknowledged Mode (or Numbered Frame).

Regarding the interfaces, each data handler has its own Service Access Point (SAP) to connect with Adaptation Layer and receive and transmit data. Also, all the TM_DH of a single user employ a common BCt-UCDATA-SAP to communicate with the Bearer Control Layer and all NUM_DH and AM_DH of a single user employ a common BCt-DATA-SAP. Now some primitives of the SAPs are described in order to exemplify the operation of this layer.

The primitives of the CBCn-SAP serve for the exchange of control messages between the Bearer Connection Layer and the Adaptation Layer. The main primitives are:

- **CBCn_CREATE_REQ** is used by the Adaptation Layer to request the BCn Manger to create a new instance of a data handler and its associated data SAP for a new connection. It receives as input parameters the Bearer Connection ID, BCnID,

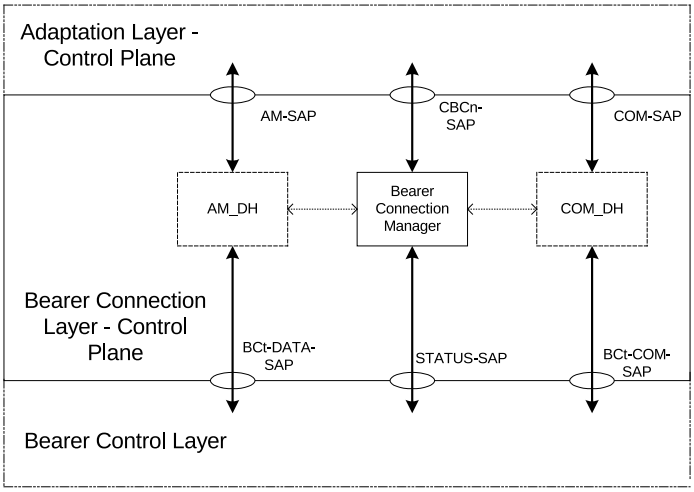

Figure 3.7: Bearer Connection Layer - Control plane
(Source: ETSI TS 102 744-3-4 Fig. 4.2)

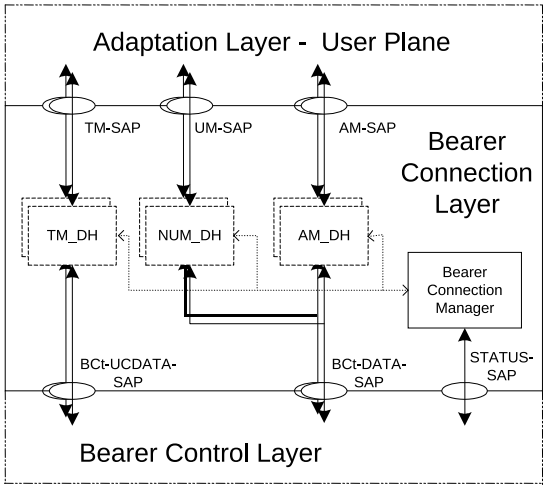

Figure 3.8: Bearer Connection Layer - User plane
(Source: ETSI TS 102 744-3-4 Fig. 4.3)

identifying the new connection, the type of connection and the QoS parameter list, among others.

- **CBCn_CREATE_CNF**. After the successful creation of the data handler and SAP the BCn responds to the Adaptation Layer with this primitive.
- **CBCn_CREAT_REJ** used when the operation of create the new connection fails.
- **CBCn_MODIFY_REQ, CBCn_MODIFY_CNF and CBCn_MODIFY_REJ** are used when some modification of the characteristics of an existing connection is requested.

With respect to the primitives of the user planes interfaces here only are described the primitives of the Acknowledged Mode (AM)-SAP because the others are similar to these

ones. The primitives of AM-SAP are the following:

- **BCn_AM_DATA_REQ** used by the higher layer to request the transmission of a data PDU. It receives as input parameters the data packet, the MUI, Message Unit ID that identifies the higher layer PDU, and the BCnID, among others.
- **BCn_AM_DATA_IND** used by the data handler to deliver a PDU to the higher layer entity
- **BCn_AM_DATA_CNF** used by the data handler to confirm to the higher layer entity that a data PDU has been successfully transmitted or to inform that a data PDU has been discarded.

3.3.8 Acknowledged Mode Operation (ARQ)

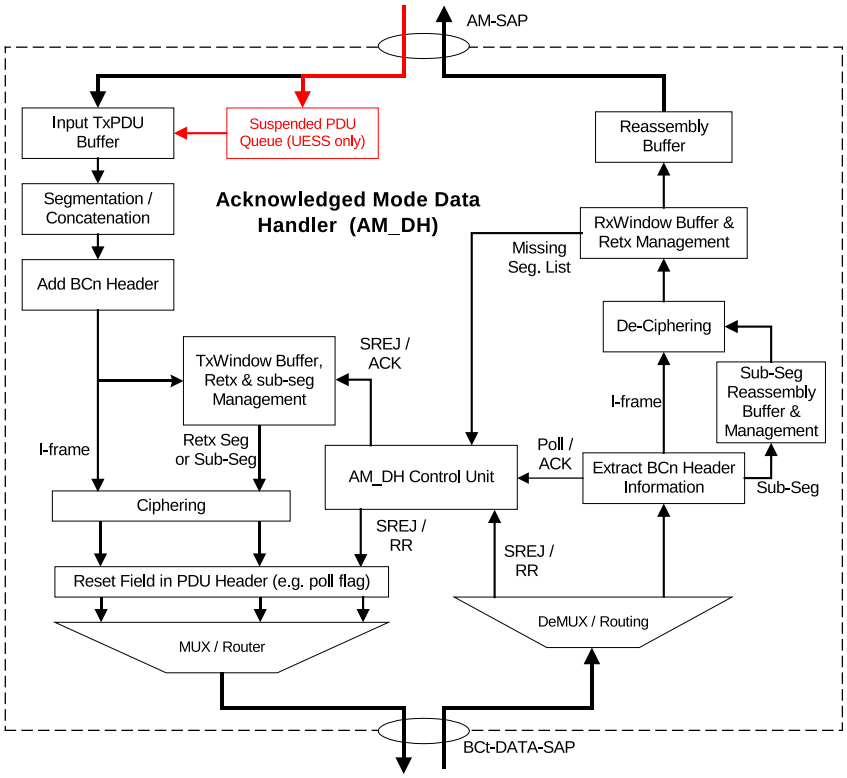

Figure 3.9: Model of an Acknowledged Mode Data Handler
(Source: ETSI TS 102 744-3-4 Fig. 5.1)

The Acknowledged Mode Data Handler, whose block diagram is represented in Figure 3.9, is composed of three main subsystems: a transmit path processing unit, a receive path processing unit and a control unit.

At the input of the transmit path there is a FIFO (First In First Out) queue, the TxPDU buffer, where the data handler stores all incoming data awaiting transmission as well as PDU's target and discard time. When the BCt layer informs of capacity for transmission, the correct amount of data is retrieved from the TxPDU and a header added to form a BCn

PDU. Its data part is ciphered and a copy is stored in the TxWindow awaiting acknowledgement from the receiving end and only is removed from there when an acknowledgement has been received or its discard time has expired. Before sending the BCnPDU, the control unit might update the header fields according to the ARQ mechanism.

Regarding the receive path processing, when a BCn PDU is received the header information or all PDU if it is a control message is sent to the control unit. Then, once all the subsegments of a PDU are received (if it was segmented), the original segment is reconstructed, de-ciphered and forwarded to the layer above.

Lastly, the AM_DH Control unit provides an interface between the transmit an receive path processing units, controls all the other units according to received control messages and header information and manages all the timers.

With respect to the ARQ mechanism it is based on the standard HDLC (High Level Data Link Control) of the International Organization for Standardization (ISO 13239). HDLC is a data link control protocol and operates in the layer 2 (Data Link Layer) of the Open Systems Interface (OSI) (see Figure 3.10). Its is employed the Asynchronous Balanced Mode, where both nodes of the point-to-point communication have equal and complementary responsibility compared to each other (there is not a master-slave behaviour).

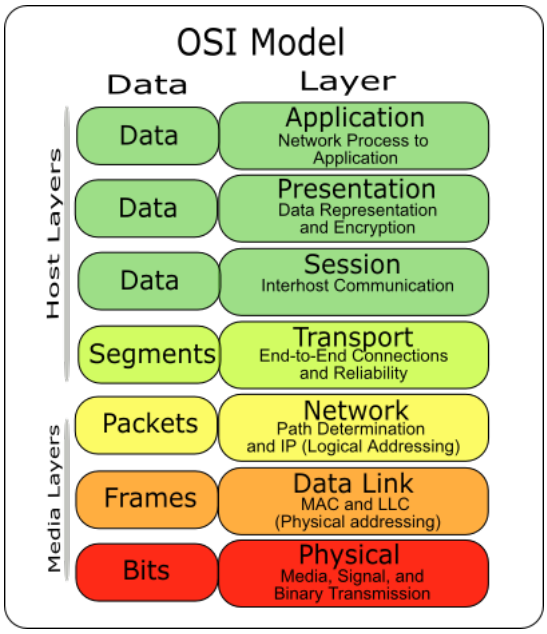

Figure 3.10: Layers of the Open Systems Interface (OSI) model
(By Original created by JB Hewitt (Johnblade) at en.wikipedia (Own work) [GFDL or CC-BY-SA-3.0], via Wikimedia Commons)

The function of the ARQ mechanism is to ensure complete and ordered transmission of data segments. For achieving that purpose several techniques are used. On the one hand data segments are numbered using a unique sequence number, ns, in a modulo 1024 space and there is a window of operation of maximum size 511 (1024/2-1). Its size is configurable depending on QoS parameters since its value has a direct impact in the maximum achievable throughput. Also missing segments detected by the receiver are added to a list (Selective Reject, SREJ, list) in order to ask to the other extreme their delivery.

Moreover, there are four different type of frames using in the BCn layer operation. Their structure is shown in Figure 3.11 and its function summed up here:

- **I-Frame** (Information Frame) carries actual user data, either new or retransmission. It can correspond with a whole Adaptation Layer (AL) PDU (Single Segment Message) or be a segment of an AL PDU (if it is the last segment the End-of-Message flag must be activated). In the header also contains the field number of sequence ns and the expected receive sequence number nr, that indicates the next-in-order segment that the sender is expecting. The field nr acknowledges implicitly up to and including $nr - 1$ segment. The Poll flag field pf is set to 1 if the sender wishes to obtain an acknowledgement of sent segments in the form of a Poll Response.
- **RR-frame** (Receive Ready Frame) is a supervisory frame used to carry either a Poll (pf set to 1) or a Poll response (pf set to 0). They ensure that acknowledgements are sent at regular intervals.
- **SREJ-Frame** (Selective Reject - Frame). This is other supervisory frame employed to carry an ordered list of missing segment sequence numbers.
- **Sub-Segment Frame**. This frame it is used to carry part of a retransmitted I-frame when the capacity offered by the BCt layer is not enough to transport the whole I-frame. Each segment can be split up into a maximum of 16 sub-segments. Apart from the fields ns, nr and pf, also present in the I-Frames, they have the field $ssegn$ indicating the number of sub-segment and the flag eos activated if the frame carries the last sub-segment of a segment.

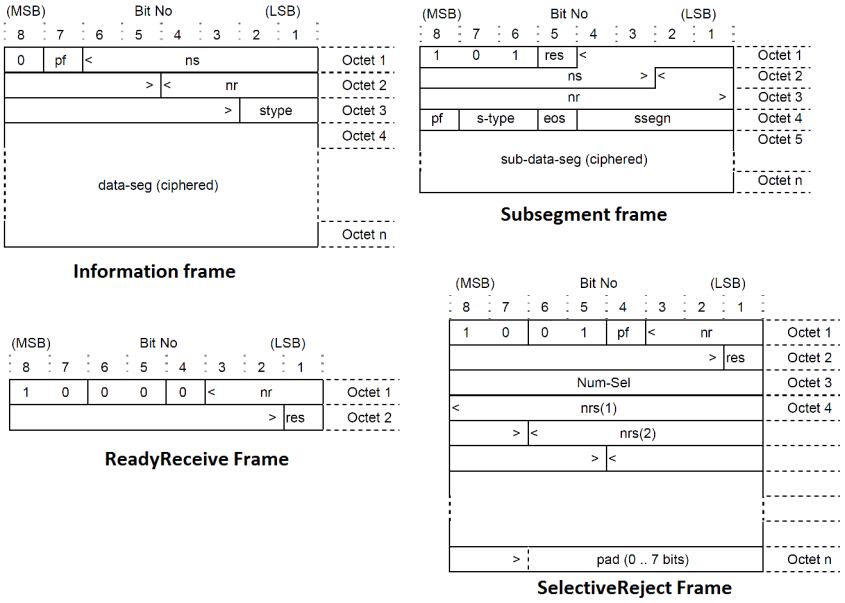

Figure 3.11: Structure of the four different frames
(Source: ETSI TS 102 744-3-3 Fig. 5.2, 5.4, 5.5, 5.7)

Other aspect of the operation of the Acknowledged Mode is the existence of three different timers to control the connection. The ACK timer controls the poll requests and responses because the system is restricted to sending one Poll at a time. Another one, the MaxIdle Timer, is used to release the resources if the connection is inactive and lastly, the

ConnFailure Timer detects the failure of the other extreme.

The ARQ mechanism is presented here briefly because it is out of the scope of this project, but if the reader is interested can read the section 5.3 of Part 3, Subpart 4 of the standard [11]. Finally, I would like to highlight that although in our link adaptation algorithms we consider that a feedback with an ACK/NAK for each transmitted frame is received continuously although with a delay equivalent to the Round-Trip-Time. But in practice this does not occur, since that a BCn frame can carry ACK/NAK of several frames and also it can happen that during a short period of time no acknowledgements are received. However this does not affect to the performance of the link adaptation algorithms, which in practice, they are executed when a feedback is received.

3.3.9 Transparent Mode Operation

After presenting the Acknowledge Mode Data Handler in the previous section, now it is introduced the Transparent Mode Data Handler. As can be seen in Figure 3.12 is very simple because it only performs buffering and, in some cases, segmentation. Contrary to others modes, ciphering in Transparent Mode is carried out in the Bearer Control Layer.

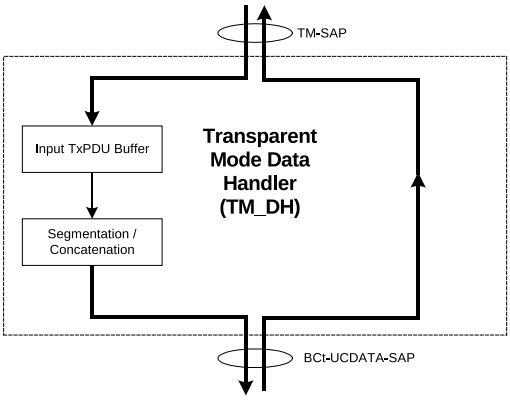

Figure 3.12: Model of an Transparent Mode Data Handler
(Source: ETSI TS 102 744-3-4 Fig. 5.7)

3.3.10 Un-Acknowledged Mode Operation

Finally, Figure 3.13 depicts a scheme of the Un-Acknowledged Mode (Numbered Frame) Data Handler. In this mode no ARQ is needed, but segmentation, ordered delivery and ciphering are required. The operation of this mode is clear just looking at the figure.

3.4 Bearer Control Layer

Below the Bearer Connection Layer, introduced in the previous subsection, is located the Bearer Control Layer. Its function is to provide a mechanism for transporting data from

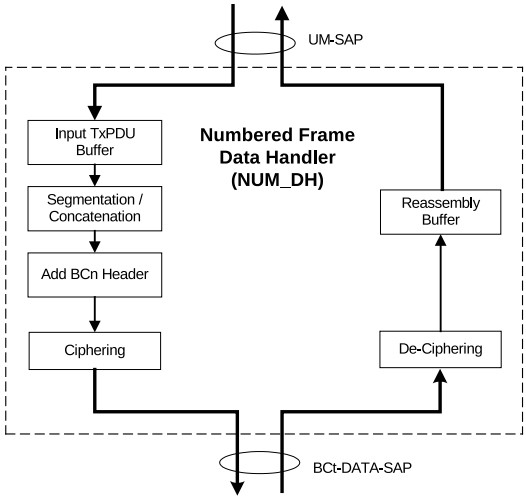

Figure 3.13: Model of a Numbered Frame Mode Data Handler
(Source: ETSI TS 102 744-3-4 Fig. 5.8)

various Bearer Connections over established physical bearers, it controls the access to the physical layer (channel resource) for each of the connections which are established.

The Bearer Control Layer is responsible for aspects related with the physical layer as:

- selection of the appropriate Primary Shared Access Bearer for initial access to the RNC
- control of initial timing offeset due to UE position
- delta timing corrections due to UE or satellite movement
- power and/or coding rate adjustments (link adaptation) of UE transmissions. This be explained in detail due to the fact that link adaptation is the centre of the project.
- coding rate adjustments of transmission from RNC (Radio Network Controller).

Other tasks realized by this layer include the following:

- admission control
- broadcast of system information
- scheduling resources in forward and return directions
- packing and unpacking of packets into frames
- ciphering in Transparent Mode
- support for sleep mode operation
- traffic monitoring and trend analysis
- requesting and releasing physical and logical resources.

3.4.1 General architecture

Through this subsection the main elements of the Bearer Control Layer are presented as well as their functions and their interfaces with the other layers.

The Bearer Control Layer in the RNC side consists of number of Bearer Control Process, each one typically controlling all the channels within a spot beam and identified by a BCt-ID. In the UE side there is only one Bearer Control Process. Their architecture is shown in Figure 3.14 for the RNC side and in Figure 3.15 for the UE side.

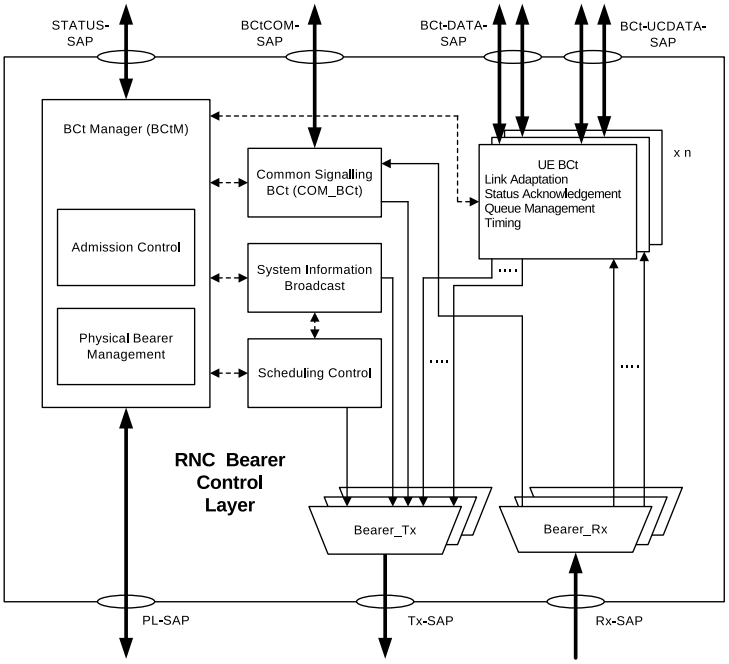

Figure 3.14: Bearer Control Layer - RNC side
(Source: ETSI TS 102 744-3-2 Fig. 4.2)

Hereafter the individual functional blocks of the Bearer Control Process are explained. The **Bearer Control Manager (BCtM)** provides the management interface to the Bearer Connection Layer (through the STATUS-SAP) and to the Physical Layer (through the PL-SAP). When a UE within the spot beam the BCtM manages request the first connection, it receives from the Connection Layer the command to create a bearer control unit for that UE (UE_BCt) as well as its associated data SAP. In Figure 3.14 is shown how in the BCt Process of the RNC there is one UE BCt for each UE with active connections, while in the UE side there is only one UE BCt.

The BCt also receives the queue status for each bearer connection and passes that information to the **Scheduling Control Unit**. This, in the RNC side, using that information and the QoS parameters of each connection, creates a schedule that allocates resources in forward and return directions to each connection of UEs. Then the BCtM executes the schedule planned by this unit.

The **System Information Broadcast Unit** on the RNC side generates the Broadcast BCt Protocol Data Units (PDUs). These contain the BulletinBoard, which is transmitted

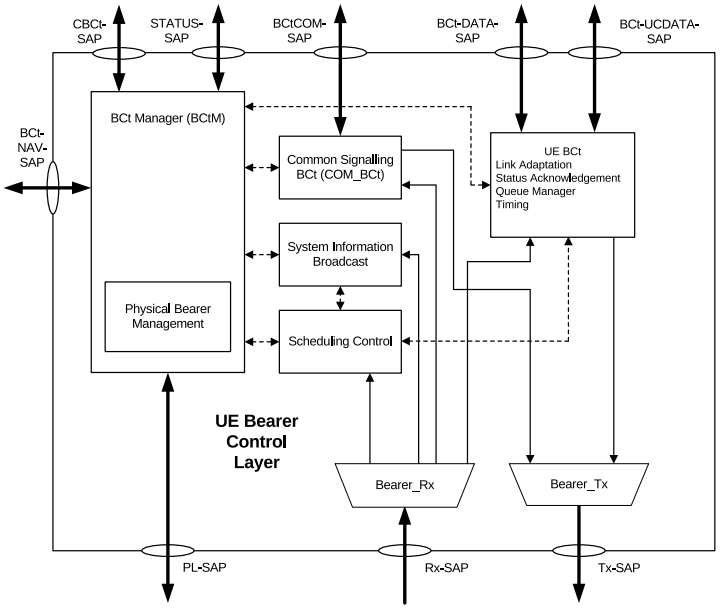

Figure 3.15: Bearer Control Layer - UE side
(Source: ETSI TS 102 744-3-2 Fig. 4.3)

periodically and carries basic network parameters, System Information transferred as a list of Attribute Value Pair (AVP) used to carry other parameters and Return Schedules, which describe the distribution of the return channel capacity. On the UE side this unit just receives and decodes the broadcast BCt PDUs.

Other elements inside the Bearer Control Process are the Bearer Transmit and Receive Buffers (Bearer_Tx and Bearer_Rx). There is one Buffer per transmit or receive bearer. On the one hand, the **Bearer Transmit Buffer** collects all the BCt PDUs and provides the Physical layer with the correct amount of data, including padding, to fill the FEC-blocks of the frames. On the other hand, the **Bearer Receive Buffer** collects from the Physical Layer all BCt PDUs decoded within a FEC block and forwards to their corresponding entity.

Lastly, the **UE Bearer Control Unit** (UE_BCt) is responsible for the UE-Specific Signalling and all data connections associated with a particular UE. In its architecture, showed in Figure 3.16, can be seen that there is a number of data SAPs, one for each bearer connection associated with the UE, and that only ciphering is performed in this layer for Transparent Mode connections (BCt-UCDATA-SAP). This unit also does the specific UE link adaptation to optimize the data rate of the system. This task will be treated later.

Regarding the interfaces to upper layer, here are presented some primitives and its parameters of the STATUS-SAP and BCt-DATA-SAP. The STATUS-SAP acts as the interface in the control plane between the Connection and Control layer, its main primitives are:

- **BCt_CREATE_REQ, BCt_CREATE_CNF, BCt_CREATE_REJ** used to request the establishment of a new connection (it triggers the creation of a UE_BCt), to confirm its successful establishment and to inform about the fail of the operation, respectively. If the connection was create successfully, the BCt layer assigns it a unique ID within the Bearer Control Process: the tBCnID (translated

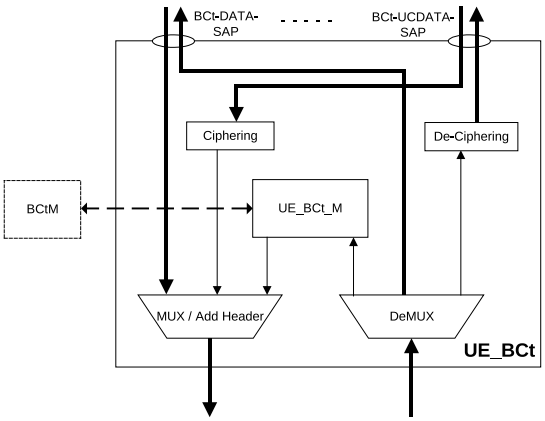

Figure 3.16: UE Bearer Control Unit *(Source: ETSI TS 102 744-3-2 Fig. 4.5)*

Bearer Connection ID).

- **BCt_MODIFY_REQ, BCt_MODIFY_CNF, BCt_MODIFY_REJ** are primitives related with the modification of some of the QoS parameters of the connection.
- **BCt_DATASTATUS_REQ** is used by the BCn Layer to send the last information about the queue status for each bearer connection. These data are then used by the Schedule Control Unit.

In the user plane the interface BCt-DATA-SAP serves for data interchange between BCn layer and BCt layer. This SAP has only three primitives:

- **BCt_TxDATA_REQ** is used by the data handler of the Bearer Connection Layer to send a BCnPDU.
- **BCt_TxDATA_IND** indicates to the Connection Layer the availability for transmit a certain quantity of data for a specific connection in the current frame.
- **BCt_RxDATA_IND** is employed in the receiver side to deliver a BCnPDU to the Connection Layer.

With regard to lower layer interfaces there exists the PL-SAP, Tx-SAP and Rx-SAP. All of them are implementation-dependent and are not detailed in the technical specification. The only information provided in the Technical Specification is that via PL-SAP the BCtM initializes and configures the physical layer channels with the correct parameters and receives via PL-SAP any timing error and C/N_0 measurements from the physical layer.

3.4.2 Data Transfer Operations

The BCtPDUs interchanged between the RNC and the UE can contain only a BCnPDU and this one only can contain one segment of Adaptive Layer data. In general the maximum size of a BCtPDU is 256 bytes although this length may also be limited by the maximum payload size of the frames.

In the forward direction (from RNC to UE), the physical bearer operates in Time Division

Multiplex (TDM) mode: the bearer is divided in frames, each one of 80 ms. On the other hand each frame is made up of several FEC blocks, having each one an integer number of BCtPDUs and filling with zeros the unused space. Each FEC block of the frame can have a different code rate, but the code rate of the first FEC block of each frame (defined in the Unique Word) should allow that the UE with worst channel conditions be able to decode the it due to in it there is broadcast information.

In the return direction (from UE to RNC), each bearer is contained within a 200 kHz wide sub-band. Moreover, each sub-band is divided in time and in frequency in slots. The slots can be allocated to a specific user or be contention slots which all the users can employ but with the risk of collision with other users and loss of information. Each slot can last 5 or 20 ms and can occupy 21, 42, 84 or 189 kHz bandwidth. Periodically, in the forward link is transmitted a special Signalling Data Unit (SDU) called *ReturnSchedule* that describes the slots allocation during a period of time in the return bearers associated with it. In Figure 3.17 is shown an example of return schedule where each 40 ms a connection transmits data of a circuit switched ISDN (Integrated Services Digital Network) connection within a 100 kHz subband.

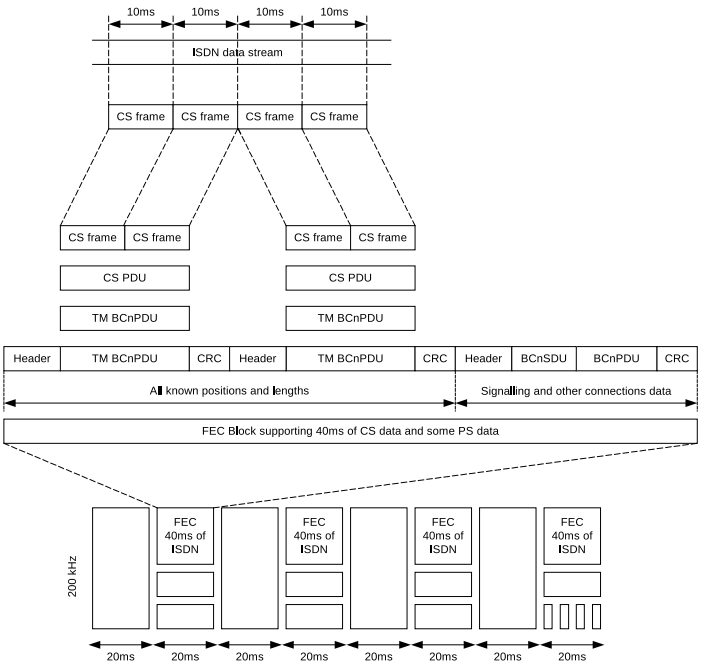

Figure 3.17: Example of return schedule where ISDN data are transmitted over BCtPDUs *(Source: ETSI TS 102 744-3-2 Fig. 6.2)*

3.4.3 Link Adaptation Operations

The objective of the link adaptation is to optimize the efficiency of the satellite radio interface increasing its throughput while keeping the Packet Error Rate (PER) at a low level (e.g. 10^{-3} for Packet Switched). The link adaptation algorithm tracks long-term channel variations and adjust the coding rate of the FEC blocks accordingly while discrete events and short-term fading are covered by the fading margin in the link budget.

Firstly, the return link operation will be explained. The Return Schedule planned by the RNC assigns a bearer type (characterised by a specific modulation and symbol rate) to the UEs, but the particular bearer subtype or coding rate is calculated by the link adaptation algorithm. This algorithm involves both the RNC and the UE.

On the one hand, the Physical Layer of the RNC measures the C/N_0 of all the received bursts from the UE and the BCt layer corrects the measurements using the information about the EIRP used by the UE. After that, the corrected measurements are averaged within 12 x 80 ms frames to obtain a more accurate value that is then provided as input to a 16-tap FIR filter. Then, a mechanism for testing the convergence of the estimated C/N_0 is employed and if divergence is detected the link adaptation algorithm returns the initial values. To the apparent link margin obtained from C/N_0, a target link margin, configurable and dependent of UE class, is subtracted and a reference level is calculated. This reference level indicates which code rate (bearer subtype) of the bearer type could be used for transmitting at the maximum (nominal) EIRP guaranteeing the QoS of the connection (PER under a threshold).

Furthermore, the link adaptation has two different modes of operation. In Backoff mode = 0 the code rate is fixed and signalled by the reference level, and the backoff value is used to control the EIRP. On the other hand, in Backoff mode = 1 the backoff value express a window below the reference level where the UE can trade-off EIRP for coding rate. If the transmission queue is almost empty or the PDU to transmit fits in lower coding rate bearer subtype, the UE can decide transmit with a lower EIRP using that lower rate bearer subtype. In this way, the UE can save battery although the efficiency of the radio interface is reduced.

Figure 3.18 shows how this works. Each UE has stored its default bearer table as the Figure 3.18 table, indicating for each bearer subtype its data transport capabilities and what is the necessary C/N_0 needed for obtain a PER of 10^-3 in a AWGN (Additive White Gaussian Noise) channel with ideal modem. Changes to the cited table are broadcasted by the RNC in the *BearerTables* and *BearerTableUpdate* SDUs. Each row of the table is a different bearer, the link adaptation algorithm has to choose which coding rate (column) uses and the EIRP of the transmission. The reference level is signalled from the RNC and the UE can employ any of the coding rates within the backoff interval having each one associated a specific dB below nominal EIRP.

Hereafter the link adaptation in the forward link is explained. With the help of the pilot and UW (Unique Word) symbols the UE measures continuously the C/N_0 in the forward link. It averages the C/N_0 over a number of forward frames specified in the *SignalQualityMeasurementInterval* AVP received from the RNC and then reports it to the RNC using the *ReceivedSignalQuality* AVP. The number of frames used to average the measured C/N_0 is determined by the RCN depending on the UE Class, for example, an aeronautical class UE can have a lower value than a land mobile class and this lower than a land class. The minimum value is 8 frames (640 ms), the default value is 128 frames (10.2 s) and the maximum value corresponds to 156 frames (20.48 s).

Once received the averaged C/N_0 value in the RNC, it calculates the optimum coding rate for each UE after applying a target fading margin. A FEC block can contain BCtPDUs for a group of UEs and all these UEs must be able to decode that FEC block correctly. The RNC should taking this into account when electing the coding rate of the FEC blocks. The first FEC block, which carries broadcast SDUs, should be coded so that the least capable

Sub type	R5T1X								L3	L2		L1		R		H1
Octets									19	21		24		28		31
Avg Kbit/sec									30,4	33,6		38,4		44,8		49,6
Sub type	R5T2Q				L8		L7		L6	L5		L4		L3		L2
Octets					19		24		29	34		40		44		48
Avg Kbit/sec					30,4		38,4		46,4	54,4		64,0		70,4		76,8
Sub type	R5T2X												L3	L2		L1
Octets													44	46		54
Avg Kbit/sec													70,4	73,6		86,4
Sub type	R5T45Q										L8	L7		L6	L5	
Octets											51	57		68	78	
Avg Kbit/sec											81,6	91,2		108,8	124,8	
Sub type	R5T45X															
Octets																
Avg Kbit/sec																
Inc. implementation loss (This will be the actual value measured by the RAN).	C/No	48,0	48,5	49,0	49,5	50,0	50,5	51,0	51,5	52,0	52,5	53,0	53,5	54,0	54,5	55,0
Control Index	6 bit value	23	24	25	26	27	28	29	30	31	32	33	34	35	36	37

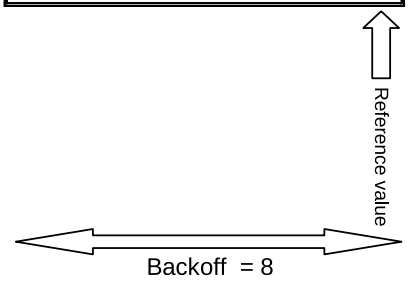

Figure 3.18: Illustration of Reference Level and Backoff
(Source: ETSI TS 102 744-3-2 Fig. 5.16)

UE can decode it. The coding rate of the first FEC block is indicated in the Unique Word of the frame and the coding rate of the rest of FEC blocks, when it is different, it is signalled using a *ForwardBearerCodeRate* AVP.

3.5 Physical Layer

One important concept to understand the technical specification of SL family of S-UMTS in general, and its physical layer operation in particular, is the shared access bearer. Bearers are physical bearers or carriers that support the transfer of data and, in this case, shared access bearers are bearers that support the transfer of data of multiple concurrent connections simultaneously. The method to distinguish the connection each packet belongs to is through its address field.

On the one hand, channels in the forward direction are allocated on a Time Division Multiplex (TDM) basis, dividing the time in slots of 80 ms. On the other hand, channels in the return direction are allocated on a Time Division Multiple Access (TDMA) basis, dividing each frequency channel in small time slots being used each one by a different user. In addition, resources in both directions are operated on Frequency Division Multiple

Access (FDMA).

With regard to the frequency bands assigned to systems employing this satellite radio interface, these are situated in L-band (region of the radio spectrum going from 1 GHz to 2 GHz). The downlink of the user link (forward direction) employs frequencies ranging from 1518 MHz to 1559 MHz. For its part, the uplink of the user link (return direction) covers frequencies from 1626.5 MHz to 1660.5 MHz and from 1668 MHz to 1675 MHz. Therefore in each direction there are 41 MHz, that are also divided into a set of 205 contiguous 200 kHz subbands.

The technical specification allows the use of wide number of different bearers that can provide data rates in the range of 4.5 kbit/s to 858 kbit/s in the forward link and in the range of 3.2 to 848 kbit/s in the return link. The physical layer offers a great flexibility since through different bearer types and subtypes it can change symbol rate (and hence bandwidth), modulation scheme and coding rate to adjust the data transmissions to the UE capabilities, mainly determined by its channels conditions (C/N_0 level) and its UE class (explained in a subsequent subsection).

3.5.1 Forward bearers

Bearer Type Identifier (Note)	Frame Duration	Symbol Rate	Modulation	Channel bandwidth	FEC Blocks per Frame
F80T0.25Q-1B	80 ms	0,25 x 33,6 ksym/s	QPSK	10,50 kHz	1
F80T1Q-1B	80 ms	1,0 x 33,6 ksym/s	QPSK	42,00 kHz	1
F80T1Q-4B	80 ms	1,0 x 33,6 ksym/s	QPSK	42,00 kHz	4
F80T1X-4B	80 ms	1,0 x 33,6 ksym/s	16-QAM	42,00 kHz	4
FR80T2.5X4/16-5B	80 ms	2,5 x 33,6 ksym/s	4-QAM/16-QAM	94,92 kHz	5
FR80T2.5X16-5B	80 ms	2,5 x 33,6 ksym/s	16-QAM	94,92 kHz	5
FR80T2.5X32-6B	80 ms	2,5 x 33,6 ksym/s	32-QAM	94,92 kHz	6
FR80T2.5X64-7B	80 ms	2,5 x 33,6 ksym/s	64-QAM	94,92 kHz	7
F80T4.5X-8B	80 ms	4,5 x 33,6 ksym/s	16-QAM	189,00 kHz	8
FR80T5X4/16-9B	80 ms	5,0 x 33,6 ksym/s	4-QAM/16-QAM	189,84 kHz	9
FR80T5X16-9B	80 ms	5,0 x 33,6 ksym/s	16-QAM	189,84 kHz	9
FR80T5X32-11B	80 ms	5,0 x 33,6 ksym/s	32-QAM	189,84 kHz	11
FR80T5X64-13B	80 ms	5,0 x 33,6 ksym/s	64-QAM	189,84 kHz	13
NOTE: The bearer type identifier notation used in the present document is defined in Annex A.					

Table 3.1: Overview of Forward Bearers Types
(Source: ETSI TS 102 744-2-1 Tab 5.1)

There are 13 types of forward bearers, all lasting 80 ms as can be seen in Table 3.1 where their modulation parameters are specified. The symbol rate can take the following values, indicated in the Bearer Type Identifier as TF, where F is the factor that multiplies the basic symbol rate of 33.6 ksymb/s. The five possible symbol rates are:

- 8.4 ksymb/s (T0.25)
- 33.6 ksymb/s (T1)
- 84.0 ksymb/s (T2.5)
- 151.2 ksymb/s (T4.5)
- 168.0 ksymb/s (T5)

In regard with the modulation scheme, it is chosen from a set of five options, listed here below along with the abbreviation employed in the Bearer Type Identifier signalled between

brackets:

- QPSK (Q or X4)
- 16-QAM (X16)
- 32-QAM (X32)
- 64-QAM (X64)
- dynamic modulation 4-QAM/16-QAM (X4/16): modulation can change from one FEC to other within the same frame.

Lastly, the last characteristic of th modulation is the channel filtering. It is used a root-raised-cosine (RRC) filter function for symbol shaping with a roll-off of 0.25 for all bearers, except for FR80T2.5 and FR80T5 which employ a 0.13 roll-off.

Now let us look inside the forward frames format. Firstly they are numbered using a 12 bit unsigned integer (0-4095) and frame number is included in a specific Signalling Data Unit (SDU). Forward frames can contain between 1 and 13 FEC blocks, being each one the output of the Turbo encoder used for channel coding. With respect with the internal structure of each FEC block, they consist of a sequence of integer number of higher layer Packet Data Units (PDUs), concretely BCtPDUs, with an optional padding with zeros at the end if it is required to fill in the FEC block as illustrated in Figure 3.19. This sequence of PDUs (a string of bits) is then scrambled before being encoded with the turbo code. It shoud be noticed that each FEC block can contain BCtPDUs of different connections of one or several UEs.

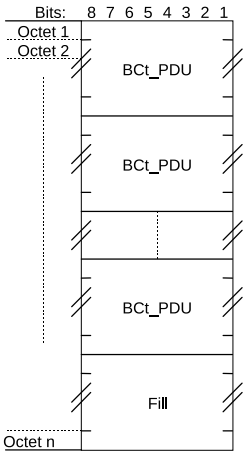

Figure 3.19: Forward FEC block structure
(Source: ETSI TS 102 744-2-1 Fig. 5.26)

Continuing with the frame structure, the bits of the FEC blocks are mapped to symbols of the chosen constellation and between each DS data symbols one pilot symbol (PS) is inserted, a predefined symbol of the most energetic symbols of the constellation. Pilot symbols assist channel estimation of E_s/N_0 and help carrier (frequency and phase) and clock synchronisation. Table 3.2 lists the number of pilot symbols per frame of each bearer and the number of FEC symbols between pilot symbol. And finally, all frames start with a special group of 40 symbols called Unique Word (UW). This symbols signal the level of codification of the first FEC block of the frame (L8, L7, L6, ..., L1, R, H1, H2, ... or H6).

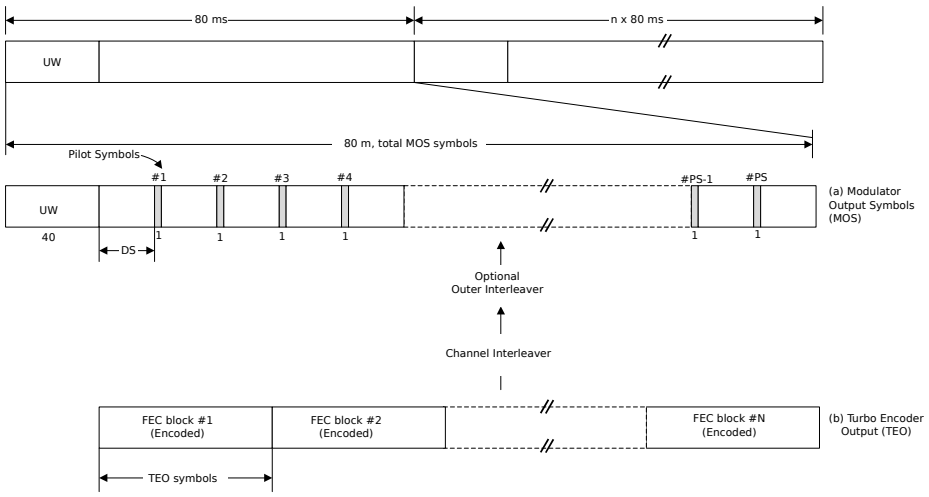

Figure 3.20: Generic Frame Format for Forward Channel
(Source: ETSI TS 102 744-2-1 Fig. 5.26)

Bearer Type Identifier (Note)	Slot Duration (ms)	Slot symbols	Start UW symbols	Pilot symbols	FEC symbols between pilot symbols	FEC symbols/ block	FEC Blocks per Frame	Total FEC symbols/ frame
F80T0.25Q-1B	80	672	40	88	6	544	1	544
F80T1Q-1B	80	2688	40	88	29	2560	1	2560
F80T1Q-4B	80	2688	40	88	29	640	4	2560
F80T1X-4B	80	2688	40	88	29	640	4	2560
FR80T2.5X4/16-5B	80	6720	40	90	73	1318	5	6590
FR80T2.5X16-5B	80	6720	40	90	73	1318	5	6590
FR80T2.5X32-6B	80	6720	40	92	71	1098	6	6588
FR80T2.5X64-7B	80	6720	40	93	70	941	7	6587
F80T4.5X-8B	80	12096	40	88	136	1496	8	11968
FR80T5X4/16-9B	80	13440	40	89	149	1479	9	13311
FR80T5X16-9B	80	13440	40	89	149	1479	9	13311
FR80T5X32-11B	80	13440	40	90	147	1210	11	13310
FR80T5X64-13B	80	13440	40	88	151	1024	13	13312
NOTE: The bearer type identifier notation used in the present document is defined in Annex A.								

Table 3.2: Frame Parameters for Forward Link Bearers
(Source: ETSI TS 102 744-2-1 Tab 5.1)

To finish this subsection only remains to explain the scrambling and the channel coding. Scrambling is a process to randomize the string of bits of each FEC block before feeding them to the channel coder. It is based on a Linear Feedback Shift Register with the characteristic polynomial 1 + X + X15. The same structure, shown in Figure 3.21, is used both in transmission and reception.

With regard to the channel coding, it is employed turbo coding. The main elements of the turbo encoder is a buffer, a S-type interleaver, two identical Systematic Recursive Convolutional Code (SRCC) encoders (see Figure 3.23) and a variable puncturer for generating the different code rates of each bearer type. The whole structure of the turbo encoder is depicted in Figure 3.22. The S-interleaver, the puncturing, channel interleaving and symbol mapping are optimised for each bearer subtype, and several matrix are provided as annex in the Technical Specification.

Lastly, to finish this subsection about the forward bearers, in Figure 3.24 is included a

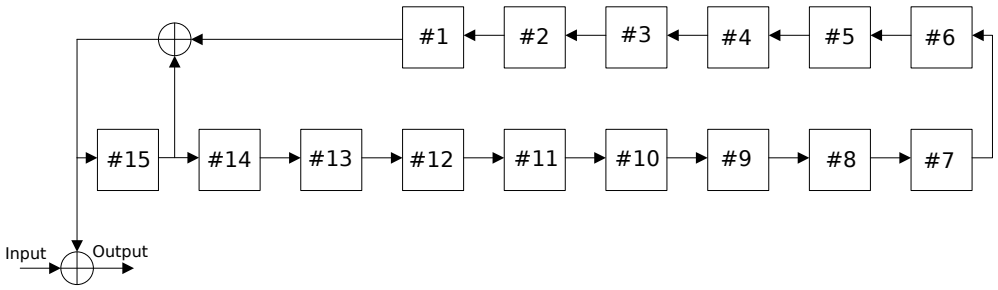

Figure 3.21: Scrambler and Descrambler Configuration
(Source: ETSI TS 102 744-2-1 Fig. 5.22)

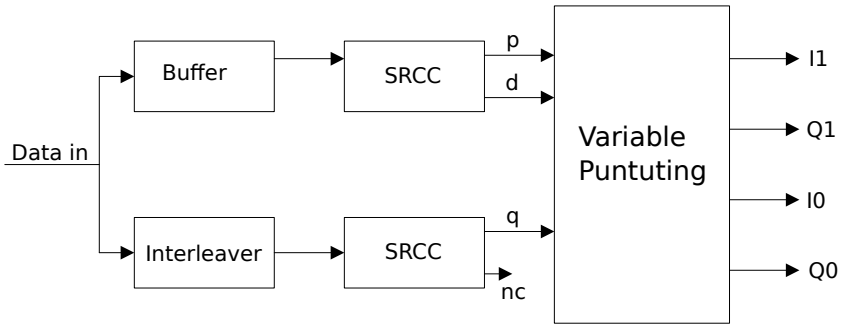

Figure 3.22: Turbo-Encoder Block Diagram
(Source: ETSI TS 102 744-2-1 Fig. 5.23)

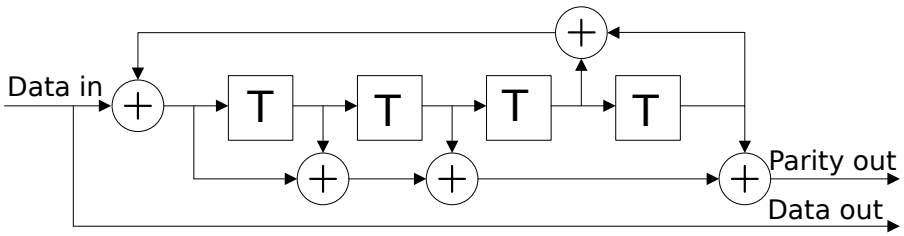

Figure 3.23: SRCC Encoder *(Source: ETSI TS 102 744-2-1 Fig. 5.24)*

block diagram of the forward bearer receiver with all the elements: de-scrambler, turbo decoder, interleaver, modulator, L-band down-converter, etc.

3.5.2 Return bearers

Contrary to the case of the forward link, return bearers are based upon two transmission strategies, burst and continuous, using a TDMA scheme. In burst mode the burst are transmitted in slots of 5 ms, 20 ms or 80 ms duration, while in the continuous mode the transmissions are based in 80 ms continuous frames just as in the forward link. Table 3.3 lists the return bearer types for must transmission mode and Table 3.4 does the same with continuous mode.

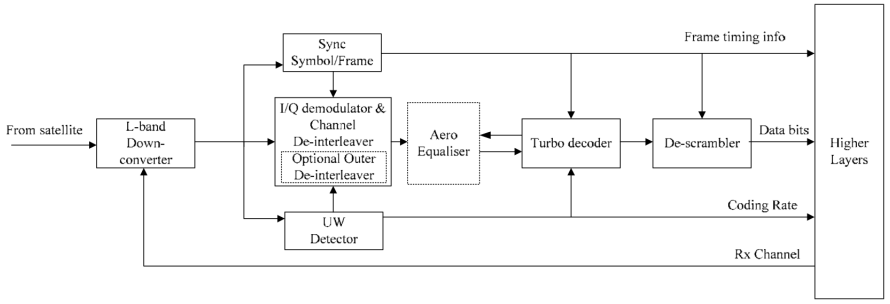

Figure 3.24: UE Receive Channel Unit Configuration
(Source: ETSI TS 102 744-2-1 Fig. 5.24)

Bearer Type Identifier (Note)	Slot Length	Symbol Rate	Modulation	Channel bandwidth	FEC Blocks per Burst
R5T1X-1B	5 ms	1,0 x 33,6 ksym/s	16-QAM	42 kHz	1
R5T2X-1B	5 ms	2,0 x 33,6 ksym/s	16-QAM	84 kHz	1
R5T4.5X-1B	5 ms	4,5 x 33,6 ksym/s	16-QAM	189 kHz	1
R20T1X-1B	20 ms	1,0 x 33,6 ksym/s	16-QAM	42 kHz	1
R20T2X-1B	20 ms	2,0 x 33,6 ksym/s	16-QAM	84 kHz	1
R20T4.5X-2B	20 ms	4,5 x 33,6 ksym/s	16-QAM	189 kHz	2
R5T2Q-1B	5 ms	2,0 x 33,6 ksym/s	π/4 QPSK	84 kHz	1
R5T4.5Q-1B	5 ms	4,5 x 33,6 ksym/s	π/4 QPSK	189 kHz	1
R20T0.5Q-1B	20 ms	0,5 x 33,6 ksym/s	π/4 QPSK	21 kHz	1
R20T1Q-1B	20 ms	1,0 x 33,6 ksym/s	π/4 QPSK	42 kHz	1
R20T2Q-1B	20 ms	2,0 x 33,6 ksym/s	π/4 QPSK	84 kHz	1
R20T4.5Q-1B	20 ms	4,5 x 33,6 ksym/s	π/4 QPSK	189 kHz	1
R80T0.5Q-1B	80 ms	0,5 x 33,6 ksym/s	π/4 QPSK	21 kHz	1
R80T1Q-1B	80 ms	1,0 x 33,6 ksym/s	π/4 QPSK	42 kHz	1
NOTE 1: The bearer type identifier notation used in the present document is defined in Annex A. NOTE 2: The R80T0.5Q-1B and R80T1Q-1B can also be used in continuous transmission mode. See clause 6.3.3.2.					

Table 3.3: Summary of Return Bearer Types for Burst Transmission Mode
(Source: ETSI TS 102 744-2-1 Tab 6.1)

Identifier	Frame Duration	Symbol Rate	Modulation	FEC Blocks per Burst
FR80T2.5X64-7B	80 ms	2,5 x 33,6 kSym/s	64-QAM	7
FR80T5X64-13B	80 ms	5,0 x 33,6 kSym/s	64-QAM	13
FR80T2.5X32-6B	80 ms	2,5 x 33,6 kSym/s	32-QAM	6
FR80T5X32-11B	80 ms	5,0 x 33,6 kSym/s	32-QAM	11
FR80T2.5X16-5B	80 ms	2,5 x 33,6 kSym/s	16-QAM	5
FR80T5X16-9B	80 ms	5,0 x 33,6 kSym/s	16-QAM	9
FR80T2.5X4-5B	80 ms	2,5 x 33,6 kSym/s	4-QAM	5
FR80T5X4-9B	80 ms	5,0 x 33,6 kSym/s	4-QAM	9

Table 3.4: Summary of Return Bearer Types for Continuous Transmission Mode
(Source: ETSI TS 102 744-2-1 Tab 6.2)

One characteristic of the return channel is the high flexibility of the return bearers. For this reason the return channel modulator has to be able to accommodate flexible channel configurations within a 200 kHz bandwidth according to the return schedule received from RNC. On the other hand, the return channel demodulator shall have a-priori knowledge of the symbol rate, modulation scheme and timeslot size for each expected burst. Figure 3.25 illustrates the high flexibility of return channel, and Figures 3.26 and 3.27 show a block diagram of the transmit channel unit configuration and receive channel unit configuration

respectively.

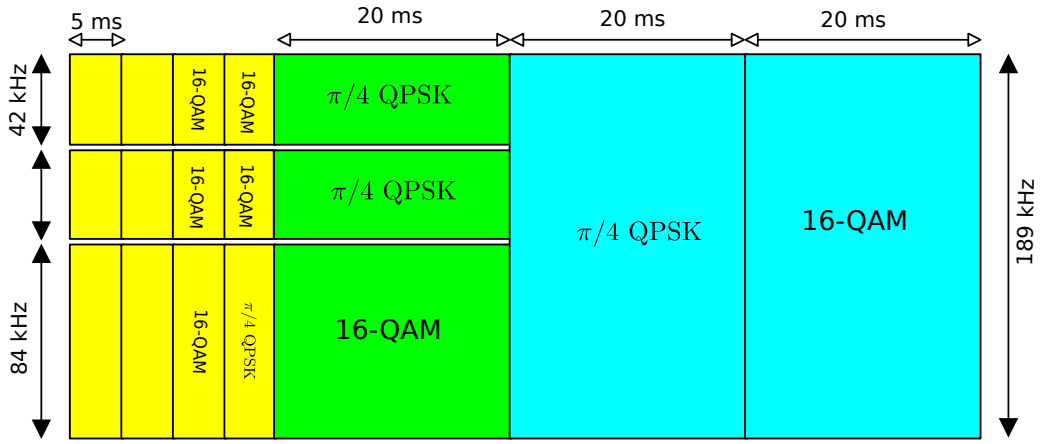

Figure 3.25: Illustration of Return Channel Flexibility
(Source: ETSI TS 102 744-2-1 Fig. 6.3)

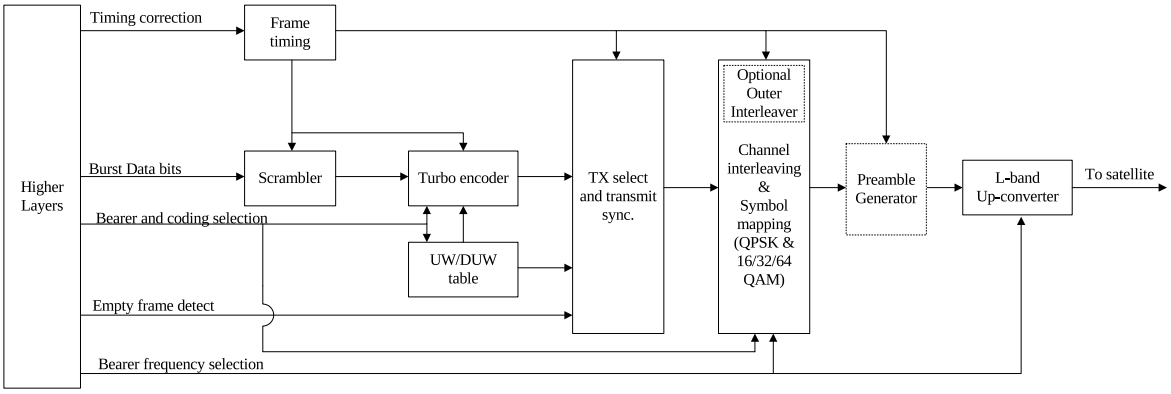

Figure 3.26: Transmit Channel Unit Configuration for Return Bearer Types
(Source: ETSI TS 102 744-2-1 Fig. 6.1)

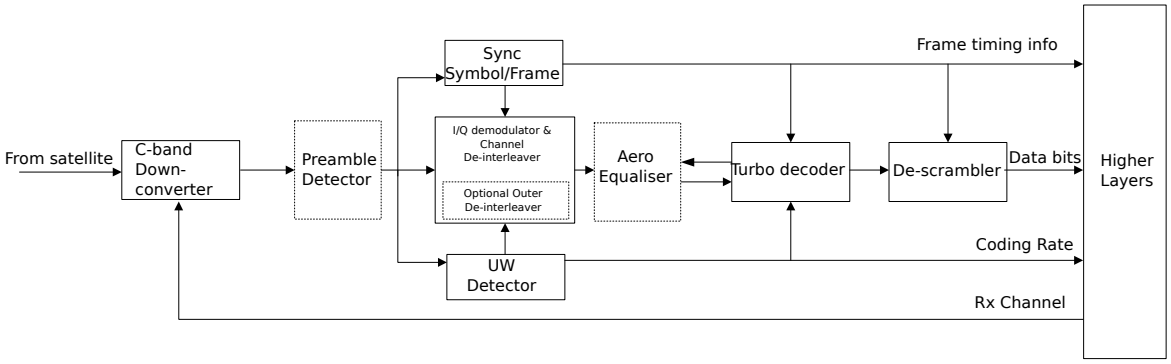

Figure 3.27: Receive Channel Unit Configuration for Return Bearer Types
(Source: ETSI TS 102 744-2-1 Fig. 6.2)

In regard to the modulation there are some differences with respect to the forward bearers.

The lowest symbol rate is 16.8 ksymb/s instead of 8.4 ksymb/s and is added a new symbol rate of 67.2 ksymb/s. The list of allowable symbol rates is the following:

- 16.8 ksymb/s
- 33.6 ksymb/s
- 67.2 ksymb/s
- 84.0 ksymb/s
- 151.2 ksymb/s
- 168.0 ksymb/S

The main differences reside in the modulation schemes employed. In the forward link four different modulations are used: QPSK, 16-QAM, 32-QAM and 64-QAM. Instead on the return link only are used 16-QAM and $\pi/4$ QPSK. The latter is a variant of the QPSK modulation that avoids large phase variations limiting the phase change from one symbol to another to 135^o rather than 180^o and also allows a differential demodulator. The channel filtering is identical to the forward channel, it uses a root-raised-cosine (RRC) filter function for symbol shaping with roll-offs of 0.25 and 0.13 depending on the bearer type.

The numbering of the return frames is relative to the forward frames. The return frame number i can start (80+SID) ms or (180+SID) after the receiving of the first symbol of the Unique Word of the forward frame number i. The use of one option or the other depends on the interleaving periods employed. SID, Self Imposed Delay, is a time that depends on the physical location of the UE and that of the satellite. When in the return schedule are used slots of 5 ms or 20 ms, the convention is to number each frame of 5 or 20 ms with a number between 0 and 15, indicating the 5 ms slot where the return frame starts. This is shown in Figure 3.28.

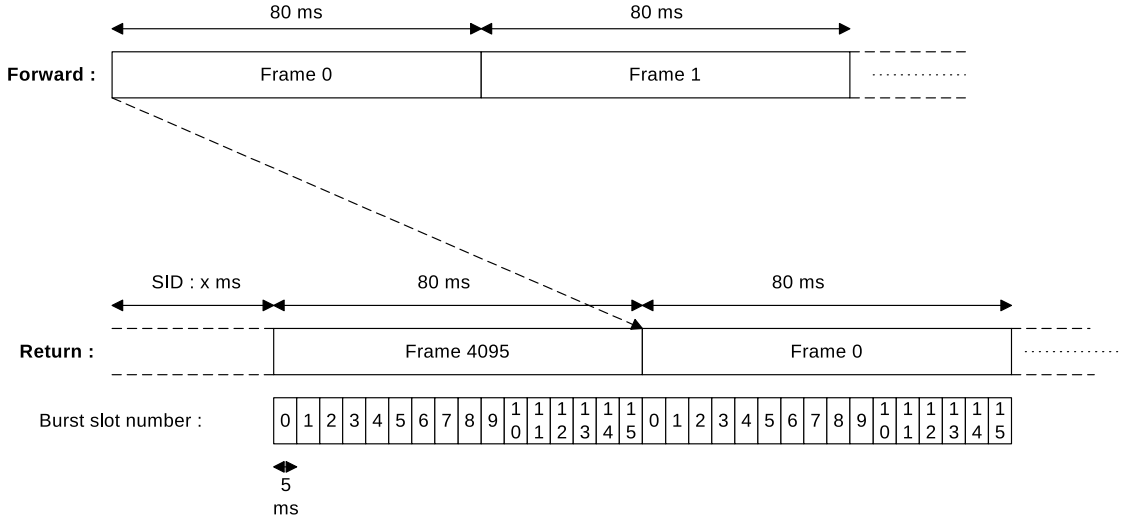

Figure 3.28: Return Frame and Slot Numbering (Referenced at the UE Antenna)
(Source: ETSI TS 102 744-2-1 Fig. 6.8)

As it was stated before, the return frames can last 5 ms, 20 ms or 80 ms. The 5 ms bursts are used to transport signalling information or short user data bursts like higher

layer acknowledgements or low bit rate voice codec frames. The 5 ms slots can be available for random access transmissions by UEs or may be reserved for use by a specific user. Before the transmission of the frame the UE must make a period guard of 0.36 ms, this is illustrated in Figure 3.29. On the other hand, 20 ms burst only can be used for reserved slots, they can not be employed for random access. They are the principal data carrying burst between the UE and the RNC. As in the case of 5 ms slots, before the transmission of a 20 ms frame there exists a period guard of 0.36 ms.

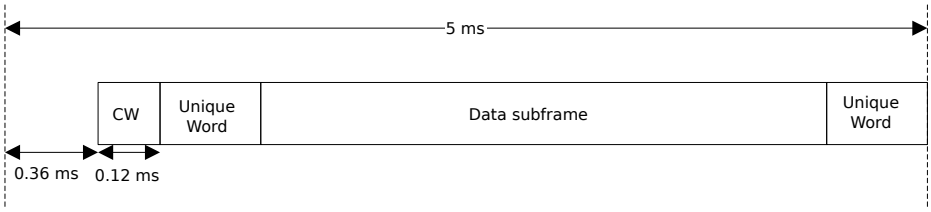

Figure 3.29: 5 ms Slot Format *(Source: ETSI TS 102 744-2-1 Fig. 6.9)*

As far as 80 ms frames is concerned, there are 8 bearer types (listed in Figure 3.4) for being used in continuous transmission mode and two bearers types (R80T0.5Q and R80T1Q) for burst mode. The latter are designed to operate in high multiuser interference scenarios and are used in a different way of the 5 ms and 80 ms bursts. Before the transmission of the data frame it is transmitted a preamble with a 11.875 kHz offset to indicate to the RNC the upcoming bursts in the following slot.

Another difference between the forward bearers and return bearers is that in 5 ms and 20 ms slots the Unique Word is repeated at the beginning and at the end. To refresh the memory of the reader, this special symbols are intented to signal the coding level used in the FEC block of the particular burst and also assist with frequency phase and clock synchronisation.

With regard to the scrambling, channel coding and structure of the FEC block there are not any remarkable difference, and everything explained for the forward bearers also applies here.

Finally, to finish the physical layer description of the SL family of S-UMTS and to end this chapter, let us comment a bit about the radio transmission and reception and the different UE classes contemplated in the Technical Specification. The UEs must have a RF transceiver with the following general capabilities:

1. The transceiver shall be designed to operate as a full duplex transceiver supporting the channelisation of 200 kHz.

2. The transceiver shall be able to tune to narrow signalling channels using nominal bandwidth sizes of 10.5 kHz, 21 kHz, 42 kHz, 84 kHz and 189 kHz wide band traffic channels.

3. The transceiver shall receive a full 200 kHz multi-bearer subband and from this 200 kHz bandwidth pick out (one) “narrow” channel using nominal bandwidth sizes of 10.5 kHz, 42 kHz and 189 kHz width.

4. The transceiver shall have a transmitter, which is capable of burst-by-burst re-tuning inside the assigned 200 kHz sub-band.

The UEs can be divided in two main groups: Land Class and Extension Class, this last group is further sub-divided into there subgroups: Aeronautical, Maritime and Land Mobile. Inside each group there exists between two and four different UE Classes depending on the gain of the antenna. In Table 3.5 are listed all classes along with the EIRP (Equivalent Isotropic Radiated Power) of the antenna in dBW (when specified in the standard) as well as the minimum G/T receiver parameter in dB/K.

Group	Subgroup	UE Classes	EIRP (dBW)	G/T (dB/K)
Land	N/A	Class 1 (Land A3 size)	20.0	≥ -10.5
		Class 2 (Land A4 size)	15.1	≥ -13.5
		Class 3 (Land A5 size)	10.0	≥ -18.5
Extension	Aeronautical	Class 4 (Enhanced Low Gain)	-	≥ -22.0
		Class 6 (High Gain)	-	≥ -13.0
		Class 7 (Intermediate Gain)	-	≥ -19
		Class 15 (Low Gain)	-	≥ -20.0
	Maritime	Class 8 (High Gain)	22.0	≥ -7.0
		Class 9 (Low Gain)	15.1	≥ -15.5
	Land Mobile	Class 10 (High Gain)	18.0	≥ -12.5
		Class 11 (Low Gain)	15.1	≥ -15.5

Table 3.5: List of UE Classes

Chapter 4

System model

4.1 Introduction

The purpose of the present project is to examine new link adaptation techniques also named techniques of Adaptive Modulation and Coding (AMC). The work I have realised for this project with Carlos Mosquera as tutor is an extension of the research made by former GPSC members Alberto Rico-Alvariño and Jesus Arnau, and Carlos Mosquera himself. First of all let us introduce what we understand by link adaptation. Link adaptation is the process of modifying the transmission parameters (modulation, coding rate and perhaps also power) depending on the channel conditions. In this work we use the terminology MCS (Modulation and Coding Scheme) which are the set of possible combination of modulation type and coding rates that are available for use. The goal of this process is to maximise the spectral efficiency of the system while maintaining the rate of errors (measured in BER, Bit Error Rate, or FER, Frame Error Rate) below a target level.

Although link adaptation is part of different terrestrial communication systems like Wi-Fi or 3G, the GPSC (Grupo de Procesado de Sinal en Comunicacións) is focused on Satellite Communications, among other research topics. That is why the here the link adaptation is applied to satellite mobile communication systems. In particular we apply our results to the satellite component of UMTS, whose radio interface was explained in detail in the previous chapter. Nevertheless the algorithms developed here are general enough to be applied to other satellite standards like the family DVB.

The behaviour of the land mobile satellite (LMS) channel hinders the use of Adaptive Modulation and Coding substantially. And additionally to the complicated nature of the LMS channel, we must add the effect of the high delay present when GEO satellites are employed, such as the commercial system BGAN, which makes use of family SL of the S-UMTS standard. This high delay causes that the Channel State Information (CSI) received by the transmitter by means of a feedback channel to be outdated even for moderate speeds.

In this chapter we make an in-depth study of the channel model employed in our simulations: the Fontan 3-state LMS channel model. Besides describing the model itself making a brief summary of the articles [14], [15], [16], [17] of Perez-Fontan et al., and the article [18] of Loo, we use a channel simulator based on the Fontan Model to obtain time series of channel samples and from these we compute other channel parameters that are of interest

in the link adaptation like outage probability and correlations and autocorrelations.

Firstly, here also is described the system model and the assumptions which are the basis for the link adaptation issue that is developed in the next chapter. We explain the signal model, the channel model and the details of the physical and link layers over the link adaptation schemes desgined and tested operate. Also, the concept of effective SNR is presented, that is of paramount importance for understanding of the simulator.

Lastly in this chapter, the simulator used to validate the link adaptation algorithms over the Land Mobile Satellite (LMS) channel is described. The simulator employed here is an object-oriented Matlab program with a big number of classes interrelated among them. The code originally was developed by Alberto Rico-Alvariño and I added some enhancements to it like the programming of the class that implements the multi-state channel (formerly only simulations with uni-state channel were available), some minor corrections, new classes to add the effect of a interference in the return channel and new functions to display the results of the simulations, specially time-domain behaviour of the link adaptation algorithm along with the channel evolution. Due to the high complexity of the simulator and with the intention to document it, the UML (Unified Modelling Language) is used to create a class diagram showing all the classes the simulator consists of and their interrelation.

4.2 System model

Through this project we consider a narrowband mobile satellite system operating in bands L (1-2 GHz) or S (2-4 GHz) in the region of the spectrum allocated to Mobile Satellite Services by the ITU-R. The system complies with the requirements of the standard S-UMTS (Satellite component of UMTS), namely the technical specification of the SL family published by the ETSI (European Telecommunications Standards Institute) as ETSI TS 102 744 [11].

Currently the service BGAN (Broadband Global Area Network) of INMARSAT makes use of this standard [19]. BGAN is a service provided by INMARSAT which can offer simultaneously voice and broadband data with guaranteed data rates on demand through a single, highly compact device on a global basis. The services have global coverage thanks to a constellation of three geostationary satellites, its coverage is shown in the map of Figure 4.1.

4.2.1 Signal model

All the signals through the system are discretised version of the real continuous signals, sampled at a sampling rate of $f_s = 1/T_{symb}$ where f_s denotes the sampling rate and T_{symb} the symbol period. The baseband discret equivalent model of the received signal y_i at a given time instant i, for both the forward and return link, is

$$y_i = \sqrt{snr} \cdot h_i^{xl} \cdot s_i + w_i \tag{4.1}$$

with

- y_i the received symbol,
- s_i the transmitted symbol,

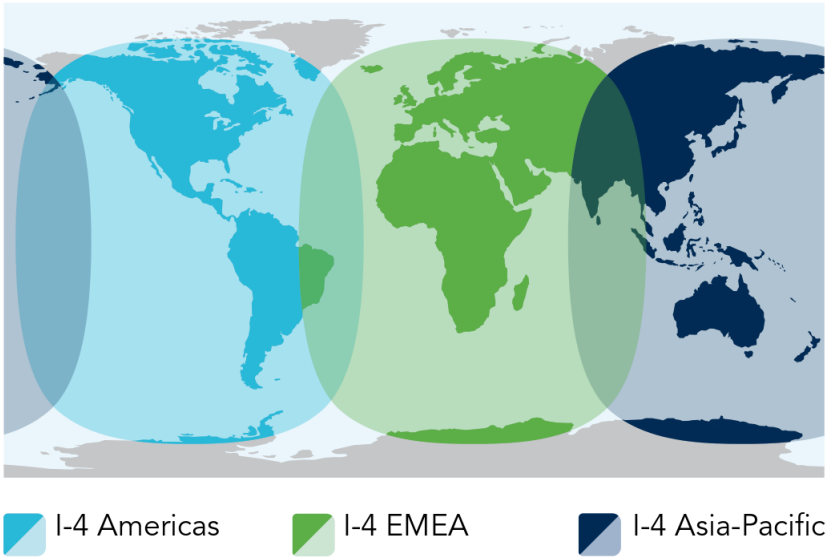

Figure 4.1: Converage of INMARSAT's BGAN service
(Source: INMARSAT webpage)

- h_i^{xl} is the channel coefficient where xl equals to fl if we refer to forward link and equals to rl for the return link,
- snr is the signal to noise ratio in natural units and
- w_i is the unit-power noise contribution.

One important feature of the algorithms presented hereafter in the following chapter is that in the design of the algorithms no particular probability density function (PDF) is assumed for the channel response, which has unknown parameters. Therefore, the methods proposed here to perform the link adaptation are expected to be robust under different channel conditions, contrary to other algorithms whose design rely on some channel model assumptions. Nevertheless, when we want to verify how the designed algorithms work in practice, we need to employ a specific channel model, but this is used in the simulation processes, rather than in the mathematical basis of the algorithms.

Channel model

For the evaluation of the link adaptation schemes the Fontan 3-state LMS channel model [14] is employed. In some cases the simulations are performed using one state (the state Line of Sight, LOS) of the channel and in other cases the whole model is employed. In each state within the Fontan model the channel follows Loo distribution [18] with a specific parameters that depend on the state. A change of state, for example from LOS conditions to a blockage of the satellite signal, changes the Loo model parameters to describe this new state of channel. Due to the importance of the channel model in the simulation process and with the idea that this project can help to future students or researches that want to employ this channel model, in the subsequent section it is explained in detail, emphasizing its implementation.

Table 4.1: Coding rate options for the return link bearer [3], $\pi/4-$QPSK constellation.

	L8	L7	L6	L5	L4	L3	L2	L1	R
Coding rate	0.34	0.39	0.46	0.53	0.61	0.69	0.73	0.77	0.81
Rate (spectral efficiency)	0.68	0.78	0.92	1.06	1.22	1.38	1.46	1.54	1.62
γ_{th} (dB)	-2.1534	-1.3663	-0.3605	0.5733	1.5948	2.6092	3.1288	3.6674	4.2367

Table 4.2: Coding rate options for the F80T1Q1B bearer [11], QPSK constellation.

	L8	L7	L6	L5	L4	L3	L2	L1	R
Coding rate	0.34	0.40	0.48	0.55	0.63	0.70	0.77	0.83	0.87
Rate (spectral efficiency)	0.68	0.80	0.96	1.10	1.26	1.40	1.54	1.66	1.74
γ_{th} (dB)	-2.1534	-1.2166	-0.0879	0.8317	1.8474	2.7278	3.6674	4.5384	5.1930

Transmitted and received symbols

The PhD thesis [20] of former GPSC member Alberto Rico-Alvariño describes well how information bits are mapped to symbols and his text is reproduced here. The transmitted symbols are the result of applying forward error coding and constellation mapping to a stream of bits; we consider a finite set of available codes. In the case of BGAN, each terminal is allocated to some bearer type, and the link adaptation process has to decide which of the bearer subtypes, i.e. which coding rate, should be used to the present transmission among a set of 9 or 10 possible coding rates that are obtained applying a different puncturing to the output of the turbo-coder.

Through this work two different bearers are employed. On the one hand, for return link simulations are employed the modulation parameters and the coding rates set of a bearer approximately equivalent to the R80T1Q-1B. The frame duration is 80 ms, the symbol rate $f_s = 33.6\ ksymb/s$, the modulation scheme employed is $\pi/4-$QPSK and the list of the coding rate is reported in Table 4.1.

On the other, for the forward link is employed the bearer type F80T1Q-1B [11] which differs from the previous one in the available coding rates (which are colected in Table 4.2) and in the type of modulation (use of QPSK instead of $\pi/4-$QPSK). In both forward and return bearers employed each frame carries a single FEC block with allows data rates between 21.6 and 55.6 kbit/s. There are a set of 9 different coding rates, going from L8 (about 8 dB below the C/N_0 neccessary to obtain a FEC Block Error Rate of 10^{-3} with the coding rate of the reference level, R).

Symbols form codewords

$$\boldsymbol{s_i} = [s_{iN},\ s_{iN+1},\ \cdots,\ s_{(i+1)N-1}] \tag{4.2}$$

of constant length N. In this case N should take the value $N = 0.08 \cdot 33600 = 2688$, but in the simulations it is rounded to the next hundred ($N = 2700$) to ease implementation of the filterings and decimatings. Each codeword see the channel samples

$$\boldsymbol{h_i^{xl}} = [h_{iN}^{xl},\ h_{iN+1}^{xl},\ \cdots,\ h_{(i+1)N-1}^{xl}] \tag{4.3}$$

where xl can refer to the forward link ($xl = fl$) or the the return link ($xl = rl$). We neglect the effect of headers or other sort of overhead.

Link layer operations

All the algorithm presented in the next chapter assume that there exists a link layer in both transmitter and receiver with some minimal functions, and that layer participates in the link adaptation process in the following way. For each send codeword, we assume that the other end feeds back an ACK if decoding was possible, and a NAK otherwise. This is modeled with the signal ϵ_i that takes the value 1 to inform of an error of the decoding, and the value 0 to inform that the decoding was successful:

$$\epsilon_i = \begin{cases} 1, & NAK \\ 0, & ACK \end{cases} \tag{4.4}$$

Performance evaluation

As said in [3], [20] and [21] determining whether a codeword will be correctly decoded or not is not an easy task since the values of the channel samples h_i^{xl} take can have large variations within the duration of a codeword, specially for moderate and high speeds as can be seen in Figure 4.2. One can think of trying to characterise the channel coefficients seen by a transmitted codeword with the value of their average SINR (maybe estimated from pilot simbols of the codeword) but in practise different channel realisations can have the same SINR and, however, offer different end-to-end performance. This is why it is important to have a method to measure the performance.

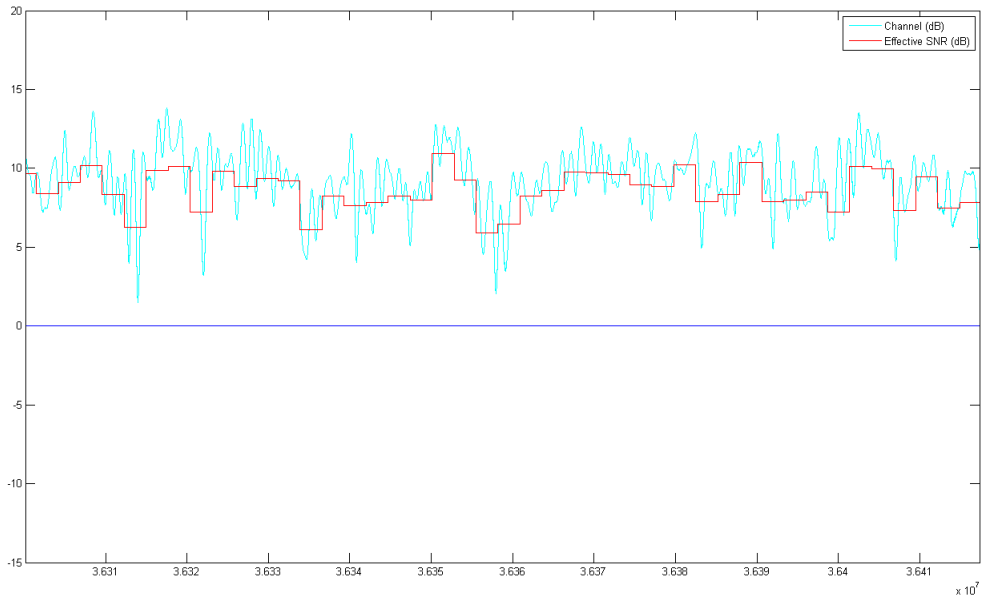

Figure 4.2: Example of channel evolution with the effective SNR of the frames

In this project, and following previous work of GPSC group, it is used an effective SNR metric (ESM), namely, the Mutual Information Effective SNR metric. Also, the use of the effective SNR allows the implementation of a simpler simulator that makes a physical layer abstraction reducing the computational load and therefore decreasing simulation time. In the last section of this chapter is described the architecture of the Mutual Information Simulator used to examine the performance of the link adaptation techniques.

For the sake of completeness we include here the equation of the effective SNR metric, which is given by

$$\Upsilon_{eff,i}^{xl} = \Theta^{-1}\left(\frac{1}{N}\sum_{k=iN}^{(i+1)N-1}\Theta\left(snr\cdot\left|h_k^{xl}\right|^2\right)\right) \tag{4.5}$$

Continuing with the explanation given in [3], the upper equation represents the SNR of an additive white Gaussian noise channel with the same mutual information as the faded channel $\boldsymbol{h_i^{xl}}$ and with $\Theta(\Upsilon)$ the mutual information over a Gaussian channel with SNR Υ and input restricted to a certain constellation $\{X_1, \cdots\cdots, X_L\}$

$$\Theta(\Upsilon) = 1 - c_L\sum_{l=1}^{L}\mathbb{E}\left[\log_2\left(\sum_{k=1}^{M}e^{-\frac{|x_l - x_k + w| - |w|^2}{1/\Upsilon}}\right)\right] \tag{4.6}$$

with $c_L = 1/(L\log_2 L)$ and $w \sim \mathcal{CN}(0, 1/\Upsilon)$.

Using this metric, we assume that the transmission of the i-th codeword fails when $\Upsilon_{eff,i}$ is below the threshold of the Modulation and Coding Scheme (MCS) used in the transmission, Υ_{th}, and that it succeeds otherwise. Mathematically we define $\epsilon_i \in \{0, 1\}$ as the error event of the i-th codeword, then

$$\epsilon_i = \begin{cases} 1 & if \;\; \Upsilon_{eff,i} < \Upsilon_{th} \quad (error : NAK) \\ 0 & otherwise \qquad\quad (success : ACK). \end{cases} \tag{4.7}$$

4.3 Channel model

In this section, the channel model used in the simulations is explained. But before moving on to the substance, in the first epigraph are explained the concept of random variable, some important distributions used within the channel model and the Markov chains. Once this is clear the following subsection goes deep into the Fontan LMS channel model.

4.3.1 Mathematical basis

The contents of this subsection are taken from the book *Principios de probabilidad, variables aleatorias y señales aleatorias* [22] and from the class notes of the subject *Caracterización de Sinais Aleatorios (CSA)*, taught in the second course of the university degree *Enxeñaría de Telecomunicación* of the University of Vigo.

In a physical experiment, the set of all possible results is named sample space, Ω. This sample space can be continuous or discrete, finite or infinite. We usually are interested in studying the probability of obtaining a group of results, an event, rather than a single result. An event is defined as a subset of the sample space. When studying a physical experiment, we frequently are interested in calculate the probability of obtain some specific outcomes or results. There are ways of coping with the definition of probability, the classical or a priori way, using the concept of relative frequency (posteriori frequency) and the axiomatic approach. In the aforementioned references the reader can find an in-depth explanation.

Here, it is employed the axiomatic definition of probability following the class notes of CSA. Given a sample space Ω, we assign to it a σ-algebra $\mathcal{F}$ (a collection of subsets), a measure of probability P is defined as:

P: $\mathcal{F} \longrightarrow [0,1] \in \mathbb{R}$ verifying:

i) $\forall A \in \mathcal{F},\ P(A) \geq 0$

ii) $P(\Omega) = 1$

iii) If $\{A_i\}_{i=1}^{\infty} \subset \mathcal{F}$ such that $A_i \cap A_j = \varnothing$, if $i \neq j$ then $P\left(\bigcup_{i=1}^{\infty} A_i\right) = \sum_{i=1}^{\infty} P(A_i)$

Its main properties are:

1) $P(\varnothing) = 0$

2) $P(A^c) = 1 - P(A)$

3) $P(A \cup B) = P(A) + P(B) + P(A \cap B)$

4) If $B \subset A$, then $P(B) \leq P(A)$

5) $0 \leq P(A) \leq 1$ for any event A of $\mathcal{F}$

6) $P(\Omega) = 1$, but if exists an event A such that $P(A) = 1$ this does not mean that $A = \Omega$

Finally, the triad $(\Omega, \mathcal{F}, P)$ is named probability space.

Now let us introduce the concept of random variable. It is a real function of the elements of the sample space Ω. A random variable is represented by a capital letter, for example, X and lower-cases are reserved for specific values the random variable can take, for example x. When using random variables, if the sample space does not belong to the real numbers a transformation is done to convert the events into intervals of the real line. A random variable can be classified into continuous, discrete or mixed. The continuous type, the single considered here, is characterised by having an uncountable infinite range and by that all events of the type $\{X = x\}$ have zero probability.

All the information of a random variable is captured in a pair of functions, related between them, that are two different ways of observing the same information: the cumulative distribution function (CDF) and the probability density function (PDF).

On the one hand, the cumulative distribution function is

$$F_X(x) = P\{X \leq x\} \tag{4.8}$$

and some of its properties are:

- $F_X(-\infty) = 0$
- $F_X(\infty = 1)$
- $0 \leq F_X(x) \leq 1$
- $P\{x_1 < X \leq x_2\} = F_X(x_2) - F_X(x_1)$

On the other hand, the probability density function is defined as the derivative of the cumulative distribution function:

$$f_X(x) = \frac{dF_X(x)}{dx} \tag{4.9}$$

This function satisfies the following properties:

i) $0 \leq f_X(x)\ \forall x$

ii) $\int_{-\infty}^{\infty} f_X(x) \cdot dx = 1$

iii) $F_X(x) = \int_{-\infty}^{x} f_X(\xi) \cdot d\xi$

iv) $P(x_1 < X \leq x_2) = \int_{x_1}^{x_2} f_X(x) \cdot dx$

Hereafter we explain some probability distributions that are used in the channel model. They are the normal or Gaussian distribution, the log-normal distribution and the Rayleigh and Rice distributions.

Normal distribution

A random variable X is Gaussian if its probability density function (PDF) is:

$$f_X(x) = \frac{1}{\sqrt{2\pi}\sigma} e^{-\frac{(x-\mu)^2}{2\sigma^2}} \tag{4.10}$$

It is represented briefly in the following way: $X \sim N(\mu, \sigma)$. The parameters within the equation are:

- $\mu \in \mathcal{R}$ is the mean of the random variable, also is named location parameter, because it signal in which place of the real line is placed the distribution.
- $\sigma > 0$ is its the standard deviation and σ^2 is its variance. This parameter indicates how sparse is the random variable. Low values indicate that the values that take the random variable are usually very closed to its mean.

An important normal distribution is the standard normal distribution, this is a random variable such that its mean is zero and its standard deviation (and hence its variance too) take the unity value, $Z \sim N(0, 1)$. Its PDF and CDF is shown if Figure 4.3. There is a very useful property, we can obtain a general random variable $X \sim N(\mu, \sigma)$ applying a transformation to Z in the following way:

$$X = \mu + \sigma Z \tag{4.11}$$

There is a function derived from the PDF of the standard Gaussian distribution that is very used, it is the Q-function. This function is employed in digital communication when

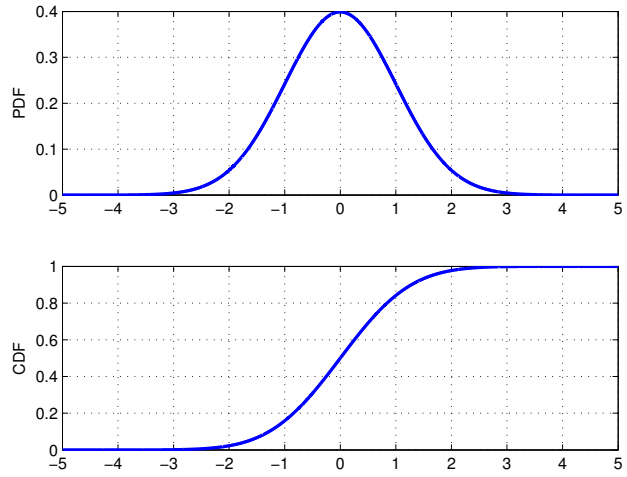

Figure 4.3: PDF and CDF of a standard Gaussian random variable

estimating the Symbol Error Rate of a continuous transmission of symbols of some constellation under a AWGN (Additive White Gaussian Noise) channel [23]. The Q-function $Q(x)$ calculates the probability of the subset $\{X \geq x\}$:

$$Q(x) = \int_x^\infty \frac{1}{\sqrt{2\pi}} e^{-u^2/2} du \tag{4.12}$$

For any normal variable $X \sim N(\mu, \sigma)$ using the CDF we can calculate the threshold x such that the probability that the random variable takes values lower than x is a given probability p_0, i.e. $P(X < x) = p_0$. This will be of interest in link adaptation where we would like to have and Frame Error Ratio (FER) lower than a given value p_0, typically a power of 10 ($10^{-1}, 10^{-2}, 10^{-3}$...). A common calculation is to obtain the threshold that will be exceeded with probability $1 - p_0$. In Table 4.3 we include the threshold relative to the mean μ for the most common p_0 used along this project, and in Figure 4.4 is shown graphically.

p_0	x such that $P(X < x) = p_0$
10^{-1}	$\mu - 1.29\sigma$
10^{-2}	$\mu - 2.33\sigma$
10^{-3}	$\mu - 3.09\sigma$
10^{-4}	$\mu - 3.70\sigma$
10^{-5}	$\mu - 4.25\sigma$

Table 4.3: Thresholds and CDF function

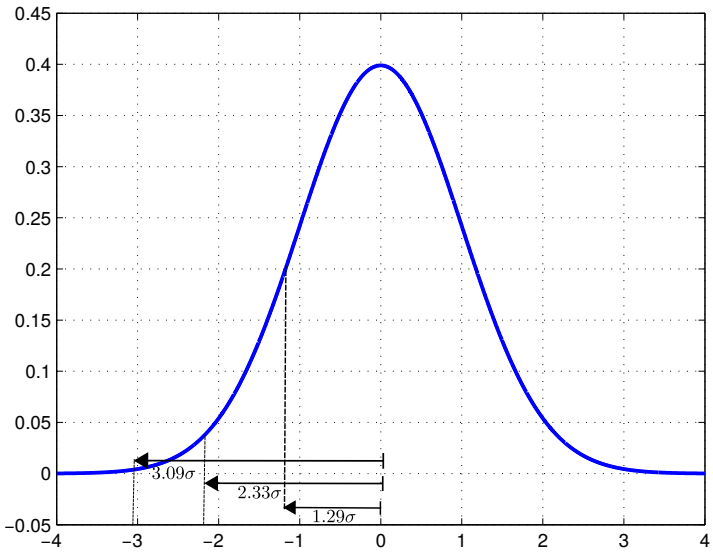

Figure 4.4: Thresholds

Log-normal distribution

A random variable X is said to be log-normally distributed, $X \sim LogN(\mu, \sigma)$, if its logarithm follows a normal distribution, i.e., if $Y = \log_{10}(X) \sim N(\mu, \sigma)$. Its PDF is

$$f_X(x) = \frac{1}{x\sqrt{2\pi}\sigma} e^{-\frac{(\log_{10} x - \mu)^2}{2\sigma^2}}, \ x > 0 \tag{4.13}$$

We can generate a log-normal distribution $X \sim LogN(\mu, \sigma)$ with the parameters μ and σ in dB from samples of a normal distribution $Y \sim N(0, 1)$ with the following transformation:

$$X = 10^{Y/20} \tag{4.14}$$

due to the fact that $Y = 20\log_{10}(X) \sim N(\mu, \sigma)$.

This distribution is very used in Telecommunications because the level of the received signal follows a lognormal distribution, i.e., the level of the signal in decibels (dB) is normally distributed.

Rayleigh distribution

Other important type of random variable is the Rayleigh distributed one. The Rayleigh distribution is a particular case of the Rice distribution that will be explained in the next subsection. The Rayleigh distribution is employed to model the so called Rayleigh fading, a situation when there is multipath (multiples replicas of the signal arrive to the antenna of the receiver) where there is not any dominant replica, i.e. in non Line of Sight (NLOS) conditions.

A Rayleigh distribution arises when solving the following problem. Let us have a bi-dimensional normal random variable $Z = (X, Y)$ with X and Y Gaussian variables, both with mean $\mu = 0$ and the same standard deviation σ: $X, Y \sim N(0, \sigma)$. The Rayleigh distributed random variable R is obtained by means of the following transformation where the modulus of a vector is calculated:

$$R = \sqrt{X^2 + Y^2} \tag{4.15}$$

This new variable, R, has a Rayleigh distribution and its PDF is

$$f_R(r) = \frac{r}{\sigma^2} \exp\left(-\frac{r^2}{2\sigma^2}\right), \ r \geq 0 \tag{4.16}$$

with σ^2 the variance of the original normal variables.

Rice distribution

As said previously, the Rice distribution is a generalization of the Rayleigh distribution allowing each of the components of the bi-dimensional Gaussian variable to have a different mean, although maintaining the constraint in the variance (both components must have the same variance σ^2). Each one of the two components of the multi-dimensional random variable are:

- $X \sim N(\mu_x, \sigma) = N(v \cos\theta, \sigma)$
- $Y \sim N(\mu_y, \sigma) = N(v \sin\theta, \sigma)$

with $v = \sqrt{\mu_x^2 + \mu_y^2}$ the modulus pointing to centre of the bi-dimensional Guassian and θ the angle signalling in which part of the plane the Gaussian is placed. All this can be understood better looking at Figure 4.5.

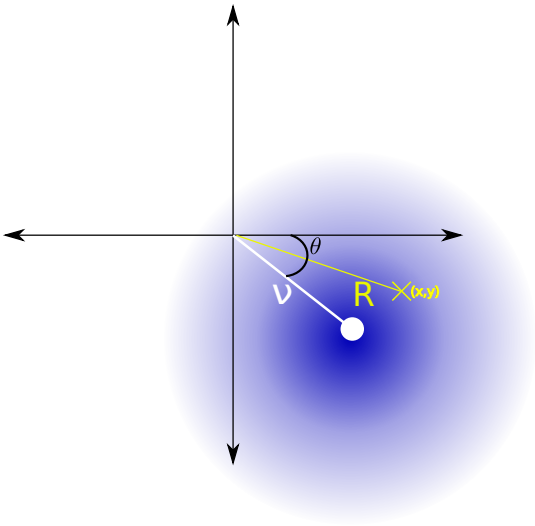

Figure 4.5: Origin of the Rice distribution
Source: article Rice distribution in the Wikipedia

Like in the Rayleigh case, we define the Rice random variable R as the modulus of a point taken from the randomly from the bi-dimensional Gaussian:

$$R = \sqrt{X^2 + Y^2} \tag{4.17}$$

and it is employed the notation $R \sim Rice(v, \sigma)$ with

- v the module of the point where the bi-dimensional Gaussian is centered.
- σ the standard deviation of each of the unidimensional Guassians

Its PDF function is

$$f_R(r) = \frac{r}{\sigma^2} \exp\left(-\frac{r^2 + v^2}{2\sigma^2}\right) I_0\left(\frac{rv}{\sigma^2}\right), r > 0 \tag{4.18}$$

with

- r the values the random variable takes,
- v the direct signal level (LOS component),
- σ the Gaussian standard deviation and
- $I_0(\cdot)$ the modified Bessel function of zero-th order.

The reader may notice that if we make $\mu_x = \mu_y = 0$, i.e. $v = 0$, the Rice distribution turns into a Rayleigh distribution. Figure 4.6 shows the PDF of a family of Rice distributed random variables where the particular case $v = 0$ (blue line) is the Rayleigh PDF.

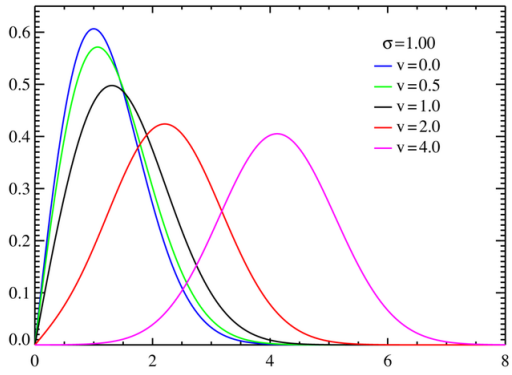

Figure 4.6: PDF of the Rice distribution
Source: article Rice distribution in the Wikipedia

When using the Rice distribution an important parameter is the Rice factor K, this is the ratio between the direct signal power and the power of the multipath. In the Fontan model the variable Multipath Power (MP) is approximately equivalent to the inverse of the Rice factor. K is also named direct to multipath signal power ratio, its expression is:

$$K = \frac{v^2}{2\sigma^2} = \frac{\mu_x^2 + \mu_y^2}{2\sigma^2} \tag{4.19}$$

This distribution is employed when the receptor has direct line of sight to the transmitter and, therefore, the received signal has a big component (LOS component) and a multipath

component with lower power, the most frequent case in satellite communications. Contrary, in some terrestrial environments and standards, like those of cellular systems (GSM, UMTS...), when the user is within a city with high buildings, multiple echoes arrive to the receiver and there is not anyone whose power stands out. In these cases is employed the Rayleigh distribution.

Markov chain

Lastly, before start the explanation of the Fontan LMS channel model, it is introduced shortly the markov chains using as source of information the English page of Markov chain in the Wikipedia.

A Markov chain (discrete-time Markov chain or DTMC), named after Andrey Markov, is a random process that undergoes transitions from one state to another on a state space. It must possess a property that is usually characterized as "memorylessness": the probability distribution of the next state depends only on the current state and not on the sequence of events that preceded it.

A Markov chain is a sequence of random variables $X_1, X_2, X_3, \cdots$, with the Markov property, namely that, given the present state, the future state and the past states are independent. Formally

$$P(X_{n+1} = x \mid X_1 = x_1, X_2 = x_2, \cdots, X_n = x_n) = P(X_{n+1} = x \mid X_n = x_n) \qquad (4.20)$$

A Markov chain can be described visually with a state diagram. Each state is represented by a circle, and the transitions from one state to another with arrows. Each arrow is labelled with the probability its transition. Of course, the process can remain in the same state apart from change to another different state. A general state diagram of a 3-state Markov chain is shown in figure 4.7. This will resemble to Electronic students to the Finite State Machines (FSM) of the Automatic and Control.

Mathematically, a Markov chain is characterised by the following elements:

- the **state space** of the chain, i.e., the states where the system can be, or in other words, the values the random variable can take. They form a finite set $\Omega = \{s_1, s_2, \cdots, s_N\}$ of N different states.
- a **transition matrix or state transition probability matrix** P such that $P = \{s_{ij}\}_{i=1}^{N}$, where s_{ij} denotes the probability of, being in state s_i, go to the state s_j.
- a **state probability vector** W such that $W = [p_1, p_2, \cdots, p_N]$ where p_i denotes the global probability of being the random process within the state s_i.

The concept of Markov chain is of paramount importance for understanding the channel model. Although it will ve developed in the following section, just tell here that in the case in question, the LMS channel in each moment can be inside three different states:

State-1: **LOS conditions**: there are no obstacles that block the signal path between the Mobile Terminal and the satellite.

State-2: **Moderate shadowing conditions**.

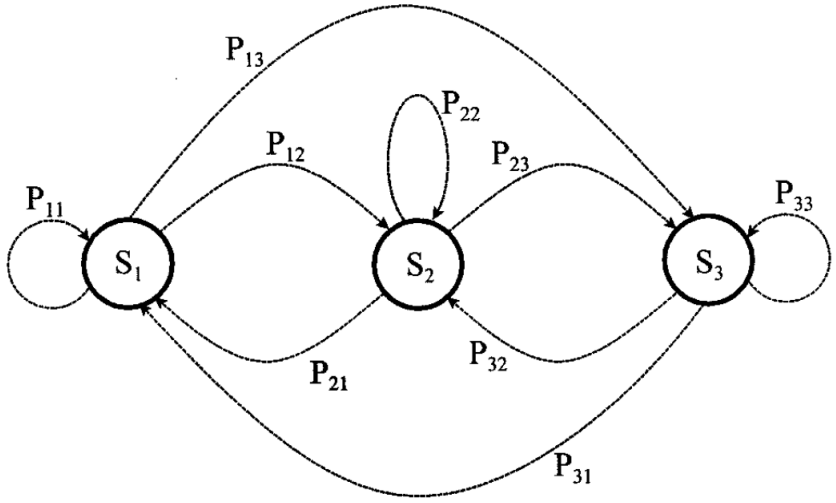

Figure 4.7: Fontán channel model.*Source: Fontán article [14]*

State-3: **Deep shadowing conditions or blockage**: there is a considerable obstacle that impedes the Mobile Terminal to receive the direct signal of the satellite or to transmit towards the satellite. Only the multipath component is received.

4.3.2 Fontán LMS channel model

Fernando Pérez Fontán et al. published in 2001 the paper "Statistical Modelling of the LMS Channel" in the IEEE Transactions on vehicular technology [14]. This article is the basis of the channel simulator employed in this project for testing the behaviour of the link adaptation algorithms. The main ideas of that paper, enhanced with other papers like [15], [16] and [17], are collected here.

The reference article of Fontán, [14], describes the principles for design and implement a land mobile satellite (LMS) channel simulator that is based on some statistical assumptions of the channel: a statistical model. This model is said to be generative since it makes it possible to generate time-series of any channel parameter whose study is required like the signal envelope and the phase.

The LMS channel is so complicated that it can not be described using a single statistical distribution due to the fact that the received signal level has a PDF of the type multi-modal. Therefore, it is used a family of complex statistical distributions (complex in the sense of not simple) along with a Markov chain rather than a simply distribution. We can express the whole channel model with the following general equation:

$$f_{total,channel}(r) = p_{s_1} f_{s_1}(r) + p_{s_2} f_{s_2}(r) + p_{s_3} f_{s_3}(r) \tag{4.21}$$

In the previous equation the constituent elements are:

- p_{s_i} is the probability of being the channel within the state s_i and
- $f_{s_i}(r)$ is the PDF of the channel conditioned by being in the state s_i

and hence, the PDF of the whole channel $f_{total,channel}(r)$ is obtained through the summation.

As stated earlier in the epigraph dedicated to the Markov chains, the Fontán model is based on a 3-state Markov chain and for the sake of clarity we include again the enumeration and meaning of each one of the three states:

- s_1 or **LOS conditions**: there are no obstacles that block the signal path between the Mobile Terminal and the satellite.
- s_2 or **moderate shadowing conditions**.
- s_3, **deep shadowing conditions or blockage**: there is a considerable obstacle that impede the mobile terminal to receive the direct signal of the satellite or transmit towards the satellite. Only the multipath component is received.

Within each state the channel follows a distribution known as Loo [18]. This distribution was proposed by Chun Loo, who has presented its mathematical fundamentals along with experimental results validating his model in an article of the year 1985 named "A Statistical Model for a Land Mobile Satellite Link". Now we include its expression and then its meaning will be discussed.

The expression of the Loo distribution is under these lines and it will be explained just after it.

$$f_R(r) = \frac{r}{\sigma_r^2 \sigma_{ln}\sqrt{2\pi}} \int_0^\infty \frac{1}{a} \exp\left[-\frac{(\ln a - \mu)^2}{2\sigma_{ln}^2} - \frac{(r^2+a^2)}{2\sigma_r^2}\right] I_0\left(\frac{ra}{\sigma_r^2}\right) da \tag{4.22}$$

The parameters present in the Loo equation are:

- $2\sigma_r^2$. **Average scattered power due to multipath**. It is the equivalent to the $2\sigma^2$ parameter of the Rice distribution 4.18.
- σ_{ln}^2. **Variance of the direct signal**. It is the equivalent to the variance of the Log-normal distribution σ^2 4.13.
- μ. **Mean value of the direct signal**. It is equivalent to the mean value of the Log-normal distribution μ 4.13
- a. **Direct signal's amplitude**. It is the equivalent to the variable v in the the Rice distribution 4.18
- r. **Received signal's amplitude**. It is what we want to characterise.

Continuing with the explanation of the Loo model, in the previous equation there is an integral because you have to think the Loo distribution as one of the marginal PDFs of the bi-dimensional random variable (also named random vector) [24]

$$f_{AZ}(a, z), \tag{4.23}$$

with $A \sim LogN(\mu, \sigma_{ln})$ and $Z \sim Rice(a, \sigma_r)$ and the Loo distribution is obtained by performing the following integration:

$$f_R(r) = \int_0^\infty f_{AZ}(a, z) da \tag{4.24}$$

Let us leave the Mathematics aside for one moment, we will describe in words what the Loo distribution says to us. When looking at the level of the received signal that goes through a Land Mobile Satellite Channel in the temporal domain, we observe that it has three different type of variations: macro-variations, mini-variations and micro-variations.

Firstly, the **macro-variations**, or very slow fading, correspond with the so-called states and are related with big changes of the transmission conditions. These changes could be a switching from having direct line of sight to have a moderate shadowing due to some trees or, even worst, due to a big building or a motorway tunnel.

Secondly, the **mini-variations**, also called slow fading, are caused by the irregularity off the obstacles (e.g. vegetative shadowing) as said in [25] and they are related with the parameter named correlation distance, which will be explained later.

And, in last place, the **micro-variations**, or fast fading, is mainly due to the multipath and to the randomness inherently character of the reception of an electromagnetic signal.

Lastly, some key parameters related with the implementation of the channel model are introduced before moving towards the next subsection.

- **Correlation distance,** d_{corr} indicates the maximum length which separates two points for who, with a frozen time, there is a significant correlation.
- **State frame length,** L_{frame}, is the minimum length, in meters, that lasts one state. Each time the Mobile Terminal moves that distance a new state of the Markov chain is drawn.
- **Length of the transition regions between states,** L_{trans}
- α is the **mean** in dB of the log-normal distribution.
- Ψ is the **standard deviation** in dB of the log-normal distribution.
- **Average multipath power, MP,** power received due to the multipath component.

On the one hand, when a simulation is performed L_{frame} and L_{trans} are converted into time durations through their relation with the mobile speed v. Well, actually, the simulator employs the number of samples equivalent to each distance, i.e. N_{frame} and N_{trans}. On the other hand, the parameters α and MP, related with the channel statistical distribution, are expressed in dB relative to the LOS level. This is done to make the channel model independent of the level of received power. Their mathematical expressions are:

$$\alpha(dB\ rel\ to\ LOS) = 20\log_{10}(e^{\mu}) \tag{4.25}$$

$$\Psi(dB) = 20\log_{10}(e^{\sqrt{\sigma_{ln}^2}}) \tag{4.26}$$

$$MP(dB\ rel\ to\ LOS) = 10\log_{10}(2\sigma_r^2) \tag{4.27}$$

The values of α, Ψ and MP depend on several factor as can be:

- The type of **environment**:
  - Open area,

	Open			Suburban			Urban			I-tree			H-tree		
	α	Ψ	MP	α	Ψ	MP	α	Ψ	MP	α	Ψ	MP	α	Ψ	MP
State 1	0.1	0.37	-22.0	-1.0	0.5	-13.0	-0.3	0.73	-15.9	-0.4	1.5	-13.3	-	-	-
State 2	-1	0.5	-22	-3.7	0.93	-12.2	-8.0	4.5	-19.2	-8.2	3.9	-12.7	-10.1	2.25	-10.0
State 3	-2.25	0.13	-21.2	-15.0	5.9	13.0	24.4	4.5	-19.0	-17.0	3.14	-10.0	-19.0	4.0	10.0

Table 4.4: Average parameters (decibels) for different states, environments and an elevation of of 40°

  - Suburban area,
  - Intermediate tree shadowed area,
  - Heavy tree shadowed area and
  - Urban area.

- The **angle of elevation** of the Mobile Terminal towards the satellite. Lower elevation angles are more problematic due to it is more easy that an obstacle provokes an blockage. For a same satellite, the elevation angle is dependent on the latitude where the Mobile Terminal is located.
- The **frequency band** employed in the communication.
- The particular **state** of the Markov channel.

In Table 4.3.2 are listed the values the parameters α, Ψ, and MP take in the simulations, which correspond to a S-band communications with an elevation angle of 40^o. These parameters were obtained by the authors of [14] from a database of the University of Bradford.

Before concluding this chapter, just two more concepts before show the two graphics that synthesise all this chapter. The channel has two different type of temporal correlation: a long-term correlation in the LOS component (log-normal distribution), ruled mainly by the correlation distance, and a short-term correlation in the non-LOS component or multipath component (Rice distribution), ruled mainly by the Doppler spread.

The correlation properties are achieved by means of filtering with two low pass filters (LPF): one in the branch of the LOS component and another in the branch of the non-LOS component. Their continuous time cut-off frequencies are:

- $f_{NLOS} = \dfrac{v}{\lambda}$
- $f_{LOS} = \dfrac{v}{d_{corr}}$

with v the Mobile Terminal speed, λ the wavelength of the signal that carriers the information and d_{corr} the correlation distance.

The normalized discrete frequencies equivalent to the previous cut-off frequencies can be easily obtained normalizing by the sampling frequency f_s (symbol rate). We calculate a channel sample for each symbol of the frame. But, how the cut-off frequencies are typically very small (in the order of $10^{-(3-5)}$) a mathematical transformation is applied to the basic scheme in order to avoid very low cut-off frequencies, this is achieved using interpolation and decimation (implicit when instead of generate $N = 2700$ random samples, 27 or 270 are generated).

The reader can look at Figure 4.8 and see an example of the evolution of the channel and can look at Figure 4.9 to see how the channel samples of a frame are generated and how they are sum up in a single value, the effective SNR.

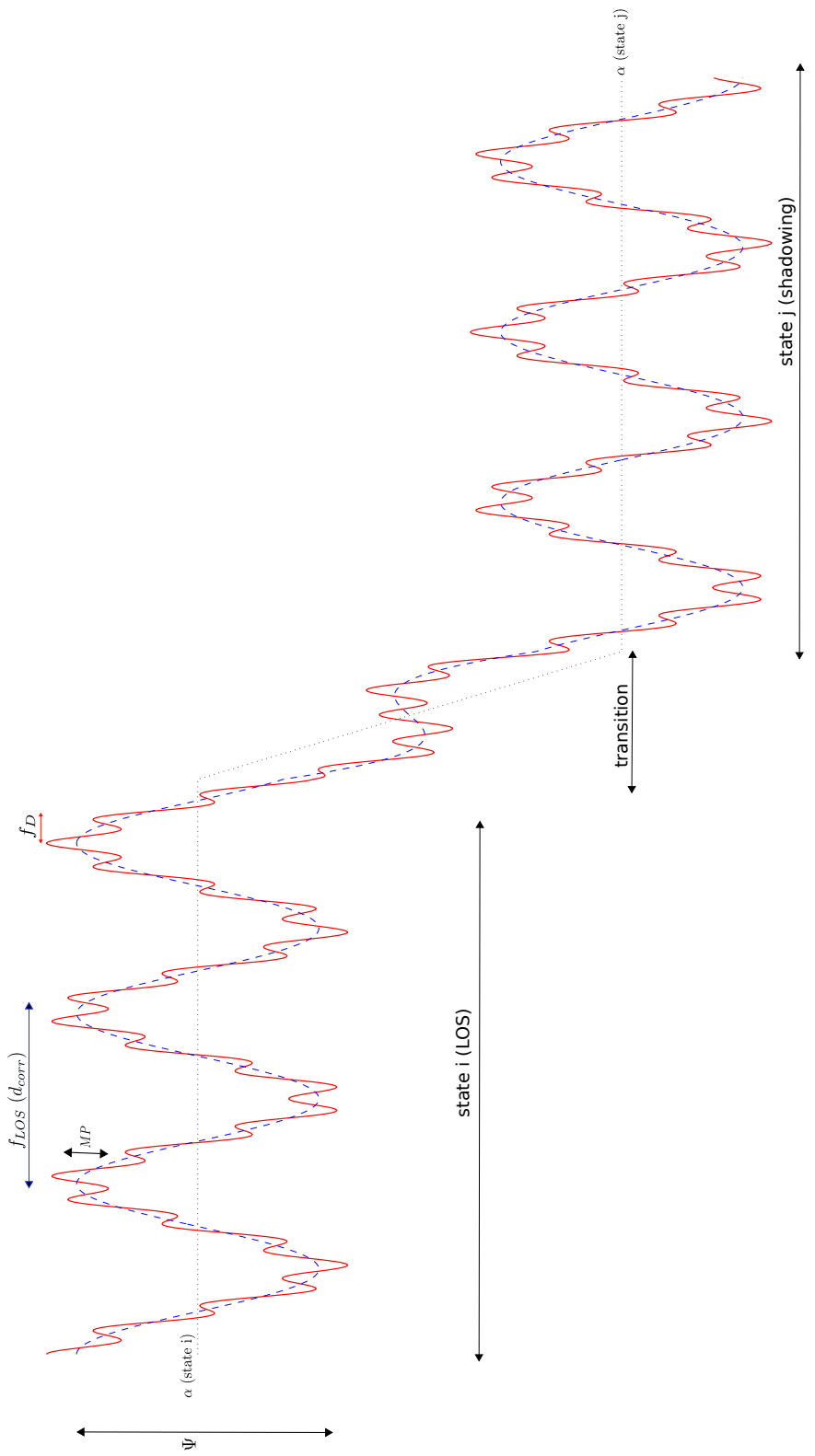

Figure 4.8: Fontán channel model

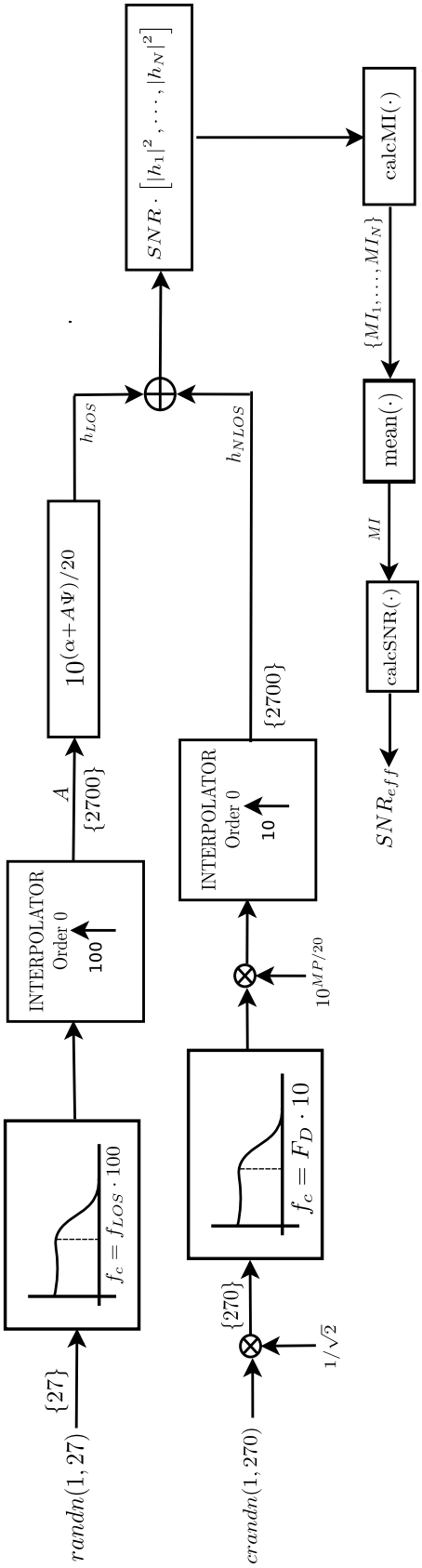

Figure 4.9: Block diagram of the channel generator

Chapter 5

Link adaptation in S-UMTS

5.1 Problem statement

The problem of link adaptation we try to solve is explained hereafter. The goal of link adaptation algorithms is to choose the MCS of each frame with the goal of maximizing the spectral efficiency of the system while maintaining the error rate (measured in Frame Error Rate, FER) under a target level p_0.

In practise, a transmitter conveys information grouped in frames to a receiver through a time varying channel. We consider the time a discrete variable, i, taking integer values, and equivalent to the number of each transmitted frame. The transmitter chooses a Modulation and Coding Scheme (MCS) for each frame i, m_i, from a set of possible MCS $\{1, 2, ..., M\}$, being M the number of total available MCS. r_j denotes de rate or spectral efficiency of MCS j. The MCS are sorted by increasing rate, i.e., $r_1 < r_2 < ... < r_M$. In the Table 5.1 it is depicted the set of MCSs employed in the forward link transmissions, these MCS are also showed in Table 4.2 with the decoding thresholds. The MCSs are taken from the forward link bearer F80T1Q1B which corresponds to frames of 80 ms, QPSK modulation and symbol rate of 33.6 ksymb/s. It should be noted that the coding rate of the channel encoder is half of the r_i values and that r_i include the factor of 2 due to the use of a QPSK constellation ($2 = \log_2(4)$).

Table 5.1: Set of MCSs (in accordance with F80T1Q1B bearer)

MCS i	1	2	3	4	5	6	7	8	9
Rate r_i	0.68	0.80	0.96	1.10	1.26	1.40	1.54	1.66	1.74

The state of the channel s_i is the maximum allowed transmission rate in time instant i. This s_i is the transformation of the effective SNR of the channel during the transmission of frame i, i.e., $SNR_{eff,i}$ into a Mutual Information value s_i or MI_i. Therefore, transmission of frame i fails (an error occurs) when s_i (or MI_i) is lower than the rate of the MCS used, r_{m_i}, otherwise it is successful.

We consider that there exists a feedback channel through which the receiver acknowledges the correct decoding of frame i and informs the transmitter about the state of the channel when frame i was received. On the one hand, the acknowledgement can be $\epsilon_i = 0$ if frame

i was decoded correctly, or $\epsilon_i = 1$ if there was an error. On the other hand, the channel quality estimated by the receiver is sent to the transmitter by means of a CQI (Channel Quality Indicator). The CQI_i indicates the index of the highest MCS supported by the channel in time instant i, and r_{CQI_i} is its rate. If no MCS is supported, then $CQI_i = 1$. The transmission of a index instead of the exact value of the channel quality allows the saving of bandwidth in feedback link.

For link adaptation on the return channel, i.e. decide the MCS used in the transmissions of the Mobile Terminal towards the satellite, we also suppose that the transmitter has some information of the state of channel through an open loop measure. This means that the Mobile Terminal apart from receiving the close loop link quality estimation via a CQI, it measures the received signal quality in the forward link and the link adaptation algorithm could make use of this value. It should be said that, due to the fact that in S-UMTS the duplexing mechanism is FDD (Frequency Division Duplex), the fading experienced by forward and return link, although similar, is slightly different. Here we considerer that the channel has a LOS component, which is the same for both forward and return link, and an independent NLOS component. In numbers, the distance between the forward link and return link sub-channels lays between 67.5 MHz and 157 MHz.

Another important thing to model in the Land Mobile Satellite (LMS) channel is the Round Trip Time (RTT), that reaches values up to 0.5 seconds in the case of geostationary satellites, the case considered here with the SL family of S-UMTS. Due to a delay of equivalent to the transmission time of d frames, when the transmitter decides the MCS of frame i, it only has available feedbacks of frames up to $i - d$, i.e., values $\epsilon_0, \epsilon_1, ..., \epsilon_{i-d}$ and $CQI_0, CQI_1, ..., CQI_{i-d}$. In most part of this project we take $d = 6$ frames, that with a frame duration of 80 ms makes RTT to take the value of 480 ms.

In Figure 5.1 it is shown the two possible different scenarios involving link adaptation: in the uppermost diagram is depicted the link adaptation in the forward link and in the down side is done the same with the return link.

Descending to the Mathematics, when the link adaptation algorithm has to choose the MCS of frame i, in general, has the following information available:

- $\epsilon_0,\ \epsilon_1,\ \cdots,\ \epsilon_{i-d}$, i.e., the sequence of ACK/NAK of the previous frames up to frame number $i - d$, where d is the number of consecutive frames a Round Trip Time corresponds to.
- $CQI_0,\ CQI_1,\ \cdots,\ CQI_{i-d}$, i.e., the Channel Quality Indicator measured by the receiver and reported to the transmitter. The CQIs have an equivalence to SNRs through the function Π: $SNR_i^{cl} = \Pi(CQI_i)$.
- $SNR_0^{ol},\ SNR_1^{ol},\ \cdots,\ SNR_i^{ol}$, i.e., the sequence of SNRs observed by the transmitter in the forward link. This is information is only employed when performing link adaptation in the return link.

In general, all the algorithms presented in this chapter choose the MCS of each frame using an LUT (Look Up Table) where the input of the LUT is the predicted SNR for time instant i. The LUT has the form a step function $\Pi(SNR)$ that maps SNR intervals to CQI values. The output of the LUT is the chosen MCS, which is the most efficient MCS that has the de-codification threshold just below the predicted SNR. In general terms, in

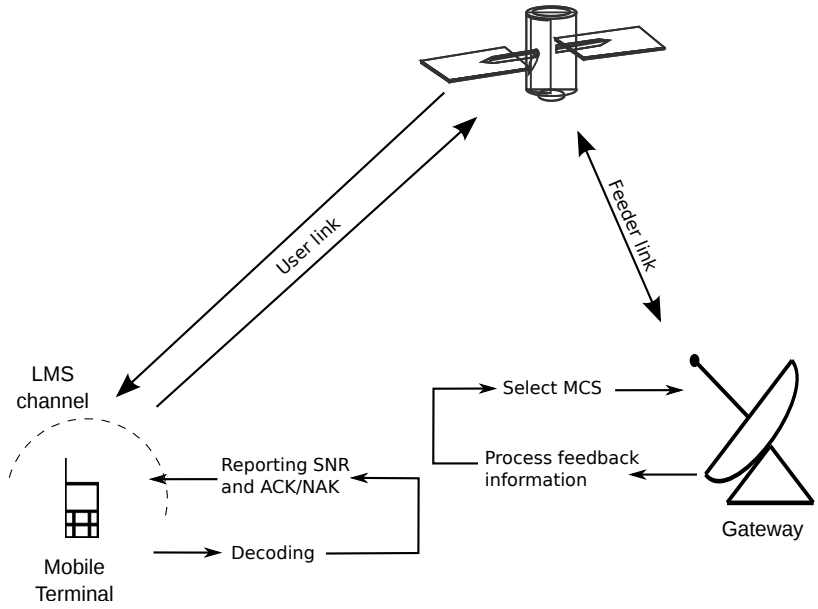

(a) Link adaptation in forward direction (Gateway to Mobile Terminal (MT))

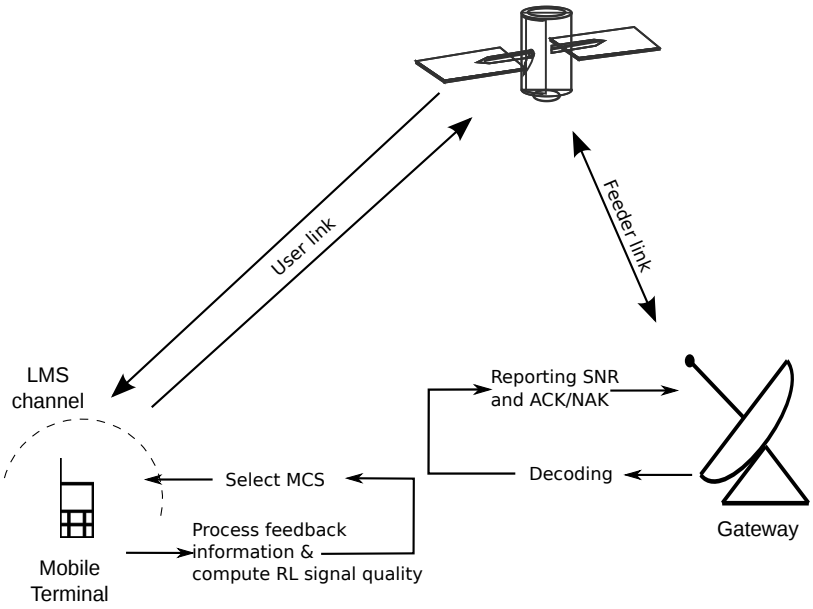

(b) Link adaptation in return direction (Mobile Terminal to Gateway)

Figure 5.1: Link adaptation process

all the studied algorithms we can express the chosen MCS with the following equation:

$$m_i = \Pi\left(\xi_i^{ol} \cdot SNR_i^{ol} + \xi_i^{cl} \cdot SNR_{i-d}^{cl} + c_i\right) \tag{5.1}$$

where

- ξ_i^{ol} and ξ_i^{ol} are the weights of the open loop SNR and closed loop SNR respectively.
- SNR_i^{ol} is the calculated SNR in open loop.

- SNR^{cl}_{i-d} is the SNR reported by the receiver in closed loop. Its is obtained using the inverse of the $\Pi(\cdot)$ function to the CQI_i received: $SNR^{cl}_{i-d} = \Pi(CQI_{i-d})$.
- c_i is a backoff margin.

The link adaptation algorithms for each frame i calculate the values of the variables of the previous equation, i.e. ξ^{ol}_i, ξ^{ol}_i and c_i using the information feed backed by the receiver (ACK/NAK ϵ_{i-d} and CQI_{i-d} along with the information it obtains in open loop SNR^{ol}_i. In each particular algorithm some of the variables in previous equation will take the value 0 or 1. All those things are shown graphically in Figure 5.25.

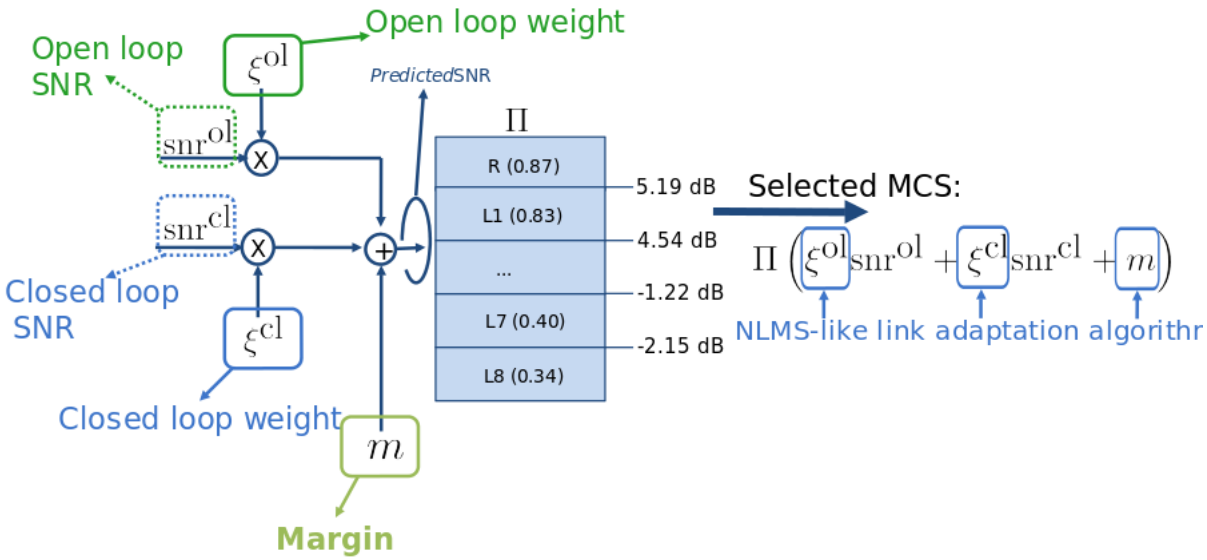

Figure 5.2: MCS selection based on a LUT

5.2 Bibliographic review: previous GPSC work

The work developed through this project is the continuation of the work realised by former GPSC members Alberto Rico-Alvariño and Jesús Arnau and my project tutor Carlos Mosquera. Therefore, it was considered interesting include here all the articles of the GPSC group related with link adaptation. In this way the reader can obtain the background to understand this project. Table 5.2 comprises all GPSC articles related with link adaptation.

The acronyms used for the authors are: AR (Alberto Rico-Alvariño), JA (Jesús Arnau), CM (Carlos Mosquera) and AT (Anxo Tato).

For finishing this section, a tag cloud is made with the words of the titles of all GPSC articles related with link adaptation, see Figure 5.3. In the tag cloud, created with an online tool, the reader can observe that most repeated terms are: Mobile-satellite (the scope where link adaptation is peformed), CSI (Channel State Information), Link-adaptation (the job we do), ACM (Adaptive Coding and Modulation) and Statistical (since we rely in a Statistical model of the LMS channel).

Year	Authors	Title
2012	AR, CM	Optimum Training for CSI Acquisition in Cognitive Radio Channels
2012	JA, AR, CM	Adaptive Transmission Techniques for Mobile Satellite Links
2013	AR, JA, CM	Statistical Cross Layer Adaptation in Fast Fading Mobile Satellite Channels
2013	JA, CM	Open Loop Adaptive Coding and Modulation for Mobile Satellite Return Links
2013	AR, JA, CM	Cross Layer Link Adaptation in Time Varying Mobile Satellite Channels with Statistical and Outdated CSIT
2014	AR, JA, CM	Balancing Closed and Open Loop CSI in Mobile Satellite Link Adaptation
2015	AR, AT, CM	Robust Adaptive Coding and Modulation Scheme for the Mobile Satellite Forward Link

Table 5.2: Articles of GPSC related with link adaptation

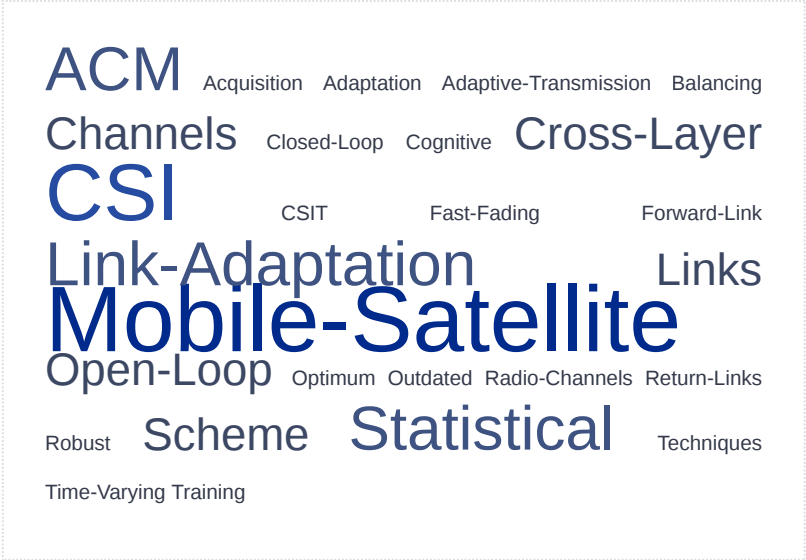

Figure 5.3: Tag cloud with the titles of the GPSC articled. Created with `http://tagcrowd.com`

5.3 Tools for analysing the link adaptation

In this section some transversal tools are introduced. They are very useful to analyse and understand the performance results of the link adaptation algorithms.

5.3.1 Correlation

The link adaptation algorithms in each step have to update the weights ξ_i and the margin c_i prior to deciding the MCS. The variables, ξ_i and c_i, can be increased in a low quantity

if an ACK is received or can be decreased in a bigger quantity if an error occurs. This is ruled by one thing: the correlation between the predicted effective SNR and the result of the transmissions (ACK/NAK), which is derived by the real effective SNR the frame suffers. Therefore, an important point to understand the results obtained with the link adaptation schemes is to know the autocorrelation of the effective SNR after a lag equal to the RTT.

In this section we compute such autocorrelation for an elevation of 40^o, the typical in our latitude, five environments of the Fontan model (Open, Suburban, Urban, I-tree and H-tree) and 10 different speeds: 1 km/h, 6 km/h, 9 km/h, 12 km/h, 20 km/h, 25 km/h, 50 km/h, 80 km/h and 120 km/h. The Table 5.3 links some of these speeds with real life situations:

Speed (km/h)	Situation
1	Almost static
6	Human walking
25	Human running or bike
50	Slow car in urban or suburban environment
120	Fast car in open environment

Table 5.3: Speeds and real situations

The results have been calculated using 20,000 consecutive values of effective SNR in dB and employing the function *autocorr* of Matlab with 7 as lag number. It has been used only 1-state of the Fontan model. The results are collected in Figure 5.4 where the abscissa axis represents the delay (from 0 to 7 frames).

In the graphics there are two values of interest. On the one hand, the autocorrelation in lag number 6, which corresponds to a RTT, and on the other hand, the autocorrelation in lag 1, which is an approximation of the cross-correlation of open loop SNR, i.e. the correlation between the effective SNR on the forward channel at time i and the effective SNR in return channel at time $i + 1$.

As observed in the graphics for 1 km/h we only have an acceptable correlation (more than 0.4) after a RTT in open, urban and i-tree environments. If we consider the minimum reasonable speed for a mobile, i.e. the 6 km/h of a human walking, only open and urban environments exceed slightly 0.2. For the rest of speeds and environments we can say that the correlation after a RTT (delay 6 in the figures) is negligible.

With respect to the open loop correlation, i.e. at lag 1, there are significant correlation (over 0.6) for speeds lower than 25 km/h in Open and Urban, for a speed of 1 km/h in Suburban and H-tree, and for speeds lower than 12 km/h in I-tree.

Its utility is that observing the values the autocorrelation takes at lags 1 and 6, it can be predicted which of the algorithms (open loop or closed loop) will outperform the other.

5.3.2 Prediction error of the effective SNR

There is a curious phenomenon observed in link adaptation that, at a first glance, can seem incorrect. The communications achieve a better performance under the LMS channel when using higher speeds. When one calculates the variance of the effective SNR finds

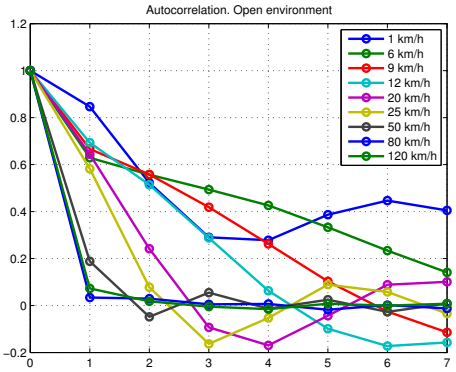

(a) Open

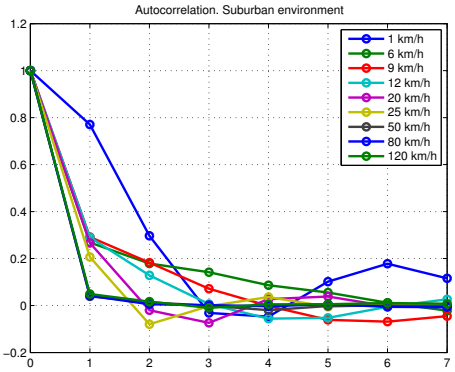

(b) Suburban

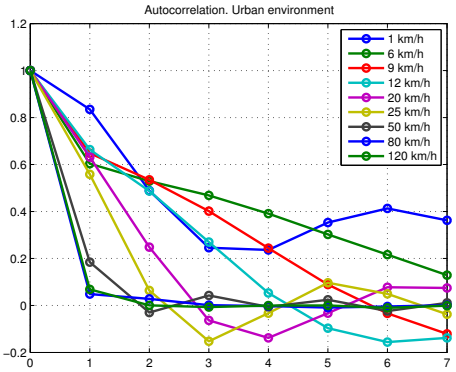

(c) Urban

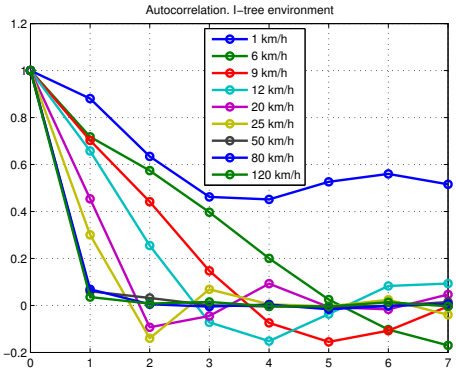

(d) Intermediate-tree shadow

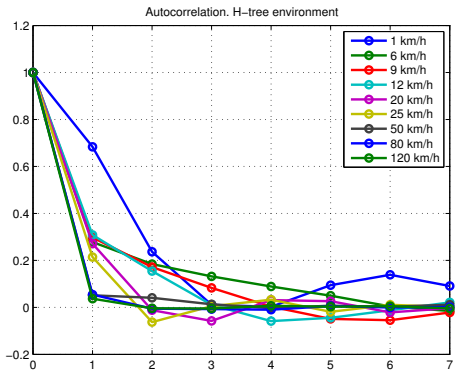

(e) High-tree shadow

Figure 5.4: Autocorrelation of the effective SNR for different environments

out that the variance decreases with the speed. This causes that, for example, at higher speeds higher throughput is achieved and the backoff margin of the algorithm is lower.

If we use the current effective SNR ρ_i to predict a future value of it a RTT later, $\hat{\rho}_{i+d}$

$$\hat{\rho}_{i+d} = \rho_i + e_i \tag{5.2}$$

we commit a prediction error e_i.

It have been calculated the prediction error for two different environments (suburban and I-tree) and several speeds (6 km/h, 25 km/h, 50 km/h and 120 km/h). The distribution of that error was found to follow approximately a Gaussian distribution. The experimental probability density function for both environments is shown in Figure 5.5 and the variance of the error in Table 5.4.

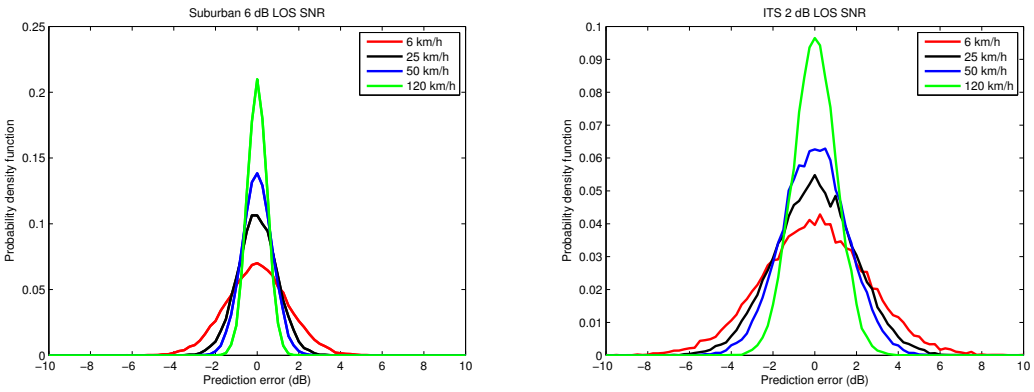

(a) Suburban environment, 6 dB LOS SNR (b) ITS environment, 2 dB LOS SNR

Figure 5.5: Distribution of the prediction error (dB)

Speed (km/h)	**Suburban**	**I-tree**
6	2.1950	6.3062
25	0.8768	3.6678
50	0.5235	2.4421
120	0.2271	1.0850

Table 5.4: Variance of the prediction error

At the light of the results and as stated early, the variance of the prediction error, and of the effective SNR itself, decreases with the speeed of the mobile terminal. The reason is that for low speeds the effective SNR coincide with the instantaneous channel values due to the channel does not change through the span of a frame. But, for higher speeds the channel has several oscillations inside one frame and the effective SNR, that is an unique value for the whole frame, does some kind of averaging, reducing therefore its variance. In Figures 5.6-5.10 is shown the evolution of the channel for five different speeds (blue line) and superimposed the values of the effective SNR for each frame (red line). The reader will be able to observe the behaviour explained previously.

5.3.3 Outage probability of 3-state channel model

Typically, the link adaptation algorithms try to maximize the spectral efficiency with a constraint on the Frame Error Ratio (FER) of, for example, $10^{-2}, 10^{-3}$, or 10^{-4}. When a simulation is carried out to test the performance of some algorithms, there are some parameters that have to be set up: target FER, environment, speed and LOS SNR.

We can define the outage probability as the probability that the channel to be in some state such that, even with the most robust MCS (Modulation and Coding Scheme), a successful

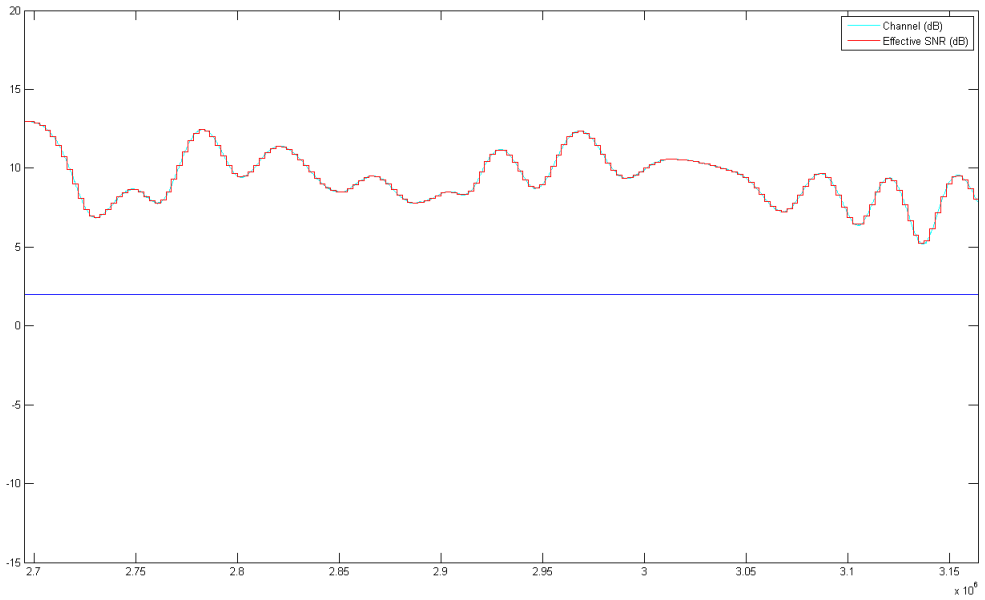

Figure 5.6: Channel and effective SNR, 1.5 km/h

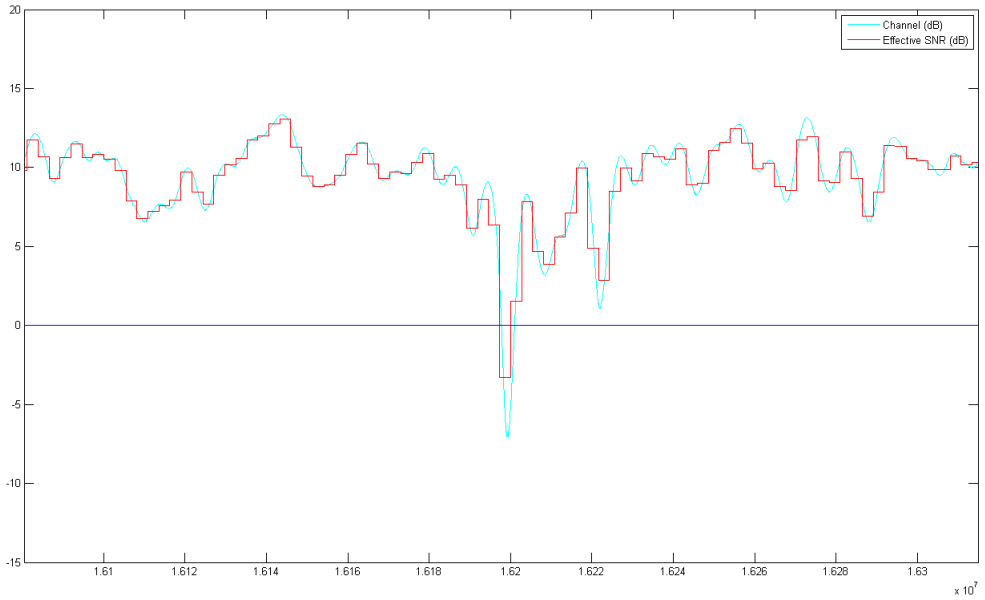

Figure 5.7: Channel and effective SNR, 6 km/h

transmission is not possible. Obviously, the FER that can be achieved is always greater than the outage probability, or in other words, if an algorithm is required to achieve a FER that is lower than the outage probability of the simulation scenario, the FER would never be reached. Therefore it is very useful to have some graphics of the outage probability for different scenarios in order to know in advance if a specific target FER can be reached.

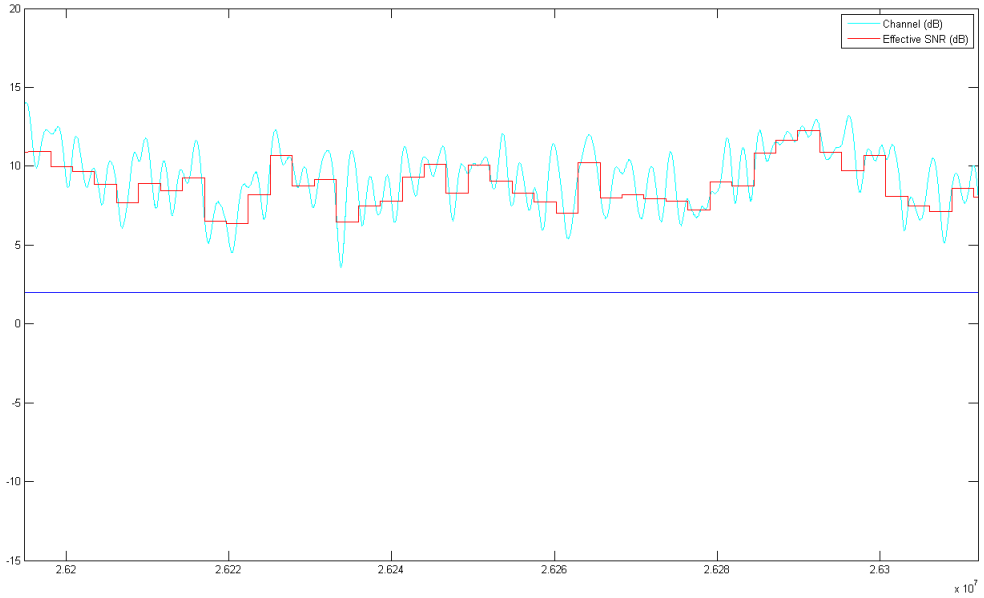

Figure 5.8: Channel and effective SNR, 25 km/h

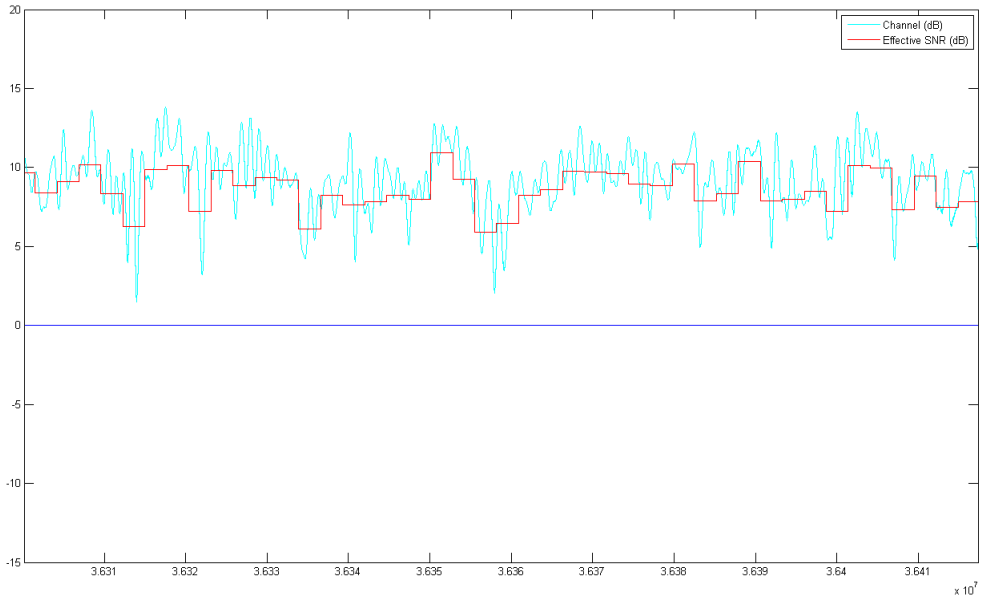

Figure 5.9: Channel and effective SNR, 50 km/h

When using the bearer F80T1Q1B the outage probability equals to the probability that the effective SNR descends below $-2.1534\ dB$, i.e. the decoding threshold of the more robust MCS (the one with lower coding rate). In Figure 5.11 we include the outage probability for the five environments and five different speeds ranging form 1.5 km/h to 120 km/h. The probability is calculated from -6 dB to 30 dB of LOS SNR in steps of 2 dB. Each value

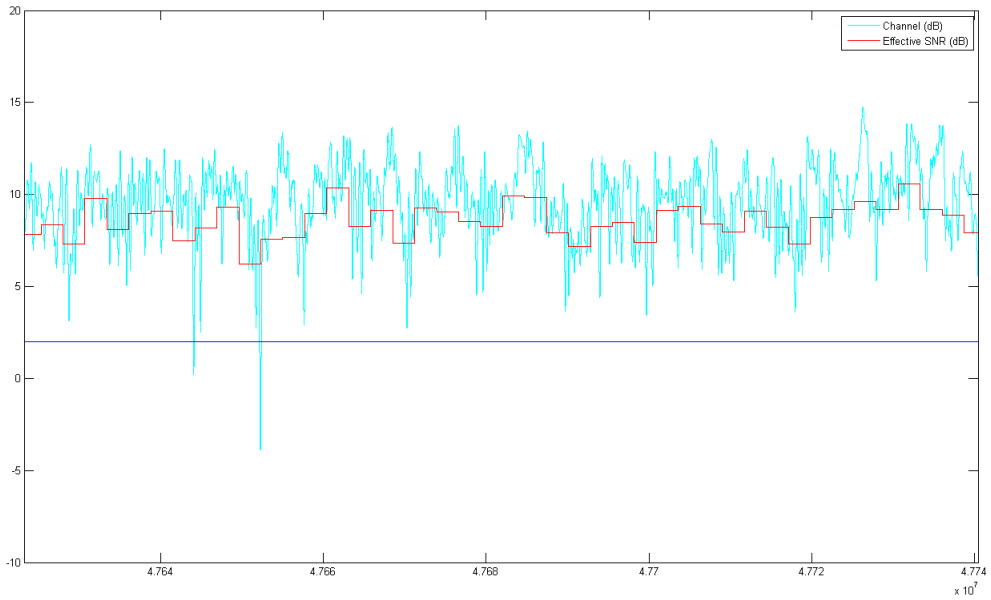

Figure 5.10: Channel and effective SNR, 120 km/h

is the average of four different realizations and in each one 50.000 frame transmissions are simulated. When there is no line in the graphic means that the outage probability if less than the minimum observable ($5 \cdot 10^{-6} = 1/(50000 \cdot 4)$).

5.3.4 Graphics with the spectral efficiency and FER

Once a simulation of some link adaptation scenario is launched and it finish, the next step is to analyse the results. The first tool is to plot in a graphic the spectral efficiency and the FER (Frame Error Ratio) achieved. Usually, the results of different algorithms are plotted together on the same figure in order to compare them, or is plotted the same algorithm under different scenarios.

The simulator has some specific methods in the class *SimulMult* named *plotTputVsSNR* and *plotFerVsSNR* that automatically plot the results of the simulation. One example of the typical graphics is shown in Figure 5.12.

5.3.5 Graphics with the evolution of the parameters

In order to have a complete understanding of how behave the algorithms, apart from use the graphics introduced in the previous epigraph, is good the see what happens in the time domain, i.e. see the evolution of the algorithm variables: ξ_i and c_i. With these graphics it can be observed how many time need the variables to converge to their final values.

Down below Figure 5.13 plots an example of time evolution of the parameters in two different scenarios: I-tree environment with a targe FER of 0.1 and suburban environment

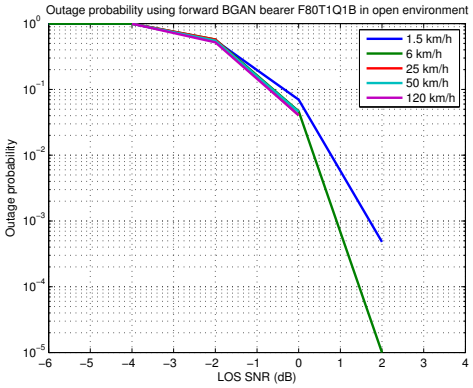

(a) Open

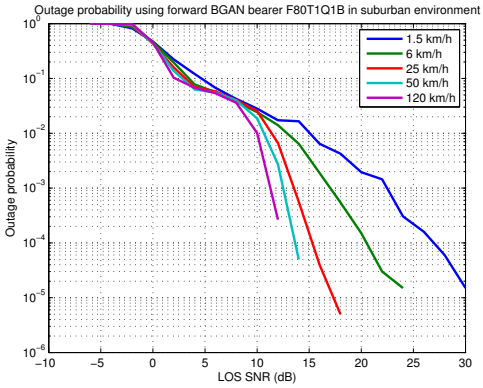

(b) Suburban

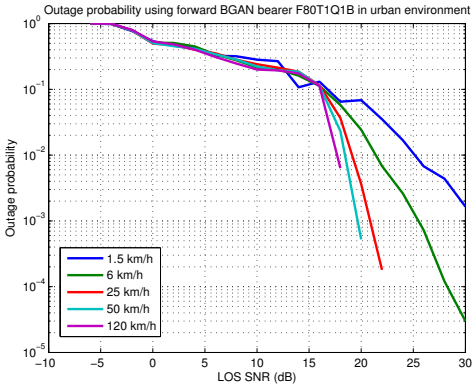

(c) Urban

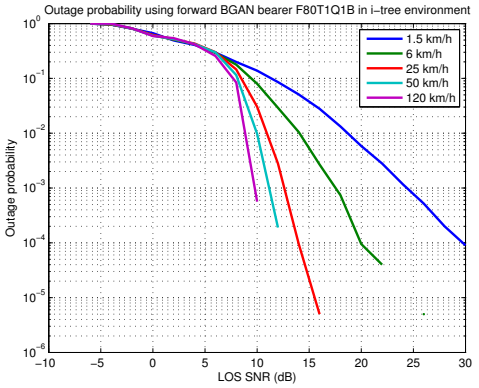

(d) Intermediate-tree shadow

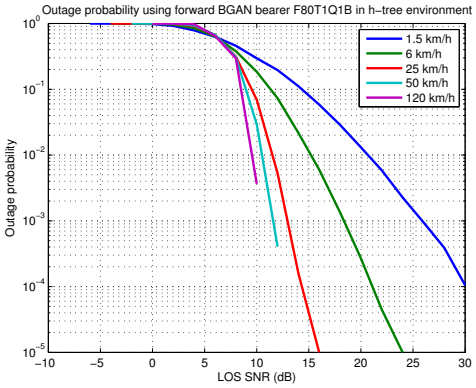

(e) High-tree shadow

Figure 5.11: Outage probability for different environments and speeds

with a target FER of 0.01. These graphic are taken from the article [26] and will be explained in detail in the next section.

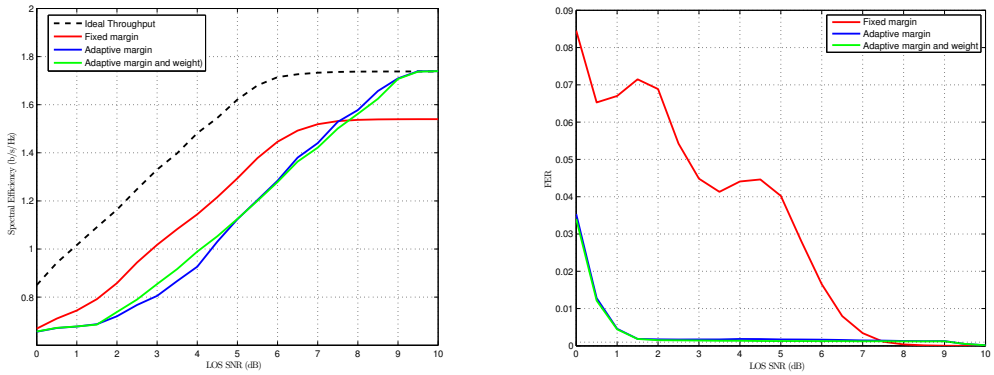

(a) Spectral efficiency (b) FER

Figure 5.12: Example of spectral efficiency and FER graphics

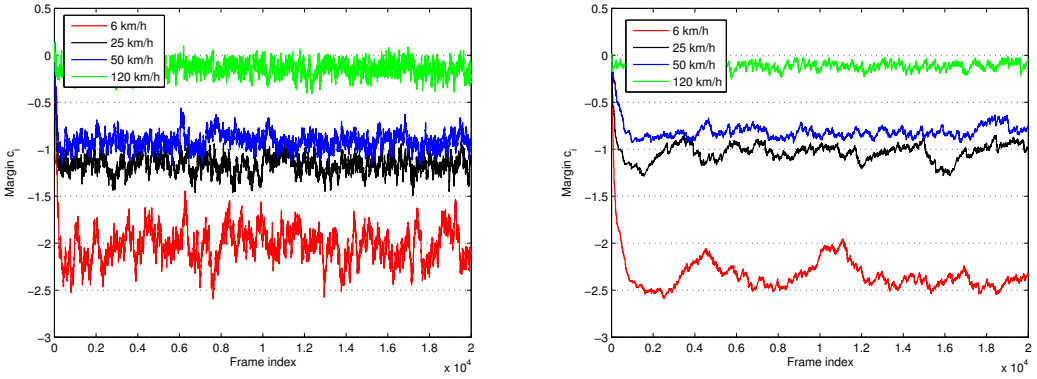

(a) I-tree, target FER of 0.1 (b) Suburban, target FER of 0.01

Figure 5.13: Example of evolution of the margin c_i

5.3.6 Graphics summarizing the link adaptation problem

Finally, it is presented the last tool. It consists in a combination of different plots in the same graphic in order to see "what happens" with the algorithm in the time domain. In the same graphic are plotted the following elements:

- **transmission result (ϵ_i)**: ACKs (successfuls) with blue circles at 0, NAKs (error) with blue circles at 1 level.
- **used MCS for each transmission (m_i)** situated at the level of the rate of the MCS itself
- **channel MI** in a red line. Its upper bound is 2 due to the fact that a QPSK constellation is employed.
- **rate allowed** in black line. It is transformation of the channel MI into the set of allowable rates of the specific bearer.

Figure 5.14 is an example of this tool for analysing the behaviour of the algorithms. It should be said that in an article of Oscar del Río Herrero and Riccardo de Gaudenzi titled *High Efficiency Satellite Multiple Access Scheme for Machine-to-Machine Communications* [27], the authors employ a similar graphic to the presented in this epigraph.

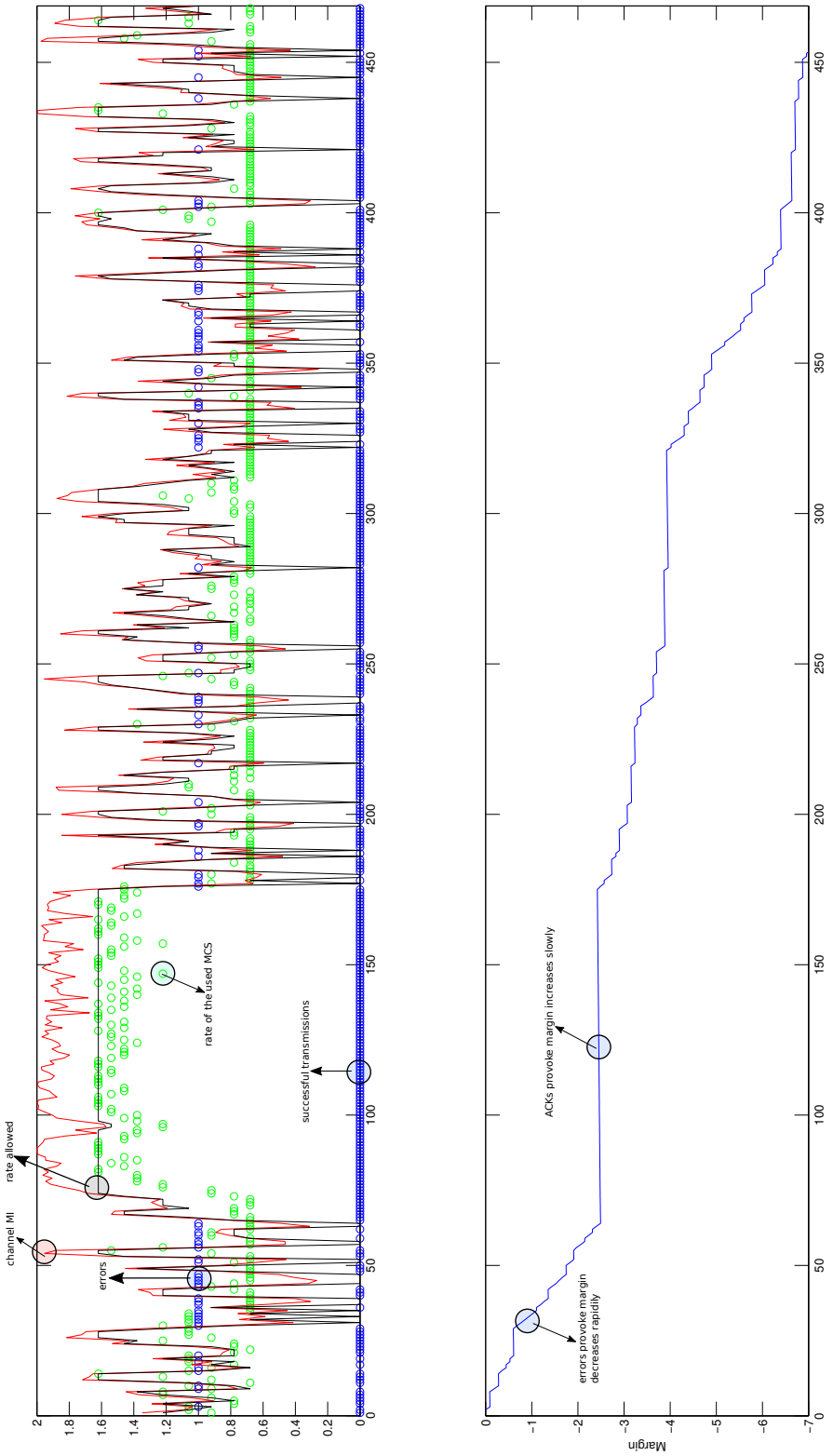

Figure 5.14: Graphical tool for analysing the time behaviour of the algorithms

5.4 Link adaptation in S-UMTS

In this section the proposed algorithms for link adaptation are presented along with their performance under the Fontan LMS channel.

My work starts analysing the results of the article *Balancing Closed and Open Loop CSI in Mobile Satellite Link Adaptation* [3] and continues extending those results to the Fontán 3-state channel model. After that, the algorithms employed in the return link are adapted to the forward link scenario. The main results for the forward link are collected in the article *Robust Adaptive Coding and Modulation Scheme for the Mobile Satellite Forward Link* [26] which I co-author and published in the SPAWC2015 conference. After that, in order to increase the spectral efficiency, new algorithms are explored. It was discovered that these new algorithms always achieve an improvement in the spectral efficiency at the expense of increasing the FER (Frame Error Ratio). Finally the concept of informed outage capacity is introduced to offer a means to compare the efficiency of our algorithms with the theoretical capacity a transmitter can achieve. The last subsection is devoted to the conclusions of this section.

5.4.1 Algorithm for return link (1-state channel)

The innovation of the article *Balancing Closed and Open Loop CSI in Mobile Satellite Link Adaptation* [3] is that proposes a new algorithm that automatically balances closed loop CSI and open loop CSI while maintaining an adaptive back-off margin. In other words, the algorithm has an adaptive margin c_i and also uses some variables to give a weight to the received close loop SNR ξ^{cl} and to give a weight to the measured open loop SNR ξ^{ol}.

The selection of the MCS is done through the following expression:

$$m_i = \Pi(\xi_i^{ol}\mathrm{SNR}_i^{ol} + \xi_i^{cl}\mathrm{SNR}_{i-d}^{cl} + c_i) \tag{5.3}$$

The algorithm for updating the margin c_i and the weights ξ_i^{ol} and ξ_i^{cl} is found as the solution of the optimization problem which follows:

$$\min_{c,\xi^{ol},\xi^{cl}} J(c,\xi^{ol},\xi^{cl}) = \min_{c,\xi^{ol},\xi^{cl}} |\mathbb{E}[\epsilon_i] - p_0|^2 \tag{5.4}$$

where p_0 is the target FER (typically 10^{-3}), ϵ_i is the error event in the i-th frame (1 for error, 0 for successful transmission) and $\mathbb{E}[\cdot]$ is the expectation operator.

Here we do not detail the steps that lead to the algorithm, this will be done in the section devoted to the robust algorithm for the forward link. It suffices to say that a stochastic gradient descent on $J(c,\xi^{ol},\xi^{cl})$ is performed (see the article [3] for more details) and that in each iteration of the algorithm the variables are updated in the following way:

$$\begin{pmatrix} c_{i+1} \\ \xi_{i+1}^{ol} \\ \xi_{i+1}^{cl} \end{pmatrix} = \begin{pmatrix} c_i \\ \xi_{i+1}^{ol} \\ \xi_{i+1}^{cl} \end{pmatrix} - \frac{\mu}{\theta^2 + \mathrm{SNR}_{ol,i-d}^2 + \mathrm{SNR}_{cl,i-2d}^2}(\epsilon_{i-d} - \tilde{p}_{0,i}) \begin{pmatrix} \theta \\ \mathrm{SNR}_{i-d}^{ol} \\ \mathrm{SNR}_{i-2d}^{cl} \end{pmatrix} \tag{5.5}$$

with $\tilde{p}_{0,i}$ following the recursion

$$\tilde{p}_{0,i+1} = \tilde{p}_{0,i} - \lambda(\epsilon_{i-d} - p_0). \tag{5.6}$$

This algorithm, named Dual, is compared with other three algorithms:

- A variant of Dual algorithm where there is only one weight: $\xi_i^{ol} = 1 - \xi_i^{cl}$
- An open loop algorithm, that only makes use of open loop SNR and where $\xi_i^{ol} = 1$ and $\xi_i^{cl} = 0$.
- A closed loop algorithm, that only makes use of closed loop SNR and where $\xi_i^{cl} = 1$ and $\xi_i^{ol} = 0$.

Hereafter we collect the simulation results taken from the article corresponding to the parameters listed in Table 5.5.

Parameter	Value
θ	10
λ	10^{-3}
μ	1
d	5 frames (GEO satellite)

Table 5.5: Values of the parameters

The results were obtained under the following conditions: Loo channel (only state LOS of the Fontán model), intermediate tree shadow environment, speeds 0.3 m/s, 3 m/s and 15 m/s, LOS SNR ranging from 0 to 10 dB and target FER 0.1 and 0.01. Now we include the graphics of the spectral efficiency and FER for three different scenarios the article considers:

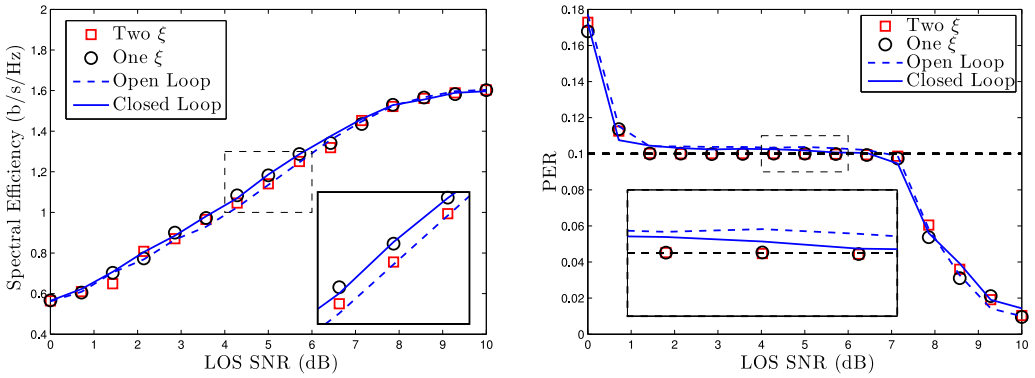

Figure 5.15: I-tree state LOS, 0.3 m/s, $p_0 = 0.1$

The authors of the article comment the three graphics of Figures 5.15-5.17 saying that the proposed methods fix the target FER more accurately than the others, and that in all cases the method with one ξ is more robust than the method with two ξ. Focusing on the former (one ξ), it always outperforms (or evens with) closed loop adaptation, and it also outperforms open loop adaptation in some cases. It shall be remarked that the target FER might not be achievable in very high or very low SNR scenarios where the variables ξ_i and c_i diverge.

In summary, under the 1-state channel (Loo distribution) the proposed dual method is shown to offer a good performance with respect to open loop and closed loop adaptation.

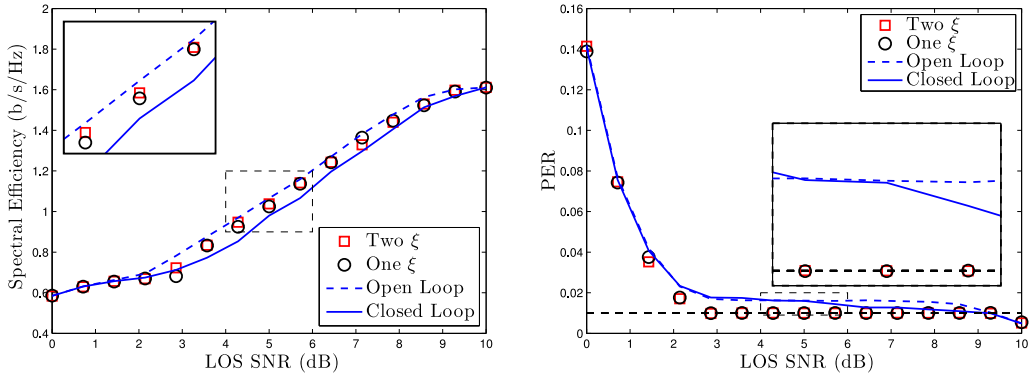

Figure 5.16: I-tree state LOS, 3 m/s, $p_0 = 0.01$

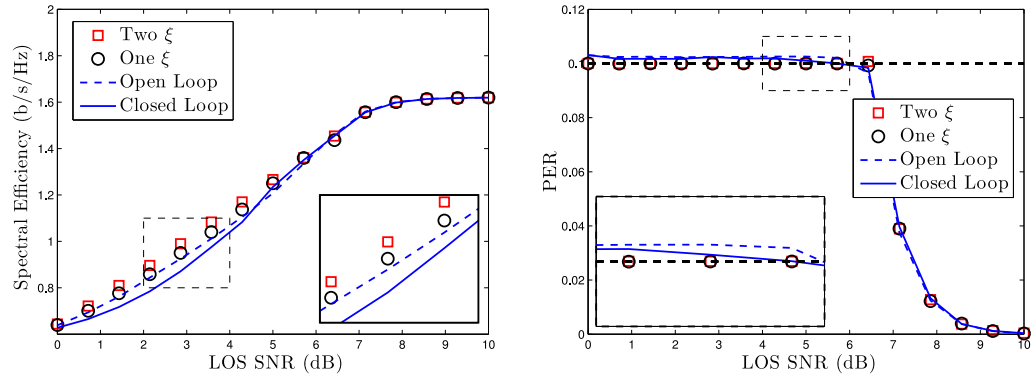

Figure 5.17: I-tree state LOS, 15 m/s, $p_0 = 0.1$

In the next subsection, the results of the simulation under the 3-state Fontán channel model are introduced.

5.4.2 Algorithm for return link (3-states channel)

Firstly, it should be said that part of the results included in this subsection are taken from an article named *Link Adaptation in Mobile Satellite Links: Schemes for Different Degrees of CSI Knowledge* that was submitted for publication to the International Journal os Satellite Communications and Networking.

In the previous subsection it was compared the performance of the Balanced Dual algorithms with Open and Closed loop adaptation algorithms but with just one state channel, the Line of Sight (LOS) state. This is not a real situation because during normal operation the Mobile Terminal will move around some environment and it will not have LOS to the satellite all the time. Therefore, it is important to test the algorithms under the whole 3-state Fontan LMS channel model.

The mutual information simulator employed for all the simulations of these project is an expanded version of the one developed by Alberto Rico-Alvariño which had implemented

only the 1-state channel. Hence, one of my first tasks was to program the whole 3-state channel model and test it. It has been used the simulator with the new functionality (3-state channel model) to obtain the graphical results illustrated in the figures here below.

In each one of the graphics are compared the two algorithms that balance the open and the closed SNR against other three algorithms: simple open loop, simple closed loop and ARF-M. The latter is an algorithm that, in contrast to the other three algorithms, it does not use any Channel State Information, in each algorithm iteration it only employs the ACK/NAK information.

Hereafter we are going to show the graphics of spectral efficiency and FER for the five scenarios of Table 5.6. The parameters of the algorithms are collected in Table 5.7.

Channel environment	**Speed (km/h)**
Open	120
Open	10
Suburban	50
I-tree	60
I-tree	12,5

Table 5.6: Trial scenarios

Parameter	**Value**
LOS SNR	0 - 26 dB
Number of transmitted frames	60,000
Environments	open, suburban, i-tree
Speeeds	120, 60, 50, 12.5 and 10 km/h
target FER p_0	0.01
θ	10
λ	10^{-3}
μ	1 for dual; 0.1 for open, closed and ARF-M
feedback delay	5 codewords (400 ms)

Table 5.7: Algorithms parameters

Now we include the five sets of graphics for the situations gathered in Table 5.6.

With regard to the FER, the algorithms converge to the target FER $p_0 = 0.01$ at a LOS SNR ranging from 12 to 16 dB. It is observed that for lower speeds the LOS SNR for which the FER is achieved is larger since at lower speeds the channel is more complicated.

With regard to the spectral efficiency, for extremely low SNRs (0-4 dB) and for extremely high SNRs (18-26) all the algorithm have the same performance in all the environments and speeds. This is due to the fact that for very low SNRs the algorithms cannot converge to the desired FER and for very high SNRs the channel is so good that there is no difference between one algorithm and others.

In the middle of the range of SNRs, between 6 dB and 18 dB, there are large differences between the spectral efficiency achieved by some algorithms and others. On the one hand, in general Closed loop has a similar performance to ARF-M and these two algorithms are who have the lower spectral efficiency. The explanation of their similar behaviour is that in the multi-state channel, even for low speeds, the autocorrelation is low, therefore, not

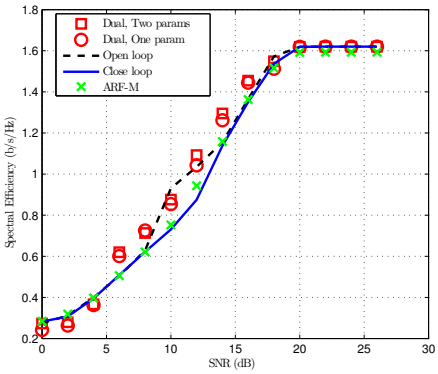

(a) Spectral efficiency

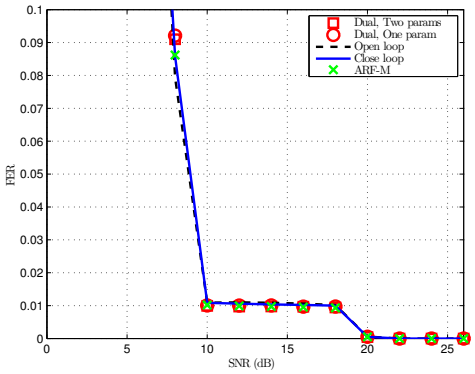

(b) FER

Figure 5.18: Spectral efficiency and FER for Open 120 km/h

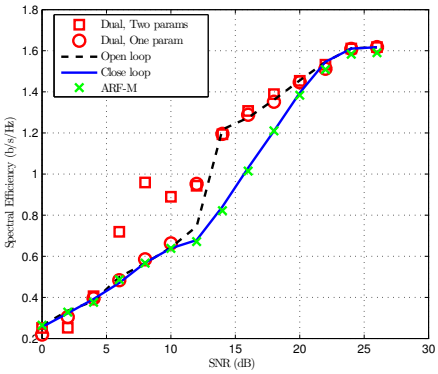

(a) Spectral efficiency

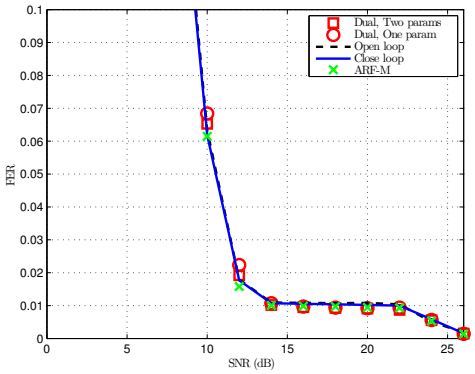

(b) FER

Figure 5.19: Spectral efficiency and FER for Open 10 km/h

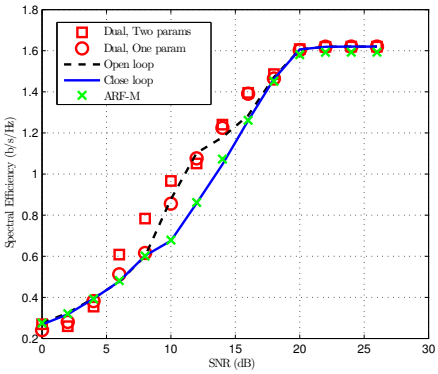

(a) Spectral efficiency

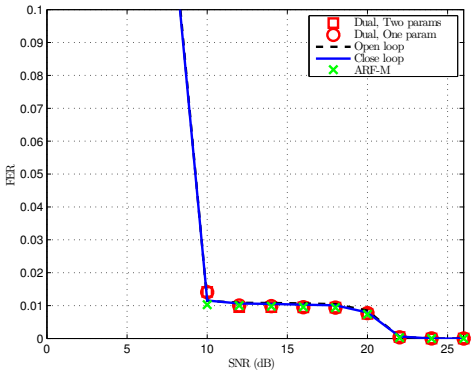

(b) FER

Figure 5.20: Spectral efficiency and FER for Suburban 50 km/h

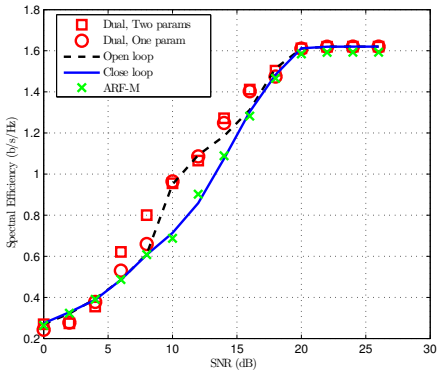

(a) Spectral efficiency

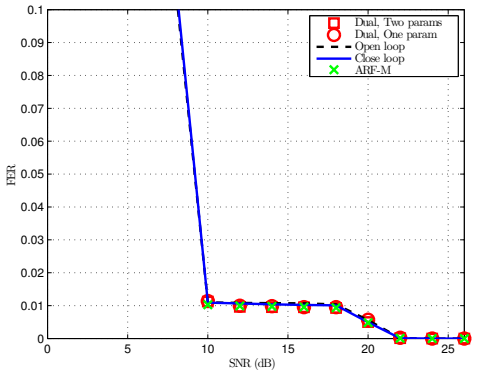

(b) FER

Figure 5.21: Spectral efficiency and FER for I-tree 60 km/h

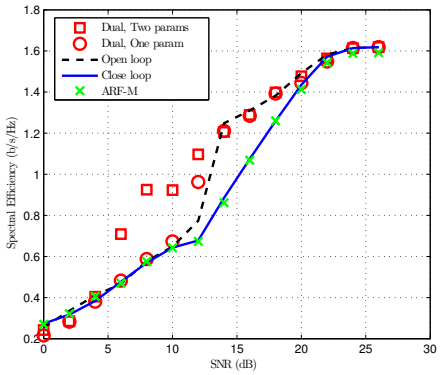

(a) Spectral efficiency

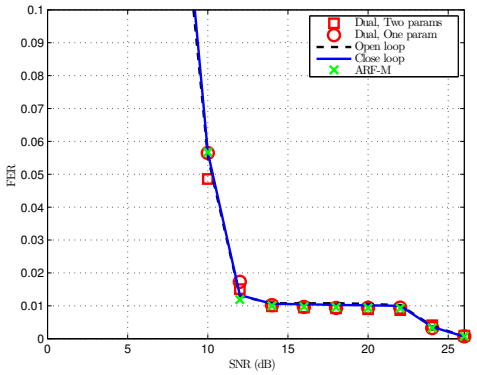

(b) FER

Figure 5.22: Spectral efficiency and FER for I-tree 12.5 km/h

using the closed loop SNR or using it, has the same effect, because after a RTT there is no correlation between the received closed loop SNR and the SNR the transmitted packet is going to suffer.

On the other hand, the Dual algorithms and Open loop always outperform Closed loop and ARF-M. Among them, the two Dual algorithms have a similar performance, but the algorithm with two parameters (two weights and a margin) almost always has a slightly better efficiency than the algorithm with one parameter (one weight and a margin). In general, both Dual algorithms are comparable to Open loop in terms of efficiency although almost always Dual algorithms match or outperform Open loop.

Curiously, there exist only one value of LOS SNR where Open loop algorithm outperforms Dual algorithms. This effect does not happen in all simulation because it is related with the time behaviour of the algorithms. In some cases, at the first value of SNR where the target FER is achieved, Open loop outperforms Dual algorithms. The reason can be that Open loop converges rapidly because it only has to adapt one variable (the margin) and Dual algorithms have to adapt until three variables (the margin and two weights). This

effect is shown in the graphics of Figure 5.23.

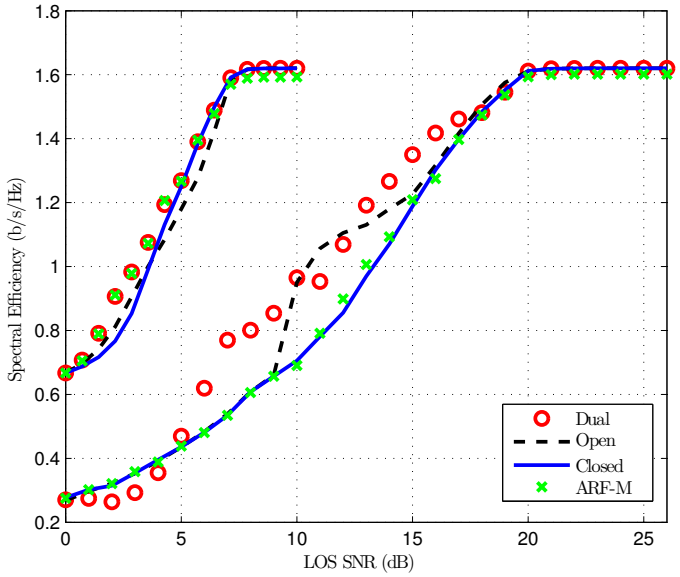

(a) Spectral efficiency

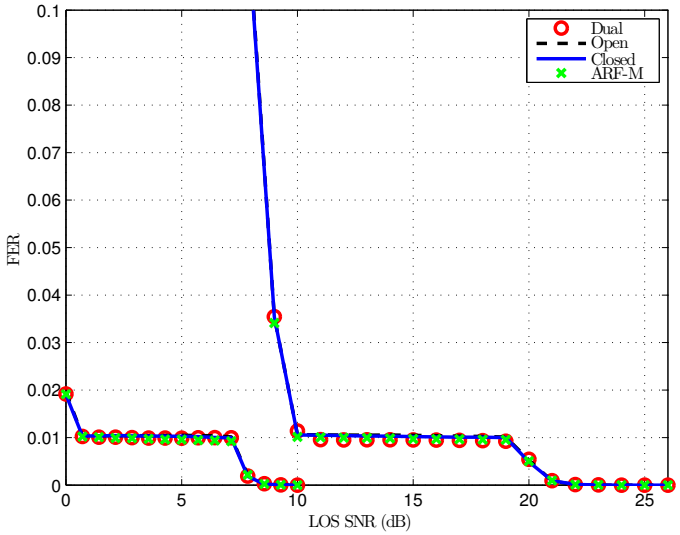

(b) FER

Figure 5.23: I-tree 60 km/h. Comparison of 3-state channel vs 1-state channel

In order to finalise this subsection, the Figure 5.23 will be commented. In this Figure we plot together the results of the simulation with just 1-state (left side graphics) and with 3-states (right side graphics). With this figure it can be understood clearly the impact of the 3-state channel. We observe that with the 3-state channel the algorithms converge to the target FER at a SNR 10 dB higher than in the LOS state. Or if we see it in terms of spectral efficiency, the maximum rate allowed by the return bearer (1.61) is achieved at a SNR 12 dB higher in the case of 3-state channel in comparison with the 1-state channel.

5.4.3 Robust algorithm for the forward link

This subsection is taken totally from the article of Alberto Rico-Alvariño, Carlos Mosquera and myself titled *Robust Adaptive Coding and Modulation Scheme for the Mobile Satellite Forward Link* published in the 16th International Workshop on Signal Processing Advances in Wireless Communications (SPAWC) [26].

Abstract

We consider the application of adaptive backoff margins to mobile satellite links. The mapping of channel state information to modulation and coding schemes is complemented by a margin which is obtained as the result of a stochastic gradient descent scheme which uses the decoding history reported by the receiver. The proposed solution does not rely on the knowledge of the channel model and its parameters, which helps to improve its robustness with respect to previous schemes. Analysis and simulations are provided to certify the potential of the exposed ideas.

Introduction

Time-varying channels are more the rule than the exception in modern wireless communications, so that adjustment of transmission parameters to the conditions of the communication channel is standard practice in many cases. This adaptation is critical to get the most of channels which evolve with time due to, for example, mobility, atmospheric changing conditions or interference. Link adaptation has been successfully included not only in several terrestrial standards but also in satellite communications; let us consider, for example, cellular technologies (3GPP LTE, IEEE 802.16), wireless local area networks (IEEE 802.11) and satellite standards (DVB-S2, DVB-RCS). Even mobile satellite links, for which the tracking of the channel conditions is difficult due to the high round trip time (RTT), conceive the use of adaptive communications [11]. Feedback, in diverse forms, is key to track the channel response and adapt conveniently. Link adaptation requires some sort of coordination between the transmitter and the receiver to be able to track the channel changes. In particular, channel state information (CSI) at the transmitter (CSIT) is necessary (or at least desirable) to apply link adaptation methods. This CSIT can be obtained by means of a feedback channel from the receiver, that reports back information on the channel quality, the decoding performance or both. Most current wireless standards include some sort of feedback mechanism that allows the application of link adaptation. Here in Figure 5.24 we show the diagram of the scenario of link adaptation in the forward link again in order to help the reader. Continuing, the channel quality indicator (CQI) can be in diverse forms such as estimated SNR or supported rate. However, a complete characterization of optimal solutions for feedback channels has proved elusive over the years, although several schemes which address a variety of practical situations exist. For the case of flat-fading channels, as those found in different types of satellite connections, the objective is the adjustment of the modulation and coding scheme (MCS) and power to maximize the spectral efficiency, subject to an error rate constraint. If we focus on the rate adaptation problem, the proposed methods consist basically of a look-up table (LUT) that matches the received SNR feedback to an MCS. This table is obtained by means of theoretical calculations or link level simulators in controlled conditions, which

lead to the selection of appropriate thresholds to switch the different MCS. If the link level simulations are representative of the scenario where the link adaptation protocol is going to operate, then the LUT-based approach will offer a near-optimal performance. However, the inaccuracy of the CSIT is a common source of performance degradation. In the case of mobile satellite links, the large RTT causes CSIT to be outdated even for moderate terminal speeds. Different techniques have been developed, such as the combination of automatic repeat request (ARQ) and multi-layer coding,or HARQ-IR protocols based on layering coding.

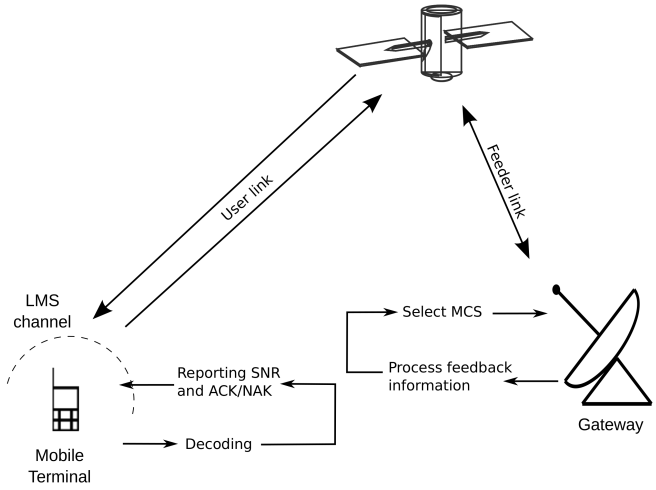

Figure 5.24: Scenario of link adaptation in the forward link

In this paper we study the application of adaptive backoff margins to mobile satellite links, in an attempt to improve on the use of unnecessarily large link margins to account for fading. ARQ will not be explicitly considered, although the related ACK/NAK will be exploited. In a previous work we applied these ideas to the return link [3], by using a judicious combination of open and closed loop quality metrics in addition to an adaptive margin. Here we focus on the forward link, by deriving as in [3] the backoff margin as a stochastic programming solution to an optimization problem.

Robust adaptive margin

Firstly, it should be said that no knowledge about the specific parameters of a channel model is assumed for obtain the algorithms. Therefore, the resulting link adaptation scheme is thought to work well in a large variety of channel conditions.

In the operation we suppose that transmitter uses a look-up table (LUT) that maps SNRs to MCS (see Figure 5.25), as explained in the section devoted to the system model. To the SNR used in the LUT it is added an conveniently chosen back-off margin c_i:

$$m_i = \Pi(\mathrm{snr}_{i-d} + c_i) \tag{5.7}$$

The application of adaptive margins with CQI information is a common strategy, also used in satellite communications for slowly variant fixed communications, although mostly

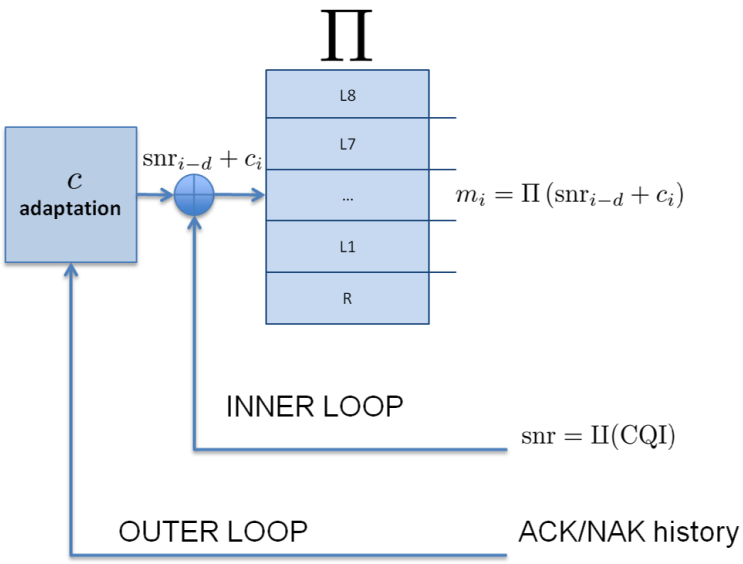

Figure 5.25: MCS selection based on a LUT

based on ad-hoc justifications. The margin c_i in (5.7) accounts for the modeling errors and the obsolescence of SNR, which is received by the transmitter at least an RTT after the corresponding block was sent. An adequate choice of c_i seems to require the knowledge of the channel statistics. Nevertheless, in an effort to obtain a flexible solution not requiring a specific knowledge about the channel, the margin can be obtained as the solution of an optimization problem for a given FER p_0:

$$\min_c J(c) = \min_c \left|\mathbb{E}[\epsilon] - p_0\right|^2 . \tag{5.8}$$

The choice of a good p_0 is not trivial, since it will have an impact on the final throughput, which will also depend on the existence of retransmission mechanisms. In practical cases $p_0 = 0.1$ is acknowledged to be a good reference [28], although this is not necessarily the case in the setting under study. If we apply a gradient descent operation to solve (5.8), then

$$c_{i+1} = c_i - \mu_i \frac{\partial J}{\partial c}\,(c_i) \tag{5.9}$$

with μ_k a sequence of positive numbers. The value of the derivative is

$$\frac{\partial J}{\partial c} = \frac{\partial \mathbb{E}[\epsilon]}{\partial c}\,(\mathbb{E}[\epsilon] - p_0) \tag{5.10}$$

so the gradient descent is

$$c_{i+1} = c_i - \mu_i \frac{\partial \mathbb{E}(\epsilon)}{\partial c}\,(\mathbb{E}(\epsilon) - p_0)\,. \tag{5.11}$$

Note that (5.11) depends on the function $\mathbb{E}(\epsilon)$ and, therefore, cannot be obtained without statistical knowledge of the channel. We propose two modifications to (5.11). First, we

substitute $\mathbb{E}(\epsilon)$ by the error ϵ_{i-d}, available at the transmitter at time instant i, so we transform the gradient descent in a stochastic gradient descent. Second, we interpret the term $\frac{\partial \mathbb{E}(\epsilon)}{\partial c}$ as a positive time varying adaptation weight, so we include its effect in μ_i. Therefore, the stochastic adaptation rule is

$$c_{i+1} = c_i - \mu_i \left(\epsilon_{i-d} - p_0\right). \tag{5.12}$$

We assume that the reported SNR feeding the LUT in (5.7) changes slowly. This is the case in [19], where the estimated SNR at the receiver is the result of an averaging operation on time designed to inform of the operation point rather than tracking the fast SNR fluctuations.

Let us denote by $p\left(c\right)$ the error probability when the margin is c. Assume that p is a continuously differentiable function, with derivative bounded by $\delta_0 < \frac{\partial}{\partial c} p\left(c\right) < \delta_1 \, \forall c$, with $\delta_0 > 0$. Let us denote by $c_\star$ the value[1] such that $p\left(c_\star\right) = p_0$. Additionally, the stepsize in (5.12) will remain constant and equal to μ. If $d = 1$ in (5.12), then the following convergence results hold.

Teorem 1 If $\mu < 2/\delta_1$, then $|\mathbb{E}(c_i) - c_\star| < \eta^i \, |\mathbb{E}(c_0) - c_\star|$, with $0 < \eta < 1$, which grants an exponential convergence of (5.12). In addition, the expectation of the mean squared error $\mathbb{E}((c_i - c_\star)^2)$ converges as

$$\lim_{i \to \infty} \mathbb{E}((c_i - c_\star)^2) < \frac{\mu}{2\delta_0 - \mu\delta_1}. \tag{5.13}$$

If $d > 0$, convergence is still expected for sufficiently low stepsize μ, although formal proof is only provided for $d = 0$ in the Appedix of [26].

In order to speed up the convergence of the adaptive (outer loop) scheme, a Normalized Least Mean Squares (NLMS) variant can also be used [**?**]:

$$c_{i+1} = c_i - \frac{\mu}{\theta^2 + \mathrm{snr}^2_{i-2d}} (\epsilon_{i-d} - \tilde{p}_{0,i}) \cdot \theta \tag{5.14}$$

with $\tilde{p_0}$ adjusted as

$$\tilde{p}_{0,i+1} = \tilde{p}_{0,i} - \lambda(\epsilon_{i-d} - p_0). \tag{5.15}$$

Numerical evaluation

We report the results of the adaptive margin approach for the forward link of the Land Mobile Satellite channel. Only one state will be considered [14], corresponding to a line-of-sight (LOS) situation. As mentioned earlier, the reported CQI by the receiver will be the result of mapping the average effective SNR to the highest supported MCS. Each frame has a duration of 80 ms. A geostationary satellite is considered, so the RTT will be approximately equal to 6 frames. Adaptation was performed with the NLMS algorithm, with $\theta = 10$ and $\mu = 1$ in (5.14) and $\lambda = 0.001$ in (5.15). Figures 5.26 and 5.27 show the evolution of the margin c_i for different speeds and simulation conditions. The cumulative FER is also shown. Due to the long duration of the frames, the variance of the effective SNR decreases for higher speeds, so the required back-off margin is lower (in absolute

[1] As p_0 is a monotonic increasing function, this value is unique.

value). In both cases the CQI is computed after mapping the effective SNR averaged during 8 frames. The margin which guarantees the target FER is a function of the speed (among other parameters), which illustrates the flexibility of the proposed adaptive solution against a fixed margin allocation. This becomes more clear in Figure 5.28, where fixed margin allocation performance contrasts with that for adaptive margin. Average spectral efficiency and cumulative FER are plotted for a LOS SNR ranging from 0 to 10 dB. Average spectral efficiency is defined as $\frac{1}{N}\sum_{i=1}^{N}(1-\epsilon_i)r_{m_i}$, with r_j the rate of the j-th MCS, and m_i the selected MCS for the transmission of i-th frame.

In the same figure we have also tested the simultaneous adaptation of the margin c and a weight ξ of the SNR, which can be of interest for those cases with a more frequent feedback of the SNR. The choice of the MCS by the LUT would follow now

$$m_i = \Pi(\xi_i \cdot \mathrm{snr}_{i-d} + c_i) \tag{5.16}$$

with the corresponding NLMS scheme

$$\begin{pmatrix} c_{i+1} \\ \xi_{i+1} \end{pmatrix} = \begin{pmatrix} c_i \\ \xi_i \end{pmatrix} - \frac{\mu}{\theta^2 + \mathrm{snr}_{i-2d}^2}(\epsilon_{i-d} - \tilde{p}_{0,i}) \begin{pmatrix} \theta \\ \mathrm{snr}_{i-2d} \end{pmatrix}. \tag{5.17}$$

A similar adaptation scheme, including also the SNR measured by the receiver, was applied in [3] for the return link. We have compared different configurations in terms of number of adaptive parameters: a fixed margin of -1 dB, adaptive margin and adaptive margin and weight. The use of adaptation (either one or two parameters) outperforms the fixed back-off margin approach, which would require the knowledge of the operation point and the channel statistics to achieve the target FER (in this example this occurs for 8 dB of LOS SNR).

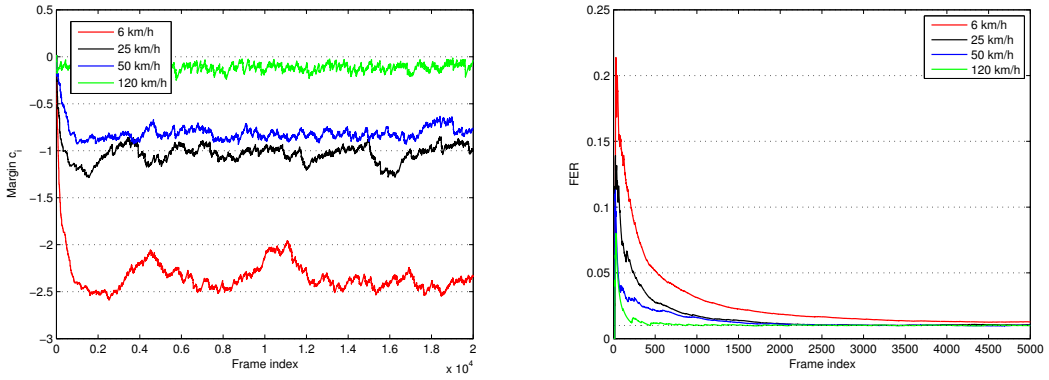

(a) Evolution of the margin

(b) Cumulative FER

Figure 5.26: Suburban environment, target FER of 0.01 and 6 dB of LOS SNR

Conclusions

In this paper we have shown the application of adaptive back-off margins to the forward link of a mobile satellite link. The mapping of the reported channel quality to the corresponding

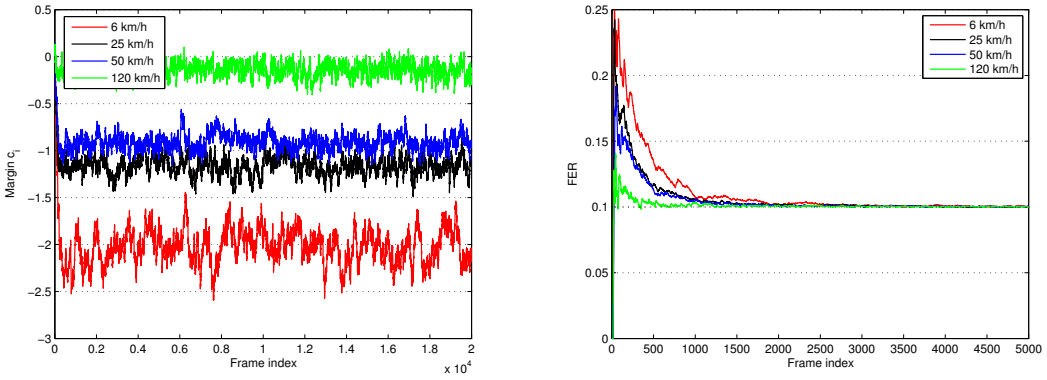

(a) Evolution of the margin (b) Cumulative FER

Figure 5.27: I-tree environment, target FER of 0.1 and 2 dB of LOS SNR

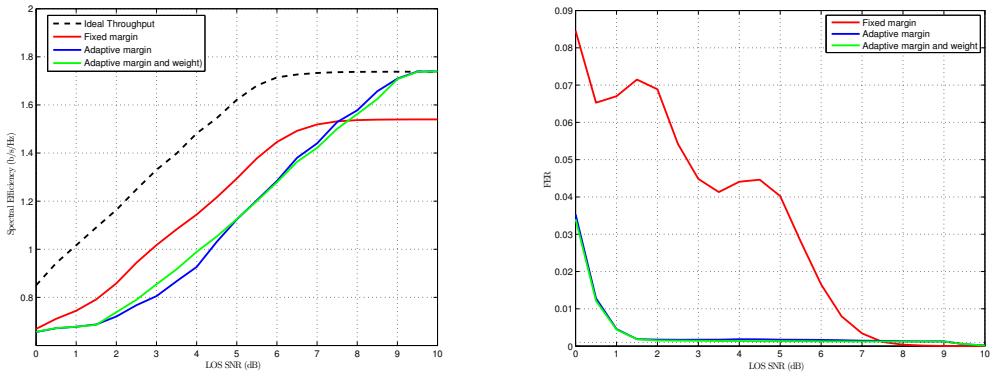

(a) Spectral efficiency (b) Cumulative FER

Figure 5.28: Urban environment, speed 5 km/h, target FER of 0.001.

transmission rate is modulated by a margin which accounts for the reliability degree of this channel information to predict the channel transmission capacity in subsequent frames.

A stochastic gradient descent algorithm was derived, and its convergence proved analytically and tested by simulations for narrowband links. Application to broadband links, with shorter frame durations,looks quite promising now that the recently published extension DVB-S2X to DVB-S2 enhances the applicability of the latter to mobile receivers by incorporating special frames able to work in very low SNR conditions.

5.4.4 A study of new algorithms

The algorithms presented in the previous subsection [26], performs very well in state-1 channel simulations (LOS conditions) adjusting the FER to the objective value, p_0, for a wide range of SNR LOS, Mobile Terminal speeds and target FERs p_0. But, when the algorithm is tested under the complete Fontan channel model, i.e., allowing transitions among all the tree states (LOS, shadowing and blocking), the value of the margin cannot

follow the channel changes, specially when $p_0 \leq 0.01$. Here a modification of the baseline algorithm is proposed in order to increase its convergence speed. Simulations are performed in order to test the new algorithm.

Problems of the baseline algorithm

The baseline equation for actualizing the value of the margin used in the MCS selection is

$$c_{i+1} = c_i - \mu_i \left(\epsilon_i - \tilde{p}_0\right). \tag{5.18}$$

that is programmed using the Normalized Least Mean Squares (NLMS) variant in order to speed up the convergence

$$c_{i+1} = c_i - \frac{\mu}{\theta^2 + snr^2_{i-2d}} \cdot \left(\epsilon_{i-d} - \tilde{p}_{0,i}\right) \cdot \theta. \tag{5.19}$$

Hereafter the baseline algorithm refers to rule adaptation provided in Equation 5.19 accompanied with the recursion to calculate $\tilde{p}_0$

$$\tilde{p}_{0,i+1} = \tilde{p}_{0,i} - \lambda \cdot \left(\epsilon_{i-d} - p_0\right) \tag{5.20}$$

with the parameters $\mu = 1$, $\theta = 10$ and $\mu = 0.001$, and snr expressed in dB.

An example of the problems of the baseline algorithm is explained thereupon with the help of Figure 5.29. During a fading period the transmissions fail and NAKs are received, this causes that the margin c_i reduces its value drastically until its programmed low bound: -7.38 dB. After that, although the channels passes through long period of good conditions, we can see that margin c_i increases very slowly, therefore MCSs with higher rate are not exploited leading to a underutilization of the channel capacity.

With the new algorithm, that takes into account the difference between the channel capacity and the throughput $(C_i - T_i)$, defined in Equations 5.21 and 5.22, this does not occur, see Figure 5.30. After the fading period (frame 16500) the margin is in its low bound, but how the channel changed to LOS conditions and difference $(C_i - T_i)$ is big, the amplifying factor of the upwards step (black curve) is high and in less than 500 frames (40 seconds) the higher MCSs are chosen again.

Modification of the baseline algorithm

In the approach applied so far it is not used some piece of information that is available at the transmitter when the MCS m_i is chosen: the past values of the channel capacity and the throughput achieved. Let r_{m_i} be the rate of the MCS selected for transmitting the frame i, ϵ_i the error event in the reception of frame i, and r_{CQI_i} the rate of the highest MCS supported by the channel when frame i is received.

The transmitter can calculate the throughput achieved in the past M transmissions as

$$T_i = \frac{1}{M} \sum_{j=i-d-M}^{i-d} r_{m_j}(1 - \epsilon_j) \tag{5.21}$$

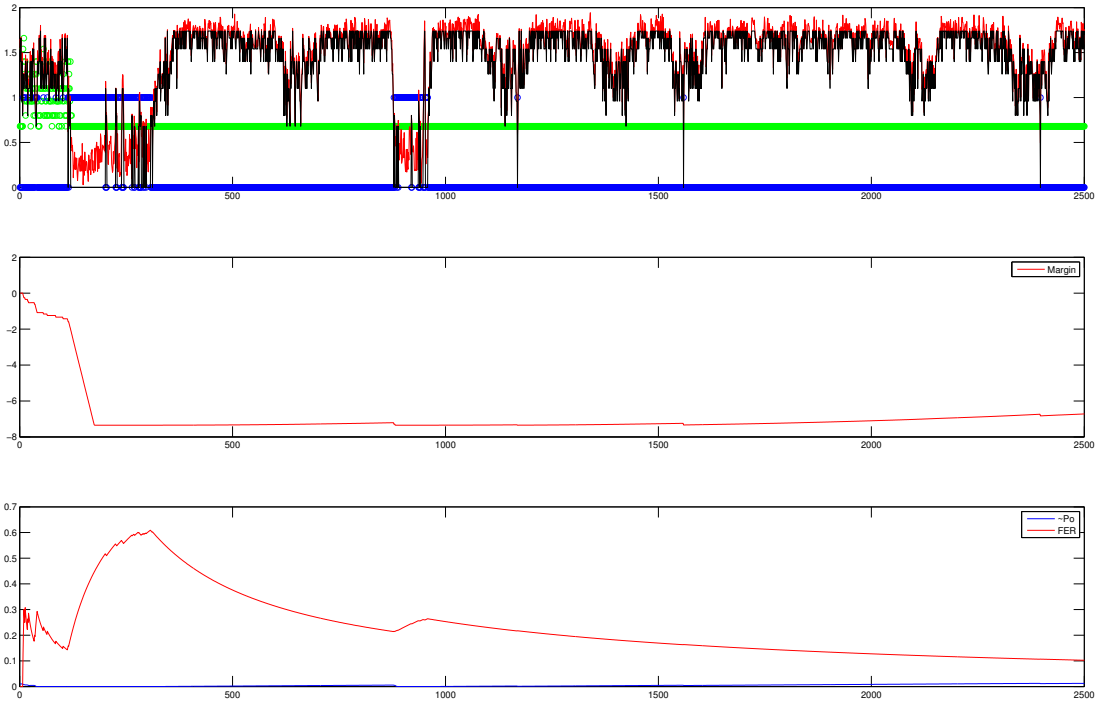

Figure 5.29: Baseline algorithm. Top: channel capacity, MCS used and errors. Middle: margin. Bottom: FER. Suburban, 6 dB LOS SNR, speed 6 km/h.

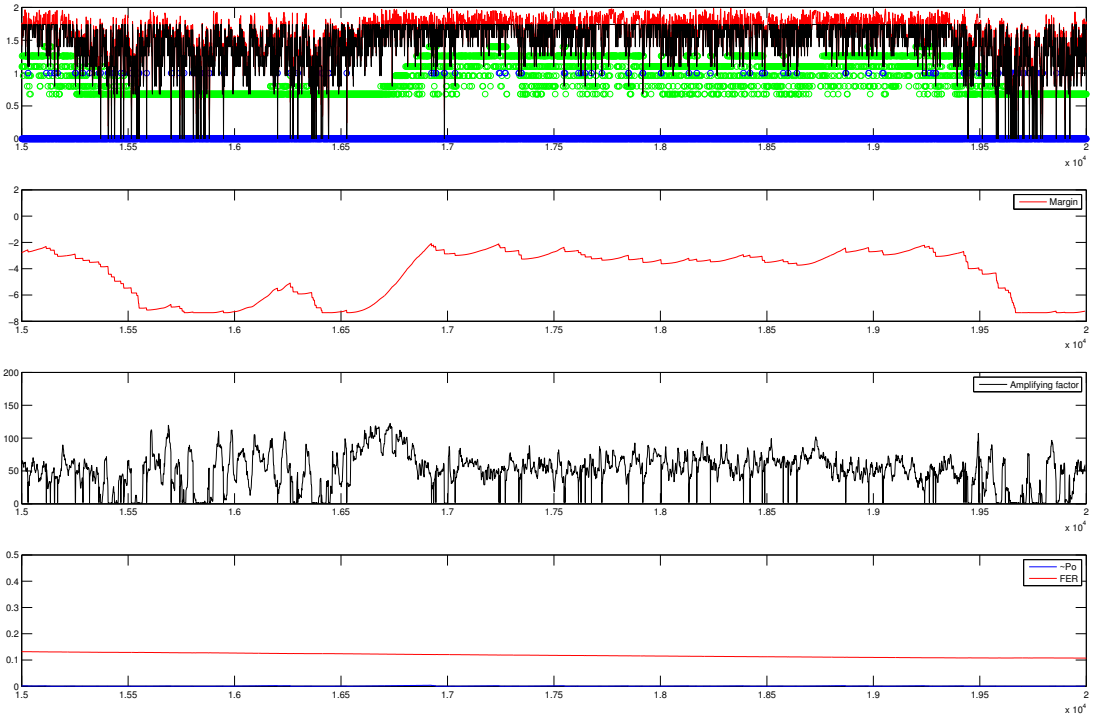

Figure 5.30: New algorithm. Top: channel capacity, MCS used and erros. Middle: margin. Bottom: FER. Suburban, 6 dB LOS SNR, speed 6 km/h.

and the channel capacity as

$$C_i = \frac{1}{M} \sum_{j=i-d-M}^{i-d} r_{CQI_j} \tag{5.22}$$

where d is the Round Trip Time (RTT) of the link, equals to 6 frames (0.48 s) in our simulations, and M takes the value 18.

Therefore, the value of $(C_i - T_i)$ can be used in order to speed up the rate of increasing of c_i when ACKs are received in the case that $(C_i - T_i)$ is big. Due to the values of $(C_i - T_i)$ are in the range of $[0, 1.74]$ if we do not want any amplification of the steps when $(C_i - T_i) = 0$ and big amplification when that value is maximum we have to apply a change of scale of that value. This change is realized through a function $f\,(C - T, \epsilon)$. The function depends on ϵ because the steps downward (NAK received) are big enough and they should not be amplified in the same way that the steps upwards (ACK received). The implemented function is different for each target FER p_0 tested, but it is believed that by means of simulations a expression of $f\,(C - T, \epsilon, p_0)$ can be obtained.

The expression of the new adaptation rule with the amplification function included on it is

$$c_{i+1} = c_i - f(C_i - T_i, \epsilon_{i-d}) \cdot \frac{\mu}{\theta^2 + snr^2_{i-2d}} \cdot (\epsilon_{i-d} - \tilde{p}_{0,i}) \cdot \theta. \tag{5.23}$$

Next, we include the expression for the amplification function (Equations 5.24-5.25) used in our simulations and we show its values when an ACK is received ($\epsilon = 0$), in Figure 5.31

- Target PER $p_0 = 0.01$

$$f(C - T, \epsilon) = \begin{cases} 150 \cdot (C - T) + 1 & if \quad \epsilon = 0 \quad (ACK) \\ 2 & if \quad \epsilon = 1 \quad (NAK) \end{cases} \tag{5.24}$$

- Target PER $p_0 = 0.1$

$$f(C - T, \epsilon) = \begin{cases} 15 \cdot (C - T) + 1 & if \quad \epsilon = 0 \quad (ACK) \\ 4 & if \quad \epsilon = 1 \quad (NAK) \end{cases} \tag{5.25}$$

There is a tenfold slope increment of the amplification function of one straight line with respect to the other. The reason is that for the baseline algorithm in the case of target PER equals to 0.1 the step upwards of the margin with each received ACK is 0.01, while in the case of target PER 0.01, the step upwards is tenfold lower, 0.001. Therefore, if we want to follow the same channel variations in both cases, the amplification factor needs to be larger in one case than in the other.

In the algorithm implemented there is a last specification. Instead of computing C as the mean of last M received values of the channel state, $C = C_i$, a correction is applied because due to the fast fluctuations of the effective SNR the transmitter cannot follow the instantaneous channel capacity transmitting without errors. So, instead of trying the algorithms to achieve a capacity C, we decrease a quantity determined by the variance. Therefore, the C used to calculate the amplification factor is C_i minus its standard deviation:

$$C = C_i - \sqrt{Var(\vec{C_i})} \tag{5.26}$$

where $\vec{C_I}$ is the vector of last M values of the channel capacity, and C_i is calculated as Equation 5.22.

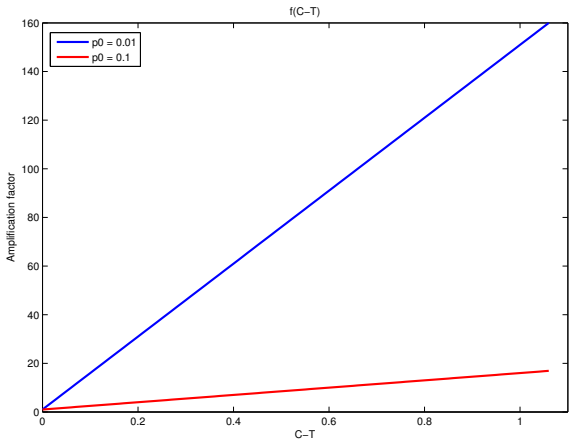

Figure 5.31: Amplification function.

Simulation results

It was performed several simulation to compare the results obtained with the new algorithm against the results offered by the baseline algorithm. The conclusion is that although the new algorithm can increase the spectral efficiency, that is always achieved at the expense of increasing the FER. This can make us think that maybe it is not possible have a better spectral efficiency. In the following subsection the theoretical limit of channel capacity is study for the 1-state Fontán channel. The results obtained show us that our robust algorithm for the forward link is quite close to the so called informed outage capacity, that is the capacity a transmitter can achieve in that conditions.

5.4.5 Informed outage capacity

There are several ways of measuring the performance of a wireless communications system, one of them is comparing the achieved throughput with the ergodic capacity and the Frame Error Ratio (FER) with some objective FER p_0. According to [29] the ergodic capacity, also named Shannon capacity, is the maximum transmission rate with arbitrary small error probability. Its use is not very practical because in fading channels the transmission time must be very long ir order to see the long-term ergodic properties of the channel. However the outage capacity is a more useful measure of the maximum reachable capacity in a particular channel. Outage capacity can be defined as the maximum transmission rate that can be achieved subject to a given outage probability, i.e., subject to a particular FER [29].

In the literature most of the work is focused on Rayleigh and Rice fading channels with no channel state information (CSI) on the transmitter. Nevertheless for our work of design link adaptation schemes is desirable to have a measure of how our algorithms performed compared with the best possible ones, i.e. the algorithms that make the best use of the available CSI. Therefore in this report is introduced a new measure of the capacity of the channel called informed outage capacity or outage capacity with CSI, that is the maximum transmission rate that can be achieved when the transmitter has some CSI subject to a given outage probability.

This new indicator is very useful because plotting it in a graphic along with the throughput achieved by a algorithm allows to see the gap to the best possible performance.

System model

In order to characterize the channel, we are going to use the effective SNR ρ. We suppose it follows a lognormal distribution, or in other words, the effective SNR in decibels is normally distributed. In the section of simulation results we verify that the effective SNR in a channel of interest, such as the Fontan 1-state Land Mobile Satellite (LMS) channel, fits well with a Gaussian distribution.

The transmitter has a partial knowledge of the real effective SNR, it has an estimation of it, $\hat{\rho}$. This can be obtained through a closed loop where the receiver informs the transmitter about the effective SNR (it is therefore a past value of the effective SNR), through an open loop where the transmitter measures the reverse channel SNR, partially correlated with the forward channel SNR or through a mixed strategy that combines open and closed loop SNR. Therefore we can model ρ as a function of its estimate used by the transmitter $\hat{\rho}$, the correlation between both of them α, the mean value of the effective SNR $\bar{\rho}$, its standard deviation σ_ρ and a standardized Gaussian random variable W:

$$\rho = \alpha\hat{\rho} + (1-\alpha)\bar{\rho} + \sigma_\rho\sqrt{1-\alpha^2}W \tag{5.27}$$

The previous equation allows us to model a wide range of cases, from no correlation ($\alpha = 0$) to perfect CSI at the transmitter ($\alpha = 1$). We consider that ρ and $\hat{\rho}$ are equally distributed, i.e.,

$$f(\hat{\rho}) = f(\rho) \sim N(\bar{\rho}, \sigma_\rho^2) \tag{5.28}$$

where $f(\cdot)$ denotes de probability density function (PDF) of the random variable. This is clearly true in the case of closed loop due to the fact that $\hat{\rho}_i = \rho_{i-d}$, in the other cases we believe that the approximation $f(\hat{\rho}) \simeq f(\rho)$ can be done.

If we calculate the PDF of ρ conditioned to $\hat{\rho}$ applying the Bayes theorem we obtain

$$f(\rho|\hat{\rho}) = \frac{f(\hat{\rho}|\rho)\cdot f(\rho)}{f(\hat{\rho})} = f(\hat{\rho}|\rho) \tag{5.29}$$

Taking into account the equation 5.27 the conditional PDF is

$$f(\rho|\hat{\rho}) \sim N\left(\alpha\hat{\rho} + (1-\alpha)\bar{\rho},\, \sigma_\rho\sqrt{1-\alpha^2}\right) \tag{5.30}$$

In Figure 5.32 we show the PDF of the effective SNR (assuming a mean of 2 dB), and its PDF conditioned to $\hat{\rho} = 6dB$ for two different values of the correlation. It can be seen that as α increases the mean of the conditional PDF tends to 6 dB and its variance tends to 0. In the limit, $\alpha = 1$, we obtain a delta in 6 dB, there is not uncertainty.

The outage capacity for a given outage probability p_0 and a given $\hat{\rho}$ is $C_{out,\hat{\rho}}$ and its expression depends on the value of effective SNR ρ_{out} that verifies

$$\int_{-\infty}^{\rho_{out}} f(\rho|\hat{\rho})d\rho = p_0 \tag{5.31}$$

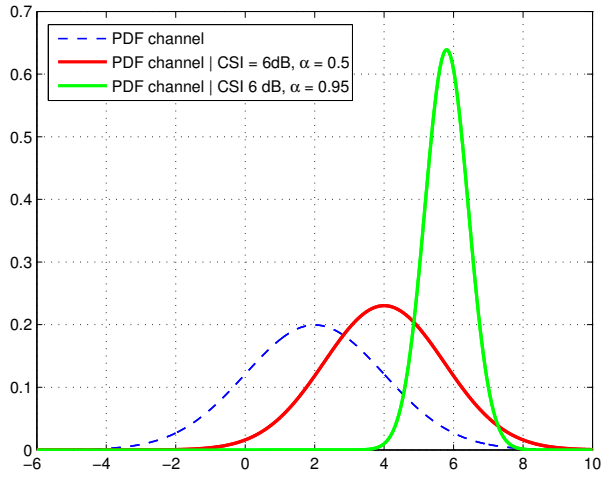

Figure 5.32: Conditional PDF of the effective SNR

If $\phi(\rho)$ is the cumulative distribution function (CDF) of 5.30 ρ_{out} can be calculated as

$$\rho_{out} = \phi^{-1}(p_0) \tag{5.32}$$

and the outage capacity for $\hat{\rho}$ as

$$C_{out,\hat{\rho}} = \log_2(1 + \rho_{out}) \tag{5.33}$$

Finally the outage capacity for p_0 is obtained integrating for all possible values of $\hat{\rho}$

$$C_{out} = \int C_{out,\hat{\rho}} f(\hat{\rho}) d\hat{\rho} \tag{5.34}$$

Outage capacity

In this section we include the graphical representation of the outage capacity with partial CSI. There are four parameters involved: the outage probability p_0, the correlation α and the mean $\bar{\rho}$ standard deviation σ_ρ of the PDF of the effective SNR. The parameters of the Gaussian distribution of the effective SNR are extracted from experimental data.50000 transmitted frames were simulated with the LOS state of the Fontan LMS channel model [14], in particular we use the 40° elevation narrow-band S-band parameters for an urban environment and a mobile speed of 5 km/h. In Table 5.8 we compare the parameters of the lognormal component of the Fontan channel (mean α and standard deviation Ψ) with the mean and standard deviation of the effective SNR obtained from the simulation (where a Rician fast fading is also added).

In Figure 5.33 we can see that the obtained experimental distribution fits well with a Gaussian, therefore the outage capacity calculated for a lognormal distribution of the effective SNR is approximately equal to the outage capacity of the channel under urban environment that follows the Fontan model. This is important for the following section

	Fontan parameters	Experimental data
mean α	-0.31	-0.30
standard deviation Ψ	0.73	0.98

Table 5.8: Simulated speeds

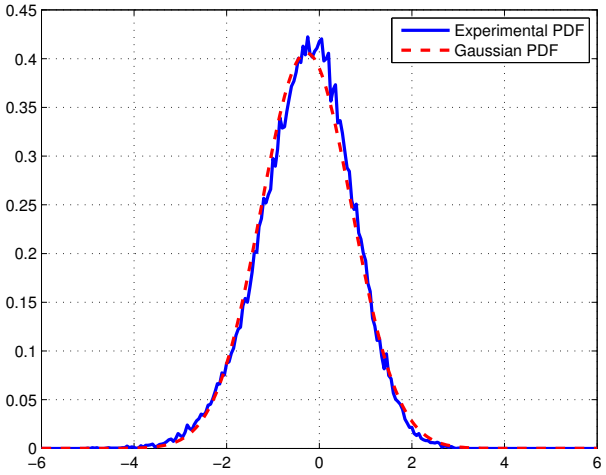

Figure 5.33: Fit of the experimental data to a Gaussian distribution

where we compare the performance of the link adaptation algorithms in terms of spectral efficiency with the outage capacity with CSI.

Now we include the six graphics of the outage capacity, by fixing one parameter ($\bar{\rho}$, α or $p0$), other is in the x-axis and the other taking a few values. In the graphics is highlighted the case presented in the paper [26]: urban 5 km/h ($\alpha = 0.28$ and $p_0 = 0.001$).

Performance of the algorithms of the SPAWC2015

Now we plot in the same graphic, see Figure 5.35, the spectral efficiency of the algorithms of the paper [26] and the constrained outage capacity with CSI. For the values of LOS SNR where the algorithm approximately achieves the objective FER of 0.001, in mean the algorithms reaches the 96.9% of the constrained outage capacity. Therefore, although there is still a 3.1% of improvement margin the performance of the algorithms is very close to the ideal case.

The optimum outage capacity

Graphics of Figure 5.34 have been calculated assuming that the maximum outage capacity is reached by requiring the same outage probability, p_0, for all the values of SNR. But actually the optimum outage capacity is a slightly larger (specially for low SNRs) if we

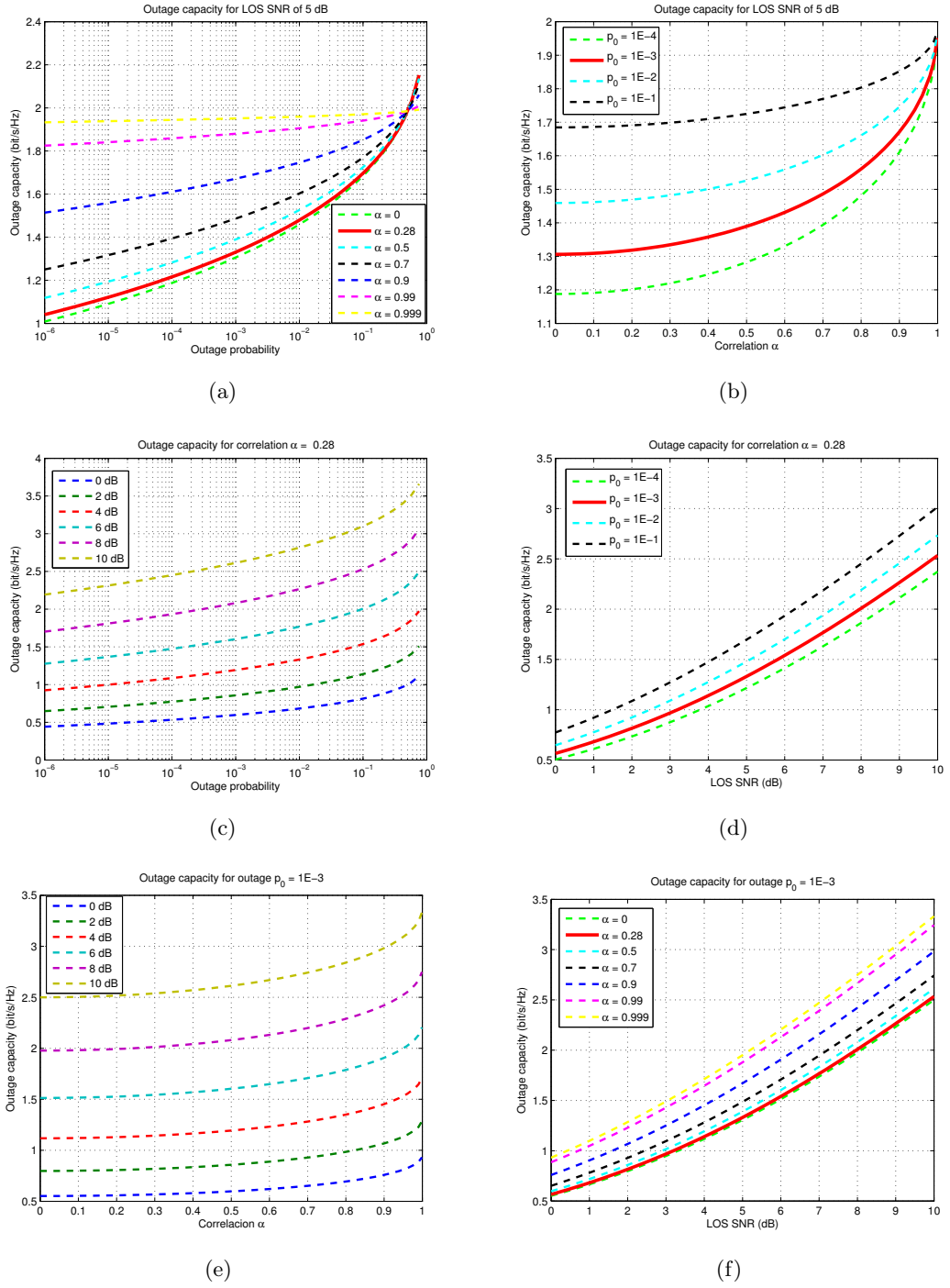

Figure 5.34: Autocorrelation of the effective SNR for different environments

allow the different SNR to have different outage probabilities with the constraint that in average the outage probability is p_0. We solved the optimization problem

$$\begin{aligned} C_{out} &= \max_{c} \mathbb{E}\{C(\rho(\hat{\rho}))\} \\ subject\ to\ & \int_{-\infty}^{\rho(\hat{\rho})} f(\rho|\hat{\rho})d\rho \leq p_0 \end{aligned} \tag{5.35}$$

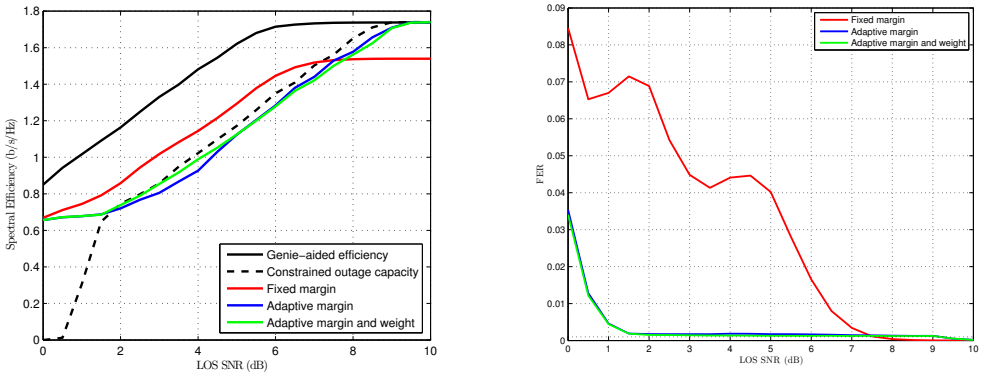

(a) Spectral efficiency

(b) FER

Figure 5.35: Performance of the algorithms under urban environment and 5 km/h

but the correct optimization problem is

$$\begin{aligned} &C_{out} = \max_{c} \mathbb{E}\{C(\rho(\hat{\rho}))\} \\ &subject\ to\ \mathbb{E}\{\textstyle\int_{-\infty}^{\rho(\hat{\rho})} f(\rho|\hat{\rho})d\rho\} \leq p_0 \end{aligned} \tag{5.36}$$

In Figure 5.36 we show the actually optimum outage capacity (in squares in the graphics), calculated with an iterative dual algorithm of gradient descent, together with the values of the outage capacity calculated following the steps of the first sections of this report. There is a big match between the curves and the squares, except for the case of $\alpha = 0.99$ where the algorithm for calculate the optimum outage capacity even diverges and gives an unusual high value of 31 for $p_0 = 0.1$. In the view of the results we conclude that the method presented in this report to calculate the outage capacity, in spite of asking the same outage probability p_0 for all SNRs, produces a results that match the optimal solution of the correct optimization problem.

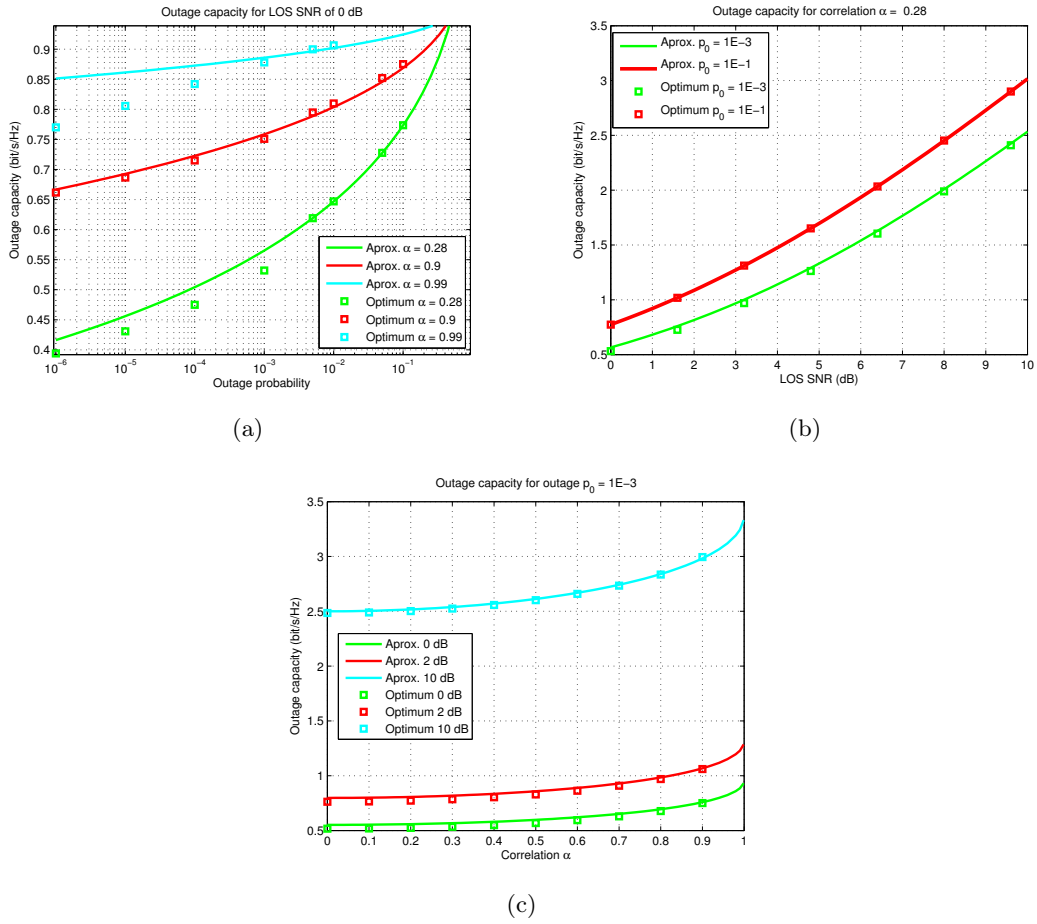

Figure 5.36: Comparison between the outage capacity obtained with the simplified method of this report and its optimal value

Chapter 6

Conclusions and Future Work

Link adaptation algorithms are widely used in terrestrial standards in order to increase the spectral efficiency of the system and in satellite communications, despite their intrinsic high delay, they can also be employed successfully.

Firstly, in Section 5.4.2 it was showed that in the return link the proposed balanced dual algorithm outperforms all other algorithms, specially in the case of the 3-state Fontán channel model. This algorithm, apart from employing an adaptive back-off margin, balances the Open Loop Channel State Information (CSI) and the Closed Loop CSI through some adaptive weights. In this way it adapts itself better to the different channel conditions.

Then, in Section 5.4.3 it was presented an algorithm with an adaptive margin for the forward link. The algorithm is named robust because it ensures the convergence of the margin to its optimal value and without relying on any assumption of the channel model. Furthermore, when compared with the use of a fixed margin, our proposal behaves better. On the one hand, with a fixed margin the target FER is only achieved in a specific operation point of LOS SNR. On the other hand, with our algorithms, target FER is guaranteed for a wide range of LOS SNRs.

Besides the study of link adaptation algorithms, we addressed the theoretical channel capacity that can be achieved by a transmitter with partial Channel State Information (see Section 5.4.5). This concept was named informed outage capacity and was found that our algorithm for the forward link reaches about the 97 % of that capacity. That means that there is no much more scope of improvement in the case of adaptive margin under 1-state channel model.

In this project we also proposed new tools (see Section 5.3) that help in the process of analysing the simulation results of link adaptation schemes. On the one hand, the autocorrelation of the effective SNR helps to predict the behaviour of the algorithms. On the other hand, the new type of graphic that includes channel capacity, MCS rate and error events, along with the evolution of the FER and the algorithm variables, is of paramount importance for understanding what is happening on the time domain with the algorithms.

This project serves too as an introduction to the SL family of the standard S-UMTS, which is summarised here in Chapter 3. This is a standardization of one Satellite Radio Interface proposed by the ITU-R. The standard is firstly put into context explaining what is IMT-2000, an initiative of the ITU-R, and exposing the main ITU-R recommendations

relative to the satellite component of IMT-2000.

Finally, some future lines of the present project are sketched. In first place, the concept of informed outage capacity, that here was studied only for the 1-state Fontán channel model, should be expanded to the 3-state model, the multi-state channel. This work is focused on link adaptation in the standard S-UMTS but the algorithms proposed here are universal and can be applied to other standards. In the future, we would like to perform some simulations using the parameters of other standards such as DVB-S2X/DVB-RCS2 where the use of smaller frames could help to increase the correlation of the open loop SNR and produce an increase of the spectral efficiency. Lastly, we can say that some field trials are scheduled to test the algorithms in a real situation. The data obtained through this way, on the one hand will serve to validate the results of this project, and on the other hand, it can help to have a better knowledge of the land mobile satellite channel.

Bibliography

[1] ITU-R Recommendation M.1167 Framework for the satellite component of International Mobile Telecommunications-2000 (IMT-2000), 1995.

[2] ITU-R Recommendation M.1850 Detailed specifications of the radio interfaces for the satellite component of International Mobile Telecommunications-2000 (IMT-2000), 10 2014.

[3] Alberto Rico-Alvariño, Jesus Arnau, and Carlos Mosquera. Balancing Closed and Open Loop CSI in Mobile Satellite Link Adaptation. In *Proc. ASMS & SPSC*, Livorno, Italy, 2014.

[4] ETSI TS 101 377-1-3 GEO-Mobile Radio Interface Specifications. Part 1; General specifications; Sub-part 3: GMR-2 General System Requirements, 03 2001.

[5] B. Evans, M. Werner, E. Lutz, M. Bousquet, G.E. Corazza, and G. Maral. Integration of satellite and terrestrial systems in future multimedia communications. *Wireless Communications, IEEE*, 12(5):72–80, Oct 2005.

[6] D.W. Matolak, A. Noerpel, R. Goodings, D.V. Staay, and J. Baldasano. Recent progress in deployment and standardization of geostationary mobile satellite systems. In *MILCOM 2002. Proceedings*, volume 1, pages 173–177 vol.1, Oct 2002.

[7] Paolo Chini, Giovanni Giambene, and Sastri Kota. A survey on mobile satellite systems. *International Journal of Satellite Communications and Networking*, 28(1):29–57, 2010.

[8] ITU-R Recommendation M.687 International Mobile Telecommunications-2000 (IMT-2000), 1997.

[9] ITU-R Recommendation M.818-2 Satellite operation within International Mobile Telecommunications-2000, 2003.

[10] ITU-R Recommendation M.1224 Vocabulary of terms for International Mobile Telecommunications-2000 (IMT-2000), 1997.

[11] ETSI TS 102 744, Satellite component of UMTS (S-UMTS); family SL satellite radio interface. Technical report, October 2012.

[12] ETSI TS 101 865, Satellite component of UMTS/IMT-2000; General aspects and principles. Technical report, 09 2002.

[13] Kai XU. Radio resource management for Satellite UMTS: Dynamic scheduling algorithm for a UMTS-compatible satellite network. Master's thesis, University of Bradford, Vigo, 2009.

[14] Fernando Pérez-Fontán, Maria Angeles Vázquez-Castro, Cristina Enjamio-Cabado, Jorge Pita García, and Erwin Kubista. Statistical modeling of the LMS channel. *IEEE T. Vehicular Technology*, 50(6):1549–1567, 2001.

[15] F. Perez-Fontan, M.A. Vazquez-Castro, S. Buonomo, J.P. Poiares-Baptista, and B Arbesser-Rastburg. S-band lms propagation channel behaviour for different environments, degrees of shadowing and elevation angles. *Broadcasting, IEEE Transactions on*, 44(1):40–76, Mar 1998.

[16] F.P. Fontan, I.S. Lago, R.P. Cerdeira, and A.B. Alamanac. Consolidation of a multistate narrowband land mobile satellite channel model. In *Antennas and Propagation, 2007. EuCAP 2007. The Second European Conference on*, pages 1–6, Nov 2007.

[17] P. Burzigotti, R. Prieto-Cerdeira, A. Bolea-Alamanac, F. Perez-Fontan, and I. Sanchez-Lago. Dvb-sh analysis using a multi-state land mobile satellite channel model. In *Advanced Satellite Mobile Systems, 2008. ASMS 2008. 4th*, pages 149–155, Aug 2008.

[18] C. Loo. A statistical model for a land mobile satellite link. *Vehicular Technology, IEEE Transactions on*, 34(3):122–127, Aug 1985.

[19] `http://www.inmarsat.com/wp-content/uploads/2013/10/Inmarsat_BGAN_Brochure.pdf`. accessed: 20-08-2015.

[20] Alberto Rico-Alvariño. Cognitive and Signal Processing Techniques for Improved Spectrum Exploitation in Wireless Communications. Master's thesis, Universidade de Vigo, Vigo, 2014.

[21] Jesus Arnau and Carlos Mosquera. Open loop adaptive coding and modulation for mobile satellite return links. In *31st AIAA International Communications Satellite Systems Conference*, Florence, Italy, 2013. American Institute of Aeronautics and Astronautics, American Institute of Aeronautics and Astronautics.

[22] Jr. Peyton Z. Peebles. *Principios de probabilidad, variables aleatorias y señales aleatorias*. Mc Graw Hill, 2001.

[23] Antonio Artés Rodríguez and et al. Pérez González, Fernando. *Comunicaciones digitales*. 2012.

[24] Alonso I. Fernández JR. Apuntes de caracterización de sinais aleatorios (csa). E.E. de Telecomunicación, Universidade de Vigo., Vigo, 2010.

[25] S. Scalise, H. Ernst, and G. Harles. Measurement and modeling of the land mobile satellite channel at ku-band. *Vehicular Technology, IEEE Transactions on*, 57(2):693–703, March 2008.

[26] Alberto Rico-Alvarino, Anxo Tato, and Carlos Mosquera. Robust adaptive coding and modulation scheme for the mobile satellite forward link. In *Signal Processing Advances in Wireless Communications (SPAWC), 2015 IEEE 16th International Workshop on*, pages 530–534, June 2015.

[27] O. Del Rio Herrero and R. De Gaudenzi. High efficiency satellite multiple access scheme for machine-to-machine communications. *Aerospace and Electronic Systems, IEEE Transactions on*, 48(4):2961–2989, October 2012.

[28] Peng Wu and N. Jindal. Coding versus ARQ in Fading Channels: How Reliable Should the PHY Be? *Communications, IEEE Transactions on*, 59(12):3363–3374, December 2011.

[29] Zhenshan Zhao and Guozhi Xu. Analysis of outage capacity in nakagami fading channels. In *Communications, Circuits and Systems Proceedings, 2006 International Conference on*, volume 2, pages 857–860, June 2006.